LATE EFFECTS OF RADIATION ON THE SPINAL CORD

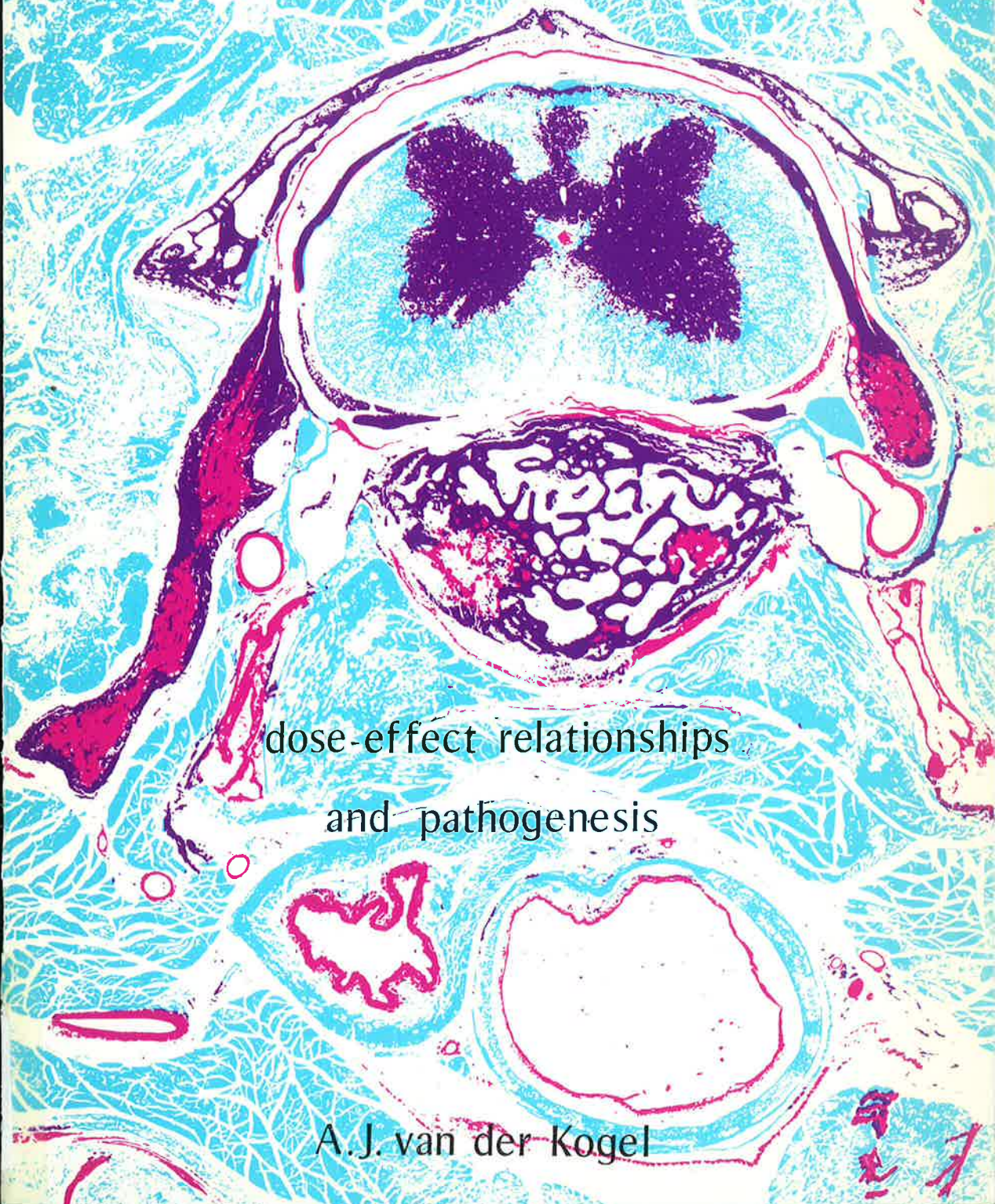

dose-effect relationships and pathogenesis

A.J. van der Kogel

LATE EFFECTS OF RADIATION ON THE SPINAL CORD

S T E L L I N G E N

1

Het optreden van late complicaties na bestraling van hersentumoren met snelle neutronen is niet toe te schrijven aan een hoger waterstofgehalte van het hersenweefsel.

W. Duncan
Brit. J. Radiol. 51 (1978) 943.

2

De bepaling van de relatieve biologische effectiviteit van neutronenstraling voor schade aan het ruggemerg op grond van de latente periode is klinisch niet relevant, aangezien er geen directe relatie bestaat met de tolerantiedosis.

J.P. Geraci et al.,
Radiat. Res. 74 (1978) 382.

3

De radonconcentratie in woningen, gemeten in verschillende landen, varieert van ongeveer 0.1 tot 2 maal de door de ICRP aangegeven limiet van 1 pCi/l. Een vermindering van de ventilatiegraad in het kader van de energiebesparing kan de radonconcentratie met een factor 5 à 10 doen toenemen. Het verdient daarom aanbeveling de hiermee gepaard gaande risico's van hogere stralingsdoses op bronchiën en longen te betrekken in beschouwingen over blootstelling aan andere door de mens toegepaste bestralingen in geneeskunde, wetenschap en techniek.

E. Stranden et al.,
Health Phys. 36 (1979) 413
J. Rundo et al.,
Health Phys. 36 (1979) 729

4

De in ICRP-27 gegeven schatting over een afnemend risico op het ontstaan van kanker na blootstelling aan straling op hogere leeftijd is niet in overeenstemming met recente gegevens, verkregen voor de overlevenden van de atoombomexplosies in Japan.

United Nations Scientific Committee on
the Effects of Atomic Radiation, 1977.

5

De veronderstellingen waarop Ellis het concept van een "nominal standard dose" voor verschillende weefsels baseert, zijn fundamenteel onjuist.

F. Ellis,
Curr. Top. Rad. Res. Quart. 4 (1968) 357.

6

Na een periode waarin technische ontwikkelingen van bestralingsapparatuur een verhoging van de genezingskansen van kanker tot gevolg hadden, lijken nu de belangrijkste mogelijkheden tot verbetering van de radiotherapie te liggen in de toepassing van experimenteel radiobiologische gegevens.

P.J.L. Scholte,
Ned. T. Geneesk. 117 (1973) 1357.

7

In tegenstelling tot bestraling van de schedel, weegt het mogelijk geringe voordeel van prophylactische bestraling van de wervelkolom bij kinderen met acute lymfatische leukemie niet op tegen de grote kans op ernstige late complicaties.

S.S. Soni et al.,
N. Engl. J. Med. 293 (1975) 113.

8

Het moet worden betwijfeld of de concentratie van methotrexaat in de cerebrospinale vloeistof een directe indicatie geeft over de weefselconcentraties in hersenen en ruggemerg.

W.A. Bleyer,
Cancer 41 (1978) 36.

9

De veronderstelling dat sommige celfuncties zoals fagocytose of de productie van collageen specifiek zijn voor cellen van een bepaalde embryonale afkomst is onjuist.

10

Beperking van het aantal proefdieren voor medisch-biologisch onderzoek, vooral in langlopende experimenten, kan worden bereikt door het gebruik van dieren van hoge kwaliteit. Deze beperking wordt echter niet bevorderd door de tendens om de proefdierkosten in een onderzoek als sluitpost op de begroting te beschouwen. Subsidiërende instanties zouden hiermee rekening moeten houden.

11

Het is de vraag of het gebruik van conserveringsmiddelen in het voedsel de houdbaarheid van de mens ten goede zal komen.

Stellingen behorende bij het proefschrift
"Late effects of radiation on the spinal cord: dose-effect relationships and pathogenesis"

A.J. van der Kogel

Amsterdam, 1 november 1979

LATE EFFECTS OF RADIATION ON THE SPINAL CORD

dose-effect relationships and pathogenesis

A.J. van der Kogel

1979

PUBLICATION OF THE RADIOBIOLOGICAL INSTITUTE
OF THE ORGANIZATION FOR HEALTH RESEARCH TNO
RIJSWIJK , THE NETHERLANDS

This work represents a thesis for a doctoral degree at the University of Amsterdam.

CONTENTS

"I selected the albino rat as the animal with which to work. By the use of the equivalent ages observations on the nervous system of the rat can be transferred to man and tested".

H.H. Donaldson, 1924

CHAPTER I

EFFECTS OF RADIATION ON ORGANS AND TISSUES

1.1 RADIATION EFFECTS ON TISSUES IN RELATION TO CELL KINETICS

Several of the most important responses of tissues and organs to ionizing radiation are the result of cellular damage leading to loss of the reproductive capacity of parenchymal cells. Most organs and tissues in the adult mammalian organism depend to a certain degree on replenishment of differentiated cells to maintain their integrity and function. These renewal systems are in a steady state equilibrium involving cell production, differentiation and cell death and these processes are regulated by complex homeostatic control mechanisms.

It is well known that there are great differences in the rate of turnover of cells in various tissue systems. Three categories can generally be distinguished:

1. Rapid renewal systems with a continuous turnover of cells at a high rate, in which specific cell types have a mean life-span of days or weeks, e.g., bone marrow, epithelium of the gastrointestinal tract, skin and testis.
2. Conditional renewal systems which show no or very little proliferation under normal conditions because of the long life-spans of the differentiated cells, e.g., liver and kidney. However, in case of damage, the destroyed cells are rapidly replaced by induced proliferation of surviving cells.
3. Static systems such as the central nervous system (CNS). In the adult organism, a fraction of all neurons is continuously lost due to death occurring at a low rate and these are not replaced by proliferation of other cells. The supporting glial cells in the nervous system, however, can be regarded as representing a conditional renewal system.

The rapid renewal systems are generally the first to show effects of total irradiation, because replacement of differentiated cells within a relatively short time interval is required. When severe damage is induced, the cells may not be able to produce offspring because a large percentage of cells which attempt division subsequently die. Several compartments or pools of cells can be recognized in these sys-

tems: a self maintaining stem cell compartment, a proliferation-differentiation compartment and a compartment of functionally mature cells with a limited life-span.

In a rapid renewal system, radiation can profoundly disturb the kinetics of cell proliferation and the transition of cells from one compartment to the other. Compensation for a partial depletion of the stem cell compartment may be evidenced by an increased rate of proliferation, e.g., due to shortening of the cell mitotic cycle and an increase in the fraction of cycling cells. However, with increasing dose level, a critical minimum of the fraction of surviving cells below which adequate repopulation within a limited time interval is no longer possible, will be reached. The dependence of these reactions on dose and time are determined by a variety of factors which may differ for various tissues and organs.

The reactions observed in skin after irradiation may serve to illustrate the significance of various parameters. It has been possible to explain the acute epithelial reaction on the basis of cellular dose response studies of the kinetics of cellular regeneration (Withers, 1967; Hegazy, 1973). The desquamative reactions are due to cellular depletion of the basal layer of the epithelium. The time of appearance of desquamation is roughly proportional to the tissue renewal time of normal unirradiated skin. Regeneration from surviving proliferating cells and from the unirradiated cells at the borders occurs. Withers (1967) has shown for mouse skin that 10-20 surviving proliferating cells per cm^2 are capable of preventing ulceration after a dose of about 16 Gy of X-rays*. After a dose of 20 Gy, a mean of only about one cell survived per cm^2 and moist desquamation and ulceration were generally observed.

1.2 CHARACTERISTICS OF CELL SURVIVAL CURVES

An important factor influencing the dose at which severe tissue damage is observed is the intrinsic radiosensitivity of the stem cells with regard to their loss of proliferative capacity. It has been possible to determine this sensitivity quantitatively for a number of cell types. With in vitro techniques, the fraction of cells which retain the capacity for unlimited proliferation after exposure to different doses of radiation is determined by scoring the number of

---

*1 gray (Gy) = 1 $J.kg^{-1}$ = 100 rad

formed colonies (Puck et al., 1955). Colony formation can be observed in vivo for some cell types, e.g., bone marrow stem cells, spermatogonia and epithelial cells of the intestine and skin (McCulloch and Till, 1962; Withers, 1967, 1974).

A cell survival curve represents the relationship between the fraction of surviving cells, commonly plotted on a logarithmic scale, and the corresponding dose plotted on a linear scale (Figure 1.1). The high dose region of the curve can be frequently characterized by two parameters describing the width of the shoulder and the slope of the exponential region of the curve. The slope of the exponential part is characterized by the D_0 value, which is the dose required to reduce the surviving fraction by a factor of e^{-1} (0.37). The extrapolation number, N, is obtained by extrapolating the exponential part of the curve to its intersection with the ordinate. The presence of the shoulder region implies that cells are able to sustain some sublethal damage without losing their capacity for unlimited proliferation, whereas accumulation of sublethal damage causes cell reproductive death. The width of the shoulder region can be expressed in the value

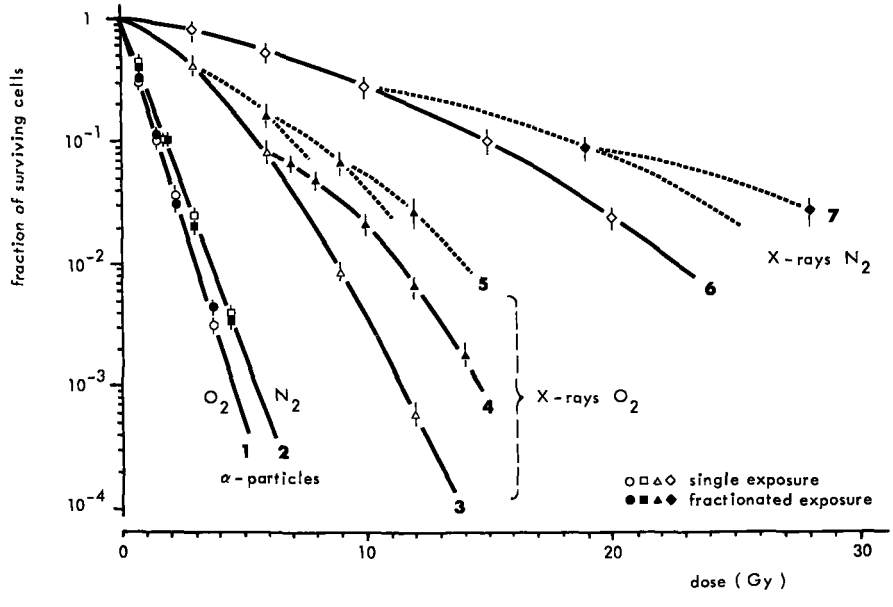

Figure 1.1

Survival curves of T-1 cells, irradiated with 3.4 MeV alpha radiation (curves 1-2) or 250 kV X-rays (curves 3-7) (Barendsen, 1966).

D_0, which is the dose obtained by extrapolating the exponential part of the curve to the abscissa at 100% survival. An important phenomenon is that surviving cells are capable of repairing sublethal damage. This is observed when the radiation dose is divided into two or more fractions separated in time (Figure 1.1). The total dose required to kill a given fraction of cells increases with an increasing number of fractions. When irradiation is carried out continuously over a longer time period, i.e., at a low dose rate, repair of sublethal damage starts already during irradiation, resulting in a cell survival curve with a very shallow slope.

The radiosensitivity of cells can be influenced significantly by their environment. Various "radiosensitizing" or "radioprotecting" agents are known. One of the most important substances affecting cell survival under normal conditions is oxygen. This is illustrated in Figure 1.1; curves 6 and 7 represent the survival of cells irradiated in the absence of oxygen. The dose modifying effect of oxygen is expressed in the oxygen enhancement ratio (OER), which is defined as the ratio of doses required to produce the same effect under anoxic and well-oxygenated conditions. For X-rays and gamma rays, the OER is 2.5-3.

With radiations differing in linear energy transfer (LET) from X-rays and gamma rays, several characteristics of cell survival curves may change. The LET is a measure of the amount of energy deposited over a certain track length of an ionizing particle and is commonly expressed in keV/µm of unit density tissue. Differences in biological effect related to the LET of the radiation are expressed by the relative biological effectiveness (RBE). The RBE can be defined as the ratio of the dose of a standard radiation (usually 250 keV X-rays) to the dose of the specified radiation required to produce the same biological effect under identical conditions. The RBE is not constant; it may vary with the type of cell, type of tissue, observed endpoint, etc. The responses of cells to radiations of different LET have been reviewed by Barendsen (1968). In Figure 1.1, cell survival curves obtained for low LET (X-rays) and high LET (alpha particles) radiation are presented. The shoulder region of the X-ray curves (3-7), representing the accumulation of sublethal damage, is absent in curves 1 and 2 resulting from alpha radiation. Furthermore, the dose modifying effect of oxygen is greatly reduced for alpha radiation and the OER is found to be close to 1.

Fast neutrons dissipate energy partly through secondary charged particles of high LET and partly through low LET protons and gamma rays. The mean LET of fast neutrons is intermediate between X-rays and

alpha particles. This is reflected in survival curves of cells irradiated with fast neutrons, which show a reduced OER of about 1.5-1.7 and a small D_Q. Survival curves of various cell types irradiated with 300 kV X-rays and 15 MeV neutrons are presented in Figure 1.2 (Broerse and Barendsen, 1973). The observed differences in survival were mainly attributed to differences in the accumulation of sublethal damage. The possible advantages of the application of fast neutrons in radiotherapy will be discussed later in this Chapter.

1.3 EARLY VERSUS LATE EFFECTS IN TISSUES

It can be seen in Figure 1.2 that for two rapidly proliferating tissues, viz. the bone marrow and the intestinal epithelium, there is

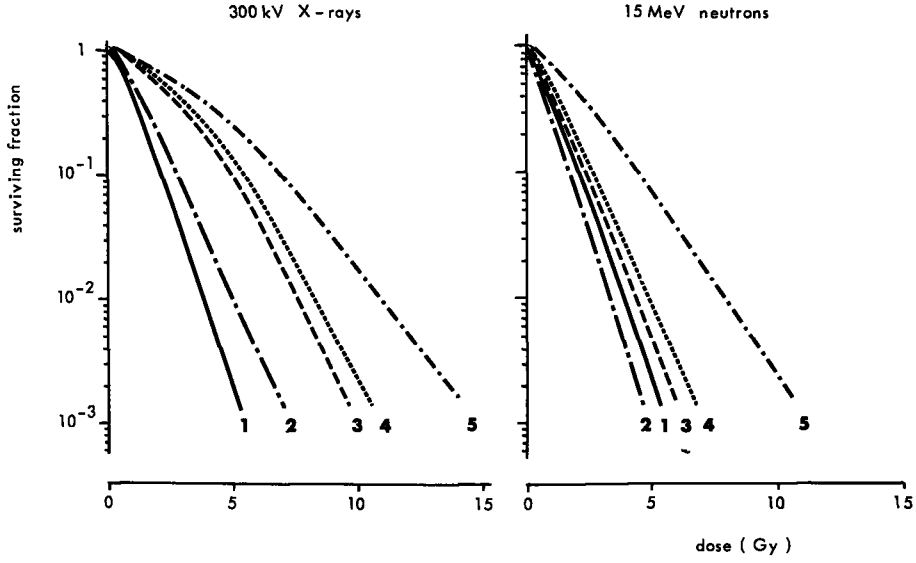

Figure 1.2

Survival curves of different types of clonogenic cells irradiated with 300 kV X-rays and 15 MeV neutrons.
Curve 1: mouse hemopoietic stem cells
Curve 2: mouse lymphocytic leukemia cells
Curve 3: T-1 cells of human kidney origin
Curve 4: rat rhabdomyosarcoma cells
Curve 5: mouse intestinal crypt stem cells
(Broerse and Barendsen, 1973).

a marked difference in the sensitivity of the stem cells. After total body irradiation, the death of the mice as a result of the treatment is primarily related to failure to maintain the functions of these two tissues. The doses at which 50% of a group of mice die (LD_{50}) from the so-called hemopoietic or intestinal syndromes are 6-9 Gy and 12-20 Gy of X-rays, respectively. These doses correspond to a surviving fraction of stem cells of 10^{-3} to 10^{-4}. The hemopoietic stem cells are among the most radiosensitive cell types, with a D_0 value of 0.73 Gy. The intestinal crypt stem cells are rather radioresistant (D_0 = 1.67 Gy) and have a large capacity for accumulation of sublethal damage (D_Q = 3.4 Gy). However, at sufficiently large doses, intestinal damage is observed earlier than death from bone marrow damage due to the shorter life time of differentiated cells. The mean life span of the epithelial crypt cells in the mouse is 3.5 days (Cheng, 1974). Besides death of cells in mitosis, death of cells in interphase within a few hours after irradiation may contribute to as much as 60% of the decrease in the number of crypt cells (Tsubouchi, 1974). Due to extensive cell death concomitant with the normal loss of epithelial cells from the villi, the intestinal surface in the mouse is denuded after about 3.5 days; this results in a massive loss of fluids and electrolytes, which may lead to the rapid death of the animal after doses of 12 Gy or more. Rapid regeneration through repopulation by surviving, proliferating cells takes place after doses of less than 12 Gy. Hyperplastic crypts are formed and these give rise to new crypts by budding and fission; the number of crypts will approach normal levels after about 21 days (Cairnie, 1975).

In the hemopoietic system of rats and mice, only 2 or 3 stem cells per thousand maintain their capacity for unlimited proliferation after doses of about 6-9 Gy of X-rays. These cells are not capable of replenishing the granulocytes and thrombocytes in the blood at a sufficient rate and to prevent the animals from dying consequent to infections and hemorrhages.

While for a number of rapid renewal systems information at the cellular level is obtained by observing colony formation *in vivo*, no technique has been developed to quantify cell survival in the conditional renewal or static systems. Effects on these systems are generally observed after latent periods of months or even years, presumably related to long turnover times of the constituent cells. In contrast to the rapidly proliferating tissues where the acute effects are obviously related to damage to the parenchymal cells and disturbances in their proliferation kinetics, damage to the microcirculation may play an important role in the development of late effects. For most of the

1.4 TIME-DOSE RELATIONSHIPS AND THE CONCEPT OF TOLERANCE DOSE

The main goal in radiotherapy is to attain a high percentage of tumor eradications while keeping the risk of severe normal tissue damage low. Although insight into the basic mechanisms leading to late types of damage are of considerable importance for the analysis and prediction of effects in tissues, this aim can be achieved only by detailed quantitative knowledge of the dose-response curves for tumors and normal tissues.

Hypothetical dose-response curves for the cure probability for two tumors with a different radiosensitivity and for the probability of severe damage in a critical normal tissue are presented in Figure 1.3B. The tumor cure probability curves are derived from the cell survival curves presented in Figure 1.3A. In this example, the original tumor volume is taken as $100\ cm^3$, containing about 10^{10} cells which all have to be killed to achieve tumor eradication. It can be seen that the cure probability rapidly increases above a certain threshold dose. However, this characteristic also applies to the probability of induction of normal tissue complications (curve N). For a tumor of type 1, the cure probability is 90% at a dose at which less than 5% normal tissue complications are observed. In contrast, for a tumor of type 2, the chance of local control is outweighed by the greater risk of complications. The recognition of these characteristics of the dose-response curves of tumors and normal tissues has led to the introduction of the tolerance dose concept (Rubin and Casarett, 1972). Tolerance doses are commonly derived on the basis of the acceptance of a low frequency of severe normal tissue damage, e.g. $TD_{5/5}$, implying that not more than 5% of the patients suffer severe late damage within 5 years after treatment. Examples of actual tolerance doses as used in radiotherapy are presented in Table 1.1.

A large variation in tolerance doses is obtained for different tissues and it can be seen that the slowly proliferating tissues are not necessarily the most radioresistant. This is in contrast to the "law" formulated by Bergonié and Tribondeau (1906), which states that radiosensitivity is directly related with the rate of cell proliferation; this view has since been reiterated in many publications. The different TD values published for the same tissue indicate that the $TD_{5/5}$ or $TD_{50/5}$ have not been definitely established for a number of normal human tissues. Moreover, the tolerance dose values are valid only for standard treatment conditions. Improvements in tumor treatment by, e.g., different fractionation schemes or combination with chemotherapy or radiosensitizers will probably be accompanied by

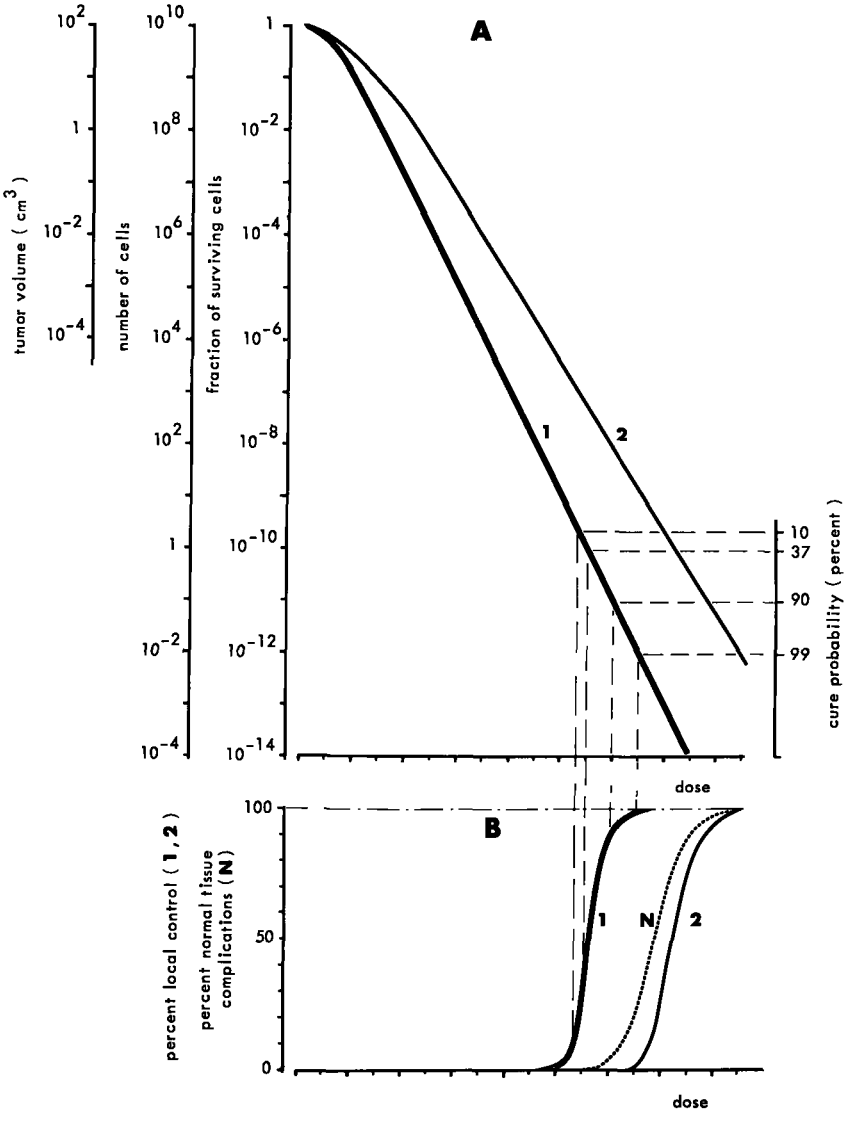

Figure 1.3

A. Relationships between tumor volume, number of cells, fraction of surviving cells and cure probability. Curves 1 and 2 are hypothetical survival curves of tumor cells with a different radiosensitivity.

B. Cure probability for the 2 tumor types as derived from the survival curves in A. The risk of normal tissue complications is represented by hypothetical curve N.

TABLE 1.1

NORMAL TISSUE TOLERANCE DOSES

organ	injury	1-5% ($TD_{5/5}$*)	25-50% ($TD_{50/5}$)	whole or partial organ	ref.**
rapid renewal systems					
skin	ulcers, severe fibrosis	55 Gy	70 Gy	100 cm^2	1
esophagus	ulcers, stricture	60	75	75 cm^2	1
stomach	ulcers, perforation, hemorrhage	45	50	100 cm^2	1
intestine	ulcers, stricture, hemorrhage	45	65	100 cm^2	1
rectum	ulcers, stricture	55	80	100 cm^2	1
bladder	ulcers, contracture	60	80	whole	1
testis	permanent sterilization	5-15	20	whole	1
ovary	permanent sterilization	2-3	6.25-12	whole	1
conditional renewal systems and static systems					
liver	acute and chronic hepatitis	35 Gy	45 Gy	whole	1
		25	40	whole	2
kidney	acute and chronic nephrosclerosis	23	28	whole	1
		20	25	whole	2
lung	acute and chronic pneumonitis	40	60	lobe	1
		30	35	100 cm^2	2
heart	pericarditis, pancarditis	40	100	whole	1
		45	55	60%	2
brain	necrosis, infarction	50	60	whole	1
		60	70	whole	2
spinal cord	necrosis, infarction	50	60	5 cm^2	1
		45	55	10 cm^2	2

*Doses refer to cumulative doses, applied as 5 fractions of 2 Gy (^{60}Co-γ-rays) per week.
TD = tolerance dose: $TD_{5/5}$: no more than 5% severe complications within 5 years.
$TD_{50/5}$: no more than 50% severe complications within 5 years.

**ref. 1: Rubin and Casarett (1972).
ref. 2: Research plan for radiation oncology (1976).

changes in tolerance dose. Therefore, each treatment must be considered in terms of the therapeutic ratio, i.e., the ratio between the tumor cure dose and the highest dose not resulting in an unacceptable level of normal tissue damage.

1.5 ISOEFFECT FORMULAS

For the prediction of tolerance doses depending on the number of fractions or the overall time of the treatment, Ellis (1968) has introduced the nominal single dose (NSD) formula (later changed in nominal standard dose). With this formula, isoeffect doses (D) involving different dose distributions in time, which are to be compared, are related to an NSD by taking into account the number of fractions (N) and the overall time (T):

$$D = NSD \times N^{0.24} \times T^{0.11}$$

The factor involving the number of fractions is related to the amount of repair of sublethal damage between subsequent fractions, whereas the exponent for the overall time is assumed to be principally related to the amount of repopulation during the overall time of the treatment. It is important to note that, in principle, these factors will vary for different tissues depending on population kinetics, capacity for repair, etc. The exponents in the original NSD formula were derived from isoeffect curves for dry desquamation of the skin. However, there is a trend in radiotherapeutic practice to use this formula for all types of normal tissues. Recent clinical and experimental data indicate that for slowly proliferating tissues such as the lung and the spinal cord, the use of other exponents might give a better approximation of the tolerance dose for various fractionation schemes (Wara et al., 1973; Field et al., 1976; Van der Kogel, 1977). Data on tolerance of the pig kidney (Hopewell, 1975) suggest that no simple mathematical expression can be used in predicting the kidney tolerance over a wide range of dose fractionation schemes. Other experimental studies (Berry et al., 1974) showed the occurrence of late subcutaneous fibrosis with treatment regimes which, on the basis of the NSD formula, were assumed to be below the tolerance level. Although the introduction of the NSD formula has been an important step in providing a system for comparison of different schedules in radiation therapy, these results from clinical and experimental studies caution against a rigid use of this formula for all tissues at risk, especially in nonconventional treat-

ment regimes. Further optimalization in radiotherapy with X-rays or gamma rays can be achieved by obtaining detailed information on the tolerance of critical normal tissues under varying conditions.

1.6 HIGH LET RADIATION

In addition to manipulation of fractionation schedules, improvements in local tumor control could result from the use of fast neutrons and accelerated charged heavy particles. Negative pions, protons, helium ions and heavy ions have a limited path length or range in tissue, depending on the initial energy. An increased amount of energy is deposited near the end of the range, at the so-called Bragg peak. By use of variable thickness absorbers, the width of this peak can be adjusted to the size of the tumor; this results in sharp boundaries of the total dose distributed in the tumor region. Negative pions and heavy ions may have an additional advantage because of a dose component of high LET which results in a higher RBE as well as in more effective killing of anoxic cells in a tumor and less repair of sublethal damage (reviewed by Raju, 1972). However, only in a few centers in the world have the large and expensive accelerators needed to produce a high intensity beam of these special types of radiation been constructed. Therefore, fast neutrons are presently still the most generally employed type of high LET radiation in radiotherapeutic treatments. The energy deposition of fast neutrons is not characterized by a Bragg peak, and tissue depth dose distributions are inferior or similar to ^{60}Co or ^{137}Cs gamma rays. Any advantage over X-rays or gamma radiation must be the result of a higher RBE for effects on tumors as compared to normal tissues. A number of studies on fundamental and practical aspects of the application of fast neutrons in clinical radiotherapy have been published in the proceedings of three congresses on this subject (Barendsen, Broerse, Van Putten, Breur, editors, 1971, 1974 and 1979).

1.7 AIMS AND OUTLINE OF THE PRESENT STUDIES

The most critical dose limiting normal tissues, sometimes indicated as type I organs, are those in which severe damage may lead to death of the patient. These organs include many tissues with a slow

turnover of cells: lung, kidney, brain, spinal cord, heart and liver. As discussed in a preceding section of this Chapter, the mechanisms leading to the primarily chronic effects observed in these organs are less well understood than those involved in the acute effects in some other tissues.

Damage to the brain and spinal cord is a particularly severe complication of radiation therapy. Encephalopathy or myelopathy may develop up to several years after treatment with curative radiation doses. This is the more dramatic because it involves patients with a prolonged regression or cure of the treated tumor. Due to the anatomical location of the spinal cord, this structure is at risk in a large number of radiotherapeutic treatments, e.g., of tumors in the neck, lungs, abdomen, testis and lymph nodes. Quantitative data on human cases of radiation myelopathy are too limited, however, to determine the dependence of the tolerance of the spinal cord on such factors as dose fractionation, dose rate, overall time of treatment and type of radiation.

One of the aims of the present study was to analyze the relationships of these factors and the tolerance of different regions of the spinal cord, to provide a basis for the improvement of radiotherapeutic treatments and to develop a radiobiological model for studies of damage to a slowly proliferating tissue. A second aim was to establish the RBE of 15 MeV neutrons as a function of the dose per fraction as a basis for the application of neutrons in radiotherapy. The third objective was to obtain an insight into the mechanisms involved in the development of damage and into the pathogenesis of the different types of lesions, which might also be of interest for insight into changes in the central nervous system occurring without radiation.

The outline of these studies as presented in the various chapters is as follows. In Chapter II entitled: "Structure of the spinal cord", a number of anatomical and histological aspects are discussed. This is given to serve as an introduction to the histopathological studies and to the discussion of the cell types which are primarily involved in the development of the various radiation induced lesions. The materials and methods used for the studies of radiation damage in the spinal cord are described in Chapter III. Rats of three inbred strains were locally irradiated on different regions of the spinal column with 300 kV X-rays or 15 MeV neutrons. The development of damage was assessed by regular observation of the movements of a rat and by tests for reflexes and muscular strength.

The time elapsing after irradiation until the development of paralysis is called the latent period. In Chapter IV, dose-latent period

relationships are analyzed with respect to the dependence on the region of the cord irradiated, the strain of rats used, the type of radiation and the experimental conditions.

That the induction of paralysis does not reflect a single pathological mechanism is shown in Chapter V. Various types of lesions are observed, depending on the region of the cord irradiated, the dose and the time after irradiation. These lesions are compared with the various syndromes of radiation myelopathy in man.

In Chapter VI, the tolerance of the spinal cord and its relationship to the number of fractions, the dose per fraction and the overall time will be discussed. It is suggested that at least two mechanisms are involved in the development of radiation myelopathy in the cervical cord and that these differ in repair characteristics and in time-dependent recovery. Isoeffect formulas and the restrictions in their application will be discussed and the rat model for spinal cord tolerance will be evaluated with respect to its usefulness for predictions in man.

In the final chapter, the effects of 15 MeV neutrons on the spinal cord tolerance are presented. The histopathological changes are compared with the X-ray induced lesions. The various factors which might contribute to the larger effectiveness of neutrons in the CNS as compared to X-rays are discussed.

CHAPTER II

STRUCTURE OF THE SPINAL CORD

As an introduction to the histopathological studies and the discussion of the cell types which are primarily involved in the development of the various radiation induced lesions, a number of anatomical and histological aspects of the spinal cord will be discussed in this chapter.

2.1 EMBRYOLOGICAL DEVELOPMENT AND ANATOMICAL CHARACTERISTICS

During early embryological development, the nervous system is formed by a longitudinal invagination of the ectoderm, the neural groove, which subsequently closes to form the hollow neural tube. The ependymal lining of the central canal forms a proliferative zone, giving rise to neurons and supporting glial cells. The neurons become arranged around the proliferative ependymal zone, while an outer marginal layer contains the fibers arising from the nerve cells. This spatial relationship is maintained, together with segmental arrangements corresponding with the vertebrae in the adult spinal cord. On transverse section, the central gray matter, containing the neurons, has the shape of the letter H, with dorsal and ventral horns. The large motor neurons are situated in the ventral horns, while the dorsal horns mainly carry sensory functions. The outer white matter contains long myelinated fibers running to and from the brain, while shorter fibers interconnect the segmental units of the cord. A dorsal and a ventral root originate from both sides of a segment of the cord; these unite to form a pair of spinal nerves, each leaving the spinal cord through a vertebral foramen.

In an early developmental stage, the spinal cord extends along the entire length of the spinal column, while the vertebral column of most mammals grows faster than the cord in later stages. Although there are differences among various species of mammals, the anatomical relationships in the adult stage in man are similar to those of the rat, with the spinal cord extending only to the second or third lumbar vertebra (Figure 2.1). Due to this difference in growth rate, the nerve roots

of the lower lumbar and sacral segments of the cord in the adult animals have to descend through the spinal canal before leaving the canal through the corresponding vertebral foramina (Waibl, 1973). Thus, they form a bundle of roots known as cauda equina.

Important differences exist among various species in the ascending and descending fiber systems in the spinal white matter. In man and the higher primates, motor activities are controlled to a larger degree by centers in the brain as compared to "lower" animals such as rodents and carnivores. As an example, the pyramidal system brings spinal motor activity under direct control of the cerebral cortex and is associated with fine digital motor activities. In primates, in contrast to, e.g., the cat, this system shows its most extensive development and a large number of fibers is directly connected with motor neurons. Interruption of the pyramidal tract at a high cervical level produces severe motor defects in primates, whereas only minor defects occur in cats (Kerr, 1975). In addition to functional differences, the locations of various fiber systems running to and from the brain also show great variation among different species (Verhaart, 1970). In Figure 2.2, the different locations of the pyramidal tract in man and the rat illustrating some of these differences are shown. This explains the difference in neurological symptoms as observed in cervical radiation myelopathy in man as compared to the rat, while histologically the lesions are similar (see Chapter V).

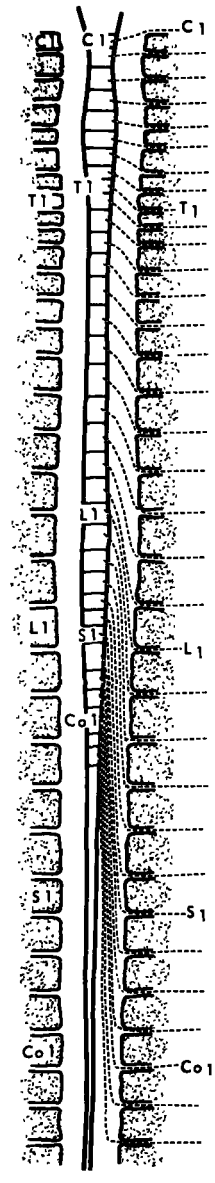

Figure 2.1

Schematic topography of the rat spinal cord, nerve roots and vertebrae.
C = cervical; T = thoracic; L = lumbar; S = sacral; Co = coccygeal (modified from Waibl, 1973).

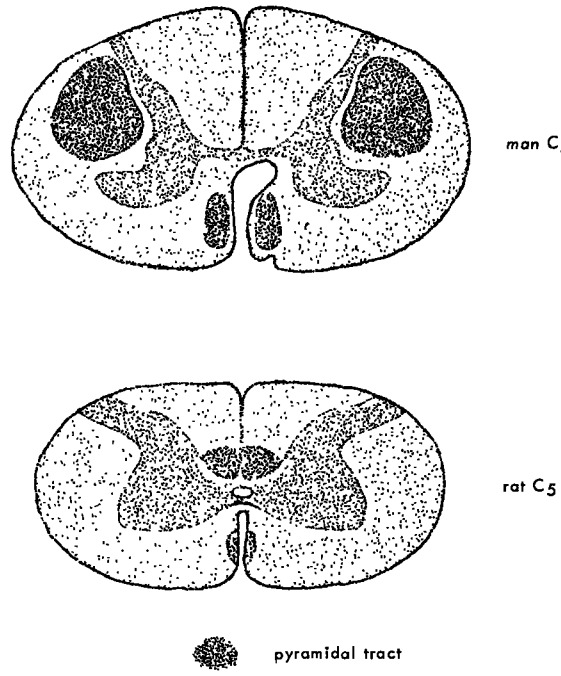

Figure 2.2
Location of the pyramidal tract at spinal cord level C_5 in man and the rat.

2.2 CELL TYPES AND THEIR FUNCTION

One of the aims of this investigation was to determine what types of cells are primarily involved in the development of radiation damage in the nervous system. To provide a basis for the understanding of the histopathological observations, the various cell types will be described, with emphasis on their function and reactions to injury. In the CNS, two main groups of cells, both of neuroectodermal origin, are recognized - namely, the neurons and the neuroglia. In addition, the Schwann cell is the main cell type present in the nerve roots and peripheral nerves.

Most neurons consist of three regions: a cell body (perikaryon) with the nucleus, a number of short dendrites and a single straight axon of considerable length. In general, the dendrites and the cell body are the receptive parts of the neuron, while the axon transmits an impulse toward its terminal branches. The cytoplasm of the peri-

karyon is characterized by so-called Nissl-bodies, which consist of large aggregates of endoplasmic reticulum and ribosomes and which are mainly concerned with the synthesis of proteins. A number of components formed in these actively producing organelles in the perikaryon are transported down through the axon. Most axons are enclosed by a myelin sheath which is interrupted at regular intervals by the nodes of Ranvier.

The oligodendrocyte forms the myelin sheath in the central nervous system (CNS). These sheaths are formed by wrapping a cytoplasmic process around the nerve axon, with spirally deposited membranes which subsequently fuse (Bunge, 1968). A number of internodal myelin segments of adjacent axons are formed by one oligodendrocyte, while the connection between the cell body and the various myelin segments is maintained. For example, in the rat optic nerve, each oligodendrocyte is responsible for the myelination of 35-50 internodes (Peters and Vaughn, 1970).

In the peripheral nervous system (PNS), consisting of spinal roots and peripheral nerves, myelin is formed by Schwann cells. Thin "unmyelinated" fibers are enclosed in troughs of Schwann cell cytoplasm, while the thicker fibers are enclosed by myelin sheaths composed of infolded Schwann cell membranes. An important difference between the PNS and the CNS is that each Schwann cell forms only one internodal segment, which remains enclosed in that cell. This internodal unit is in turn enveloped by a neurilemmal tube composed of a basal membrane and endoneural collagen. This structure is not present around the CNS myelin sheath. A considerable number of Schwann cells are involved in the myelination of one axon. For example, the last lumbar dorsal root in the adult rat has a length of about 40 mm and, with a mean internodal length of 900 µ, more than 40 Schwann cells form the myelin sheath of one axon in this root (Berthold, 1974).

The maintenance of the myelin sheath depends on the metabolic integrity of the supporting cell. A continuous renewal of the different chemical components of myelin takes place, with half-lives varying from 18 days up to more than one year (Smith, 1968). The presence of degenerate myelin within the oligodendroglial cytoplasm, so-called "myelinoid bodies", is thought to represent a morphological expression of myelin turnover (Hildebrand, 1977). Inhibition of RNA and protein synthesis in oligodendroglial cells by Actinomycin D results in extensive destruction of the central myelin sheath within 48 h (Rizzutto and Gambetti, 1976). Schwann cells and oligodendrocytes are not only involved in the maintenance of the myelin sheath, but also actively participate in the selective removal of axoplasmic material in both

normal and diseased nerve fibers (Spencer and Thomas, 1974). This mechanism of selective phagocytosis appears to be a partial expression of the more general phagocytic potential of Schwann cells and oligodendrocytes (Cook and Wisniewsky, 1973).

Astrocytes are irregularly shaped glial cells which occupy the spaces between capillaries, nerve fibers and neuronal cell bodies with their large number of processes. All capillary surfaces are enclosed in astrocytic processes and lamellae, the pericapillary glial sheath (Wolff and Bär, 1976). It is generally assumed that almost all exchange of materials between the blood and the neurons takes place through the astrocytic cytoplasm, thereby providing a protected environment for the neurons. Astrocytic processes are also involved in the isolation of receptive surfaces, e.g., by ensheathment of axon terminals synapsing on large motor neurons.

Another protecting structure of the CNS is the blood-brain-barrier (BBB), which prevents the entrance of proteins and other large molecules from the blood into the CNS. It has long been assumed to be a static mechanical barrier situated in the capillary basal lamina and/or the astrocytic processes. Using tracer substances detectable with the electron microscope, the BBB was shown, however, to be a more dynamic structure, represented by endothelial tight junctions and the low pinocytotic activity of endothelial cells (Reese and Karnovsky, 1967) (Figure 2.3). Transport of metabolic substances across the BBB

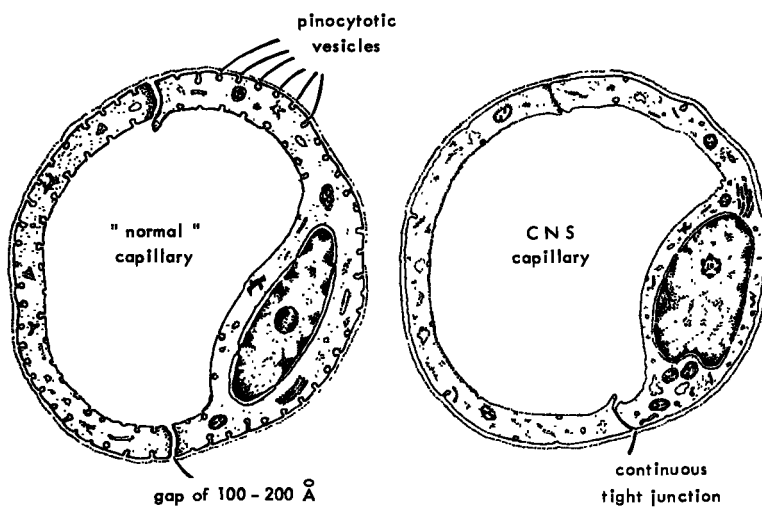

Figure 2.3

The blood-brain barrier.
Morphologically this structure is represented by continuous tight junctions between CNS capillary endothelial cells and the low pinocytotic activity of these cells.

occurs via lipid or carrier mediation. Recently, eigth independent transport systems which can be selectively altered by pathological or toxicological conditions have been described (Pardridge and Oldendorf, 1977). In addition, opening of endothelial tight junctions may occur, for example, by hypertension (Rapaport, 1976), resulting in vasogenic edema due to leakage of proteins.

A third type of glial cells, the microglial cell, is much disputed with regard to its origin and function. In the older literature, its main function was thought to be phagocytic, as a "macrophage" of the CNS, and most authors argued for a mesodermal origin from a perivascular histiocyte (review by Cammermeyer, 1970). In some recent literature, microglial cells are thought to be identical with glial precursor cells or multipotential glia of neuroectodermal origin (Kerns and Hinsman, 1973; Skoff, 1975). These cells might divide and transform into oligodendrocytes or astrocytes or, when necessary, phagocytes.

2.3 REACTIONS TO INJURY

The extent to which glial cells or exogenous cells are involved in phagocytic activity in different types of lesions, has been shown to depend on the degree of trauma (Vaughn and Skoff, 1972; Adrian and Williams, 1973). In highly inflammatory lesions such as stab wounds, most phagocytes appear to be derived from proliferation of blood mononuclear cells. In areas with secondary degeneration peripheral from a lesion (Wallerian degeneration), the phagocytes are predominantly endogenous, resulting from proliferation of glial precursor cells. In less severe chronic lesions, e.g., those resulting from intoxications, phagocytic activity might be restricted to the oligodendrocytes, which have been observed to digest their own myelin under these circumstances (Cook and Wisniewsky, 1973). Mature oligodendrocytes are assumed to be unable to divide or migrate (Blakemore, 1972). Finally, astrocytes also play a role in phagocytosis, but their reaction varies in intensity with different types of lesions. Astrocytes are especially concerned with the repair of lesions, by proliferation and subsequent formation of scar tissue. A schematic representation of the reactions of cells to injury in the CNS is given in Figure 2.4.

It has been suggested that the situation in the peripheral nervous system is comparable to that in the CNS, with a dual source of macrophages dependent upon the type of lesion (Stenwig, 1972). In traumatic lesions such as cutting or crushing of the nerve, many macrophages ap-

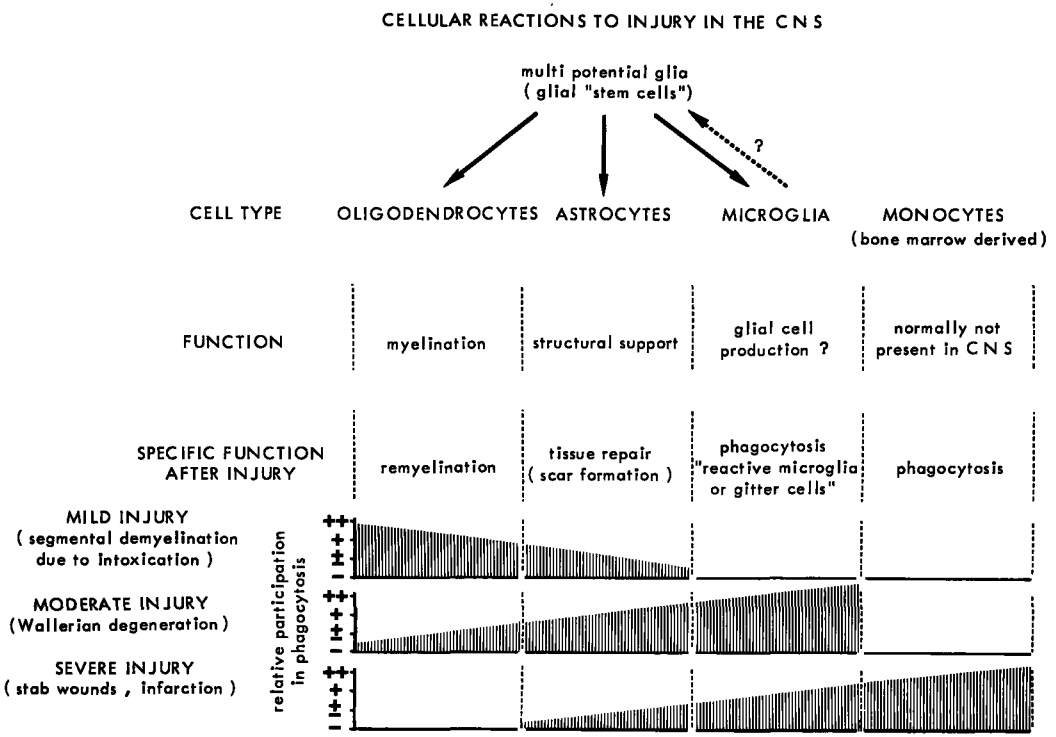

Figure 2.4

Schematic representation of the reactions of glial cells and monocytes to injury in the central nervous system. The relative participation in phagocytosis of the various cell types is indicated by an arbitrary scale for different grades of injury.

pear to be of hematogenous origin, while, in a number of neuropathies, phagocytosis is performed by Schwann cells.

The neurilemmal tube, consisting of a basal lamina and a collagen sheath, is found external to the cytoplasmic membrane of all Schwann cells. This structure is very resistant in all types of lesions and serves as a template for proliferating Schwann cells and regerating axonal sprouts. Whether new Schwann cells arise from preexisting Schwann cells has been questioned by Liu (1973), who showed the development of new Schwann cells from primitive perivascular mesenchymal cells. These cells moved into the neurilemmal tube and subsequently showed the electron microscopical characteristics of Schwann cells, together with a new basal lamina. No neurilemmal tube is present in the CNS, which is thought to be the reason for the very slow or incomplete regeneration occurring in this part of the nervous system after damage. However, in an experimental demyelinating disease of the CNS in mice, remyelination by newly generated oligodendroglial cells has been shown to occur (Herndon et al., 1977). These cells appeared to originate in the area adjacent to the lesion.

2.4 CELL KINETICS

Although the proliferative behaviour of different types of glial cells has been studied qualitatively under various pathological conditions, only few data are available on the cell kinetic parameters in either the normal or diseased nervous system. In the brains of mice and rats, there is a region with a continuous production of glial precursor cells - viz., the subependymal layer of the lateral ventricles. The subependymal cells have a cell cycle time of about 18 hours and an S phase (period of DNA synthesis) of 8.5 hours (Lewis, 1968), which is in the same range as the corresponding values for other somatic cells. However, no specific regions similar to the subependymal layer have been found in other parts of the brain and the spinal cord. More recently, cell kinetic parameters of proliferating glial cells outside the subependymal layer have been reported (Korr et al., 1975). A cell cycle time of 20 hours was established for glial cells and endothelial cells. The fraction of proliferative glial cells is only 0.004 and a constant exchange between this growth fraction and the nongrowth fraction was observed.

In summary, it can be stated that many different types of cells are present in the CNS and PNS, damage of which can be responsible for

loss of function; some of the cells might respond to damage by proliferation in order to restore the integrity of the system. The development of damage by radiation is generally attributed to death of cells during or after mitosis and it can be assumed that the time of appearance of lesions depends on the kinetics of the target cells.

CHAPTER III

MATERIALS AND METHODS FOR STUDIES OF RADIATION DAMAGE IN THE RAT SPINAL CORD

3.1 ANIMALS

Young adult male WAG/Rij rats aged 12-14 weeks and weighing 200-300 g were used in most experiments. The WAG/Rij rats are descendants of an albino Wistar strain obtained in 1953 from the Glaxo Laboratories (Greenford, Middlesex, England). The experiments were performed with the rats in their 35th-45th generation of inbreeding. They were kept under specific pathogen free (SPF) conditions until introduction into the experiments at a young adult stage. Although attempts were made to keep the quality constant, a percentage of rats, fluctuating through the years, suffered from chronic respiratory disease, probably of viral origin. This resulted in some experiments in the death of 10-20% of the rats at ages in excess of one year, due to severe cyanosis and weight loss.

Because studies of CNS damage require observation times of 12-18 months, a long life-span of the animals is a requirement for optimal studies. The mean life-span of male WAG/Rij rats is 21.5 months with a maximum observed at 33 months (Hollander, 1976). In one experiment, 9-month-old rats were irradiated to compare the threshold dose for the induction of paralysis with that of 3-month-old rats. These rats could be followed-up without problems for at least 12 months after treatment.

Due to the long time period of inbreeding, the rats can be regarded as genetically homogeneous, minimizing the individual variations in reactions to experimental conditions and treatments.

To study the general validity of the results obtained, at least for the species, two other strains were used in some comparative studies. The BN/Bi is a Brown Norway strain obtained from Microbiological Associates Ltd. (Bethesda, Maryland, USA) in 1963; the rats were used from about the 20th generation of inbreeding. The third strain used is the (WAG/Rij x BN/Bi)F_1 hybrid.

Groups of 5 rats were housed in Makrolon polycarbonate cages (38 x 25 x 15 cm). Water and food pellets (Hope Farms, Woerden) were available ad libitum.

3.2 ANESTHESIA

For local irradiation of the spinal cord, the animals were anesthetized; for most experiments, this was achieved by intraperitoneal (i.p.) injection of Nembutal (sodium pentobarbital, 60 $mg.kg^{-1}$) which resulted in deep anesthesia lasting for 1-2 hours. For low dose rate experiments, this period is too short. Therefore, a combination with a potentiating drug was used. An injection of cloramphenicol (100 $mg.kg^{-1}$) was followed 10 minutes later by a reduced dose of Nembutal (45 $mg.kg^{-1}$). It has been shown (Adams, 1970) that chloramphenicol prolongs the anesthetic action of pentobarbital in rats by a factor of 2-3 and, in mice, even up to a factor of 35, by inhibition of the metabolism of the barbiturate in the liver. In the present experiments, prolongation by a factor of 2-4 was observed; this was adequate for continuous irradiation during 8 hours.

It is of interest to inquire whether the experimental results are influenced by the action of pentobarbital on the respiratory and cardiovascular systems. Especially a local decrease in oxygen tension might lead to a reduced effect of radiation. Zeman (1966) reported a threefold increase in oxygen tension as recorded in the ventral gray horn of the spinal cord when rats breathed a mixture of 95% O_2 + 5% CO_2 instead of air for 15 minutes. Therefore, experiments were performed with rats breathing 95% O_2 + 5% CO_2 from 20 minutes before to 5 minutes after irradiation, to study the possible effects of higher oxygen tensions.

More recently, a semiclosed-circuit inhalation system, employing the volatile halogenated anesthetic halothane, was developed (Figure 3.1). The use of inhalation anesthesia has the advantage of a controllable depth and duration time, followed by a rapid awakening. In a report on halothane anesthesia in rats (Kaczmarczyk and Reinhardt, 1975), a mixture of 99% O_2 + 1% halothane was recommended. This caused a 400% increase in arterial oxygen tension and about a 25% increase in arterial carbon dioxide tension. No respiratory depression was observed and no rats died during a 6-hour period. However, in our experiments, this 6-hour period was observed to be critical, because some rats had respiratory arrest necessitating thoracic massage for resuscitation in the 7th hour. During 3 subsequent days, the same rats could be anesthetized for a maximum period of 6 hours/day without respiratory arrest.

Ethrane, a drug related to halothane, was used in some experiments. It has all the advantages of halothane (Price, 1975); however, its biotransformation is reported to result in a reduced amount of

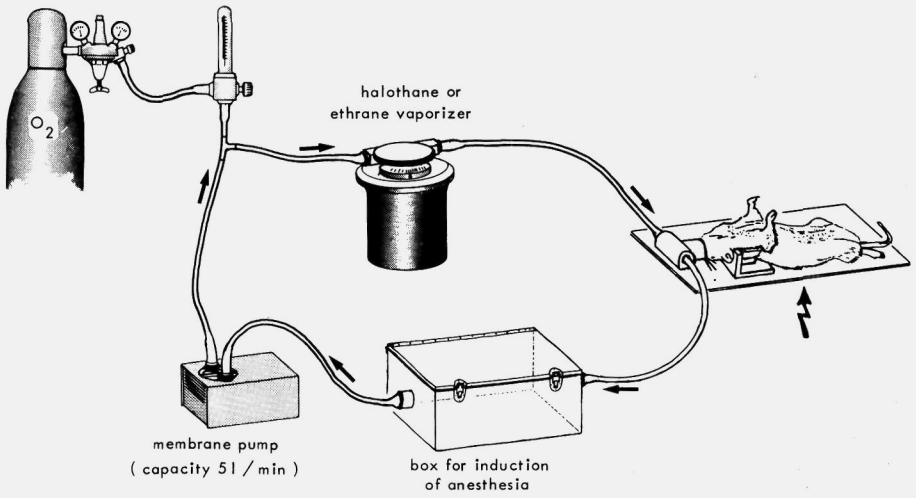

Figure 3.1

Circuit for inhalation anesthesia with halothane or ethrane. O_2 is added at a rate of 0.3 l/min to prevent buildup of CO_2.

hepatotoxic metabolites, while it causes no respiratory depression. This method appeared to be promising for a long period of anesthesia with spontaneous respiration. However, a disadvantage could be the high serum level of inorganic fluoride, which might lead to nephrotoxicity (Mazze et al., 1977).

In conclusion, three methods of anesthesia were used to evaluate possible side effects, particularly a decreased oxygen tension. Pentobarbital was routinely used; however, especially in low dose rate and multifractionation experiments requiring prolonged or repeated periods of anesthesia, ethrane-oxygen inhalation is favored.

3.3 IRRADIATION TECHNIQUES AND DOSIMETRY

3.3.1 X-rays

Irradiations were carried out with a Philips-Müller X-ray generator operated at 300 kV, 10 mA. With an added filter of 1 mm Cu, a half-value layer (HVL) of 3 mm Cu was obtained. The dose rate was 3

$Gy.min^{-1}$ (300 $rad.min^{-1}$) at a focus to skin distance (FSD) of 20 cm. In one experiment, the dose rate was reduced to 0.065 $Gy.min^{-1}$, at a FSD of 1 m. Groups of at least 5 rats were used at each dose level. The anesthetized rats were placed on a 4 mm thick horizontal lead shield. In an initial series of experiments, lumbar vertebrae 2-5 (L2-L5) were irradiated from the lateral side through a circular hole of 25 mm diameter in the lead shield. A 2 cm wide plastic clip was fitted around the back of the rat just behind the last rib. This clip was lined up with the hole, resulting in a reproducible localization and providing the advantage of pushing kidney and intestinal loops outside the radiation field (Figure 3.2). The rats were turned 180 degrees halfway through each exposure, in order to obtain a homogeneous dose distribution in the spinal column.

As illustrated in Figure 2.1, region L2-L5 of the vertebral column contains the last part of the lumbosacral spinal cord and the first part of a bundle of nerve roots, the so-called cauda equina. This anatomical situation is similar to that in man. Most nerve roots of this region are running to and from the hind legs, but the cell bodies of the motor nerves, the large ventral horn neurons, are situated more rostrally and outside the field of radiation. In histopathological studies, the main aspect of the radiation-induced lesions was found to be degeneration of the nerve roots (Chapter V). This radiculopathy differed essentially from the radiation myelopathy as commonly described for the cervical/thoracic region of the spinal cord in man. Therefore, two other regions of the rat spinal cord were also studied. In a few experiments, an adjacent area, region T12-L2, containing the lumbar enlargement of the spinal cord was irradiated. Most of the cell bodies of the nerves which supply hind legs, bladder and rectum are situated in this region. Irradiations were carried out from the lateral side with a rectangular field of 15 x 20 mm^2 (Figure 3.3).

The third region that was irradiated in a number of experiments, C5-T2, contains the cervical enlargement of the spinal cord. The neck region of the rats was irradiated from the dorsal side with a rectangular field of 15 x 20 mm^2 (Figure 3.4). The anterior boundary of the field was at a distance of 5 mm from the caudal edge of the skull.

The absorbed doses were measured with a Baldwin Ionex ionization chamber using a R/Gy conversion factor of 0.96×10^{-2}. To estimate the absorbed dose inside the spinal canal, thermoluminescent dosimetry was performed. A number of LiF rods (LiF-700 rods - Harshaw Chemie N.V., De Meern, The Netherlands) of 1 mm diameter and a length of 6 mm in a vinyl tube were inserted into the spinal canal of a sacrificed rat and

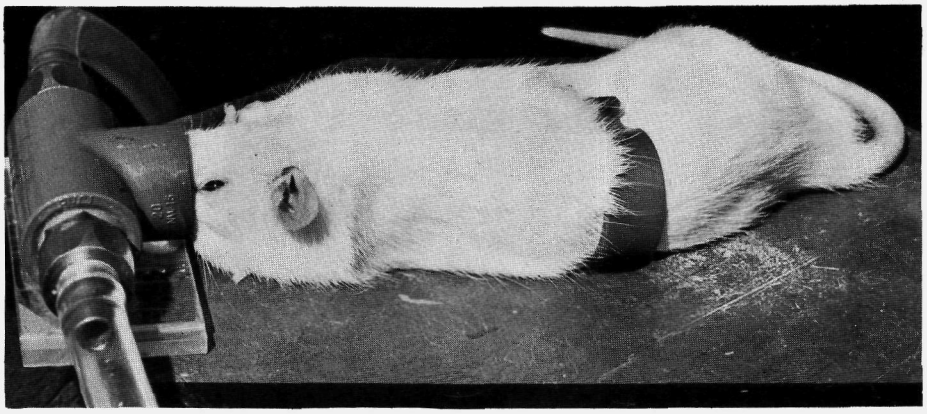

Figure 3.2

Experimental arrangement for irradiation of region L2-L5.

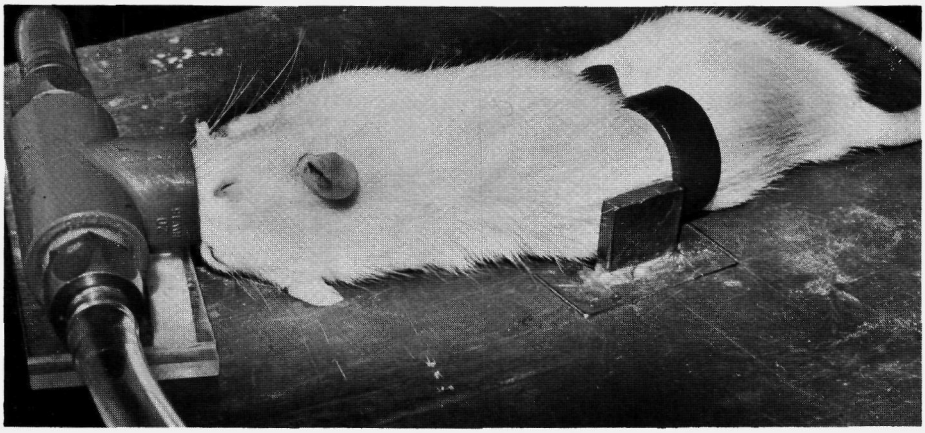

Figure 3.3

Experimental arrangement for irradiation of region T12-L2. The plastic clip marks the caudal edge of the radiation field.

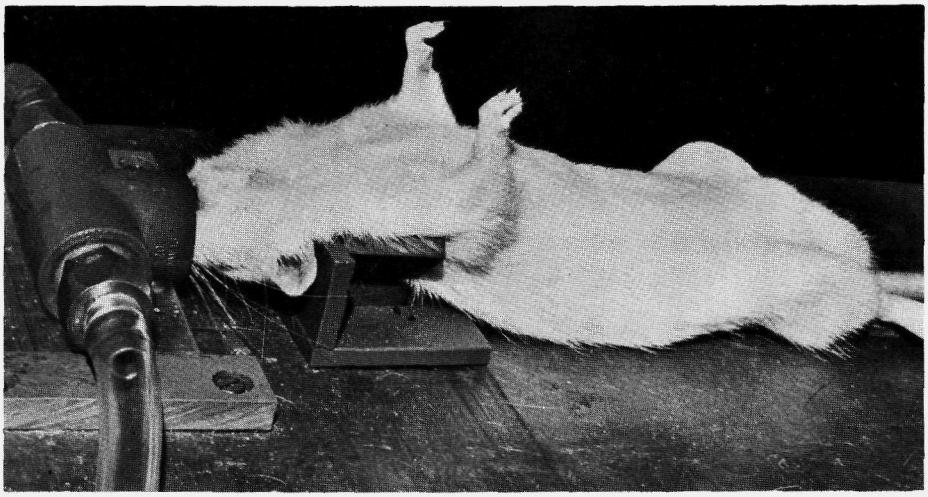

Figure 3.4
Experimental arrangement for irradiation of region C5-T2.

irradiated (Figure 3.5). Doses were obtained with a Harshaw TLD reader. These experiments gave information on the dose distribution in the spinal canal inside and outside the field. The dose was reduced to 3-5 percent of the central dose at a distance of 10 mm outside the beam behind the shielding. In the cervical region, absorbed doses were also measured inside the esophagus, because this organ together with the trachea is situated in the direct vicinity of the vertebral column. The dose in these organs was found to be equal to about 90% of the spinal cord dose.

In some experiments in which region L2-L5 was irradiated with single doses of 60 Gy or more, damage to the skin was expected to be very severe and this would certainly interfere with the health of the animal during the latent period before spinal cord damage was observed. Therefore, the skin was incised and retracted from the radiation field. Skin and underlying muscle were prevented from dehydration by a cover of gauze soaked in physiological saline. After irradiation, the skin was sutured back over the irradiated area and healing was uneventful in all animals.

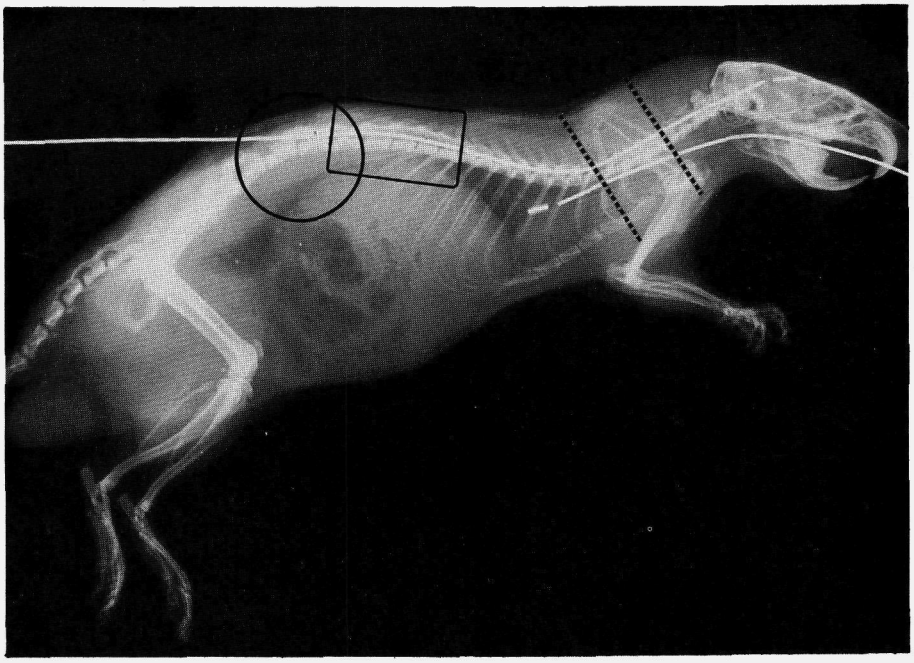

Figure 3.5

Radiograph showing tubes inside the spinal canal and the esophagus of a sacrificed rat. For thermoluminescent dosimetry, LiF rods can be inserted into the tubes. The three radiation fields are indicated.

3.3.2 Neutrons

15 MeV monoenergetic neutrons were produced with a Texas Nuclear neutron generator by bombardment of a tritium target with 270 keV deuterons at a current of 3-5 mA. The anesthetized rats were placed behind a steel collimator of 35 cm thickness containing 10 horizontal circular holes of 25 mm diameter. Using the plastic clip for alignment, approximately the same region of the lumbar spinal column was irradiated as in the X-ray experiments. Most of the rats irradiated in the cervical region died within 2 months due to infections with the characteristics of Pneumocystis carinii pneumonitis, which was not observed in any other experiments.

The absorbed doses were determined with tissue-equivalent (A-150 plastic) ionization chambers (Broerse and Barendsen, 1967). With an argon flushed Magnox chamber, which has a low neutron sensitivity, the

gamma component of the total dose was determined to be 3-4% (Zoetelief and Broerse, personal communication). Additional measurements with a Geiger-Müller counter confirmed this latter result.

According to the protocol for neutron dosimetry for radiobiological and medical applications (Broerse, editor, 1976) the absorbed neutron dose is specified in muscle tissue (ICRU, 1977). Therefore, the dose measured in A-150 tissue equivalent plastic is corrected with the ratio of kerma in muscle to the kerma in A-150 plastic. However, absorbed doses may differ in various tissues due to differences in elemental composition. The hydrogen content of the tissue is of most importance, since for the neutron energies used in radiotherapy the largest part of the dose is deposited by recoil protons. The elemental composition of rat brain and spinal cord and the kerma values are compared with the human brain, spinal cord and muscle in Table 3.1. These data show that no large differences exist between the composition of human and rat brain and spinal cord, and that the kerma values for these tissues are only 1.5-3% higher than the kerma for muscle. The neutron beam is less well collimated as compared with X-irradiations.

TABLE 3.1

ELEMENTAL COMPOSITION AND KERMA FACTORS OF A-150 TISSUE EQUIVALENT PLASTIC AND SOME HUMAN AND RAT TISSUES

compound or tissue		percent elemental weight H	C	N	O	rest*	kerma for 14.5 MeV neutrons (10^{-10} Gy.cm^2)	reference
A-150		10.1	77.6	3.5	5.2	3.6	.689	ICRU 1977
muscle	man	10.2	12.3	3.5	72.9	1.1	.661	ICRU 1977
brain	man	10.7	12.1	1.3	71.4	4.5	.679	ICRP, 1975
brain	man	10.4	16.1	3.9	68.4	1.2	.672	Kim, 1974
spinal cord	man	10.6	19.2	3.7	65.0	1.5	.682	Kim, 1974
brain	rat	10.6	13.8					**
spinal cord	rat	10.5	20.8	2.1	63.2	3.4	.676	**

* The main other elements are Na, Mg, P, S, Cl, K, Ca. For the calculation of kerma values for brain and spinal cord a mean kerma of 0.12 x 10^{-10} Gy.cm^2 is taken for these rest elements. Kerma values for A-150 and muscle are from ICRU 1977.

**Element analyses of rat spinal cord and brain (only C and H) were carried out by the Element Analytical section of the Institute for Organic Chemistry TNO, Utrecht, The Netherlands under supervision of W.J. Buis.

The dose was reduced to 15-20 percent of the central dose at 20 mm from the boundary. The dose rate varied from 0.03-0.2 Gy.min^{-1}, depending on ion current and target condition.

3.4 ASSESSMENT OF DAMAGE

The rats were weighed and examined every two weeks, but this was extended to daily examination when they showed signs of sickness or were expected to develop paralysis within a short time interval. This procedure resulted in less than 1% loss of animals due to unexpected deaths.

Changes in neurological status were scored by observing movements of a rat inside the cage or on a smooth surface and by simple tests for reflexes and muscular strength. Also the development of muscular atrophy and urinary incontinence was noted. The types and progression of signs showed differences related to the region of the cord irradiated and to the distribution and severity of the lesions within a particular region.

Different grades in the development of damage were scored according to signs of increasing severity and depending on the region irradiated.

3.4.1 Region L2-L5

Irradiation of this region resulted in a marked muscular atrophy of the hind legs and this was scored separately from the development of paralysis. Muscular atrophy was usually the first sign of damage, although dependent on the dose and type of radiation. Four stages were distinguished:

1. Absence of detectable atrophy;
2. Slight but distinct atrophy, generally starting with muscles of the lateral part of the thigh. Reduced general muscular tension;
3. More generalized atrophy, with strongly reduced muscular tension;
4. Severe atrophy of both hind leg and hip musculature.

Impairment of motor function and other neurological signs were scored separately as follows:

$\pm$ When rat is walking on a smooth surface, the feet tend to turn outwards. After lifting the rat by the tail, the feet are not immediately placed in the normal position upon contact with the surface.

+ Definite weakness and impaired use of the hind legs. Fasciculations of the toes when rat is lifted by the tail;

++ Severe paresis. Reduced reaction to pressure and pain stimuli applied to the feet.

+++ Paraplegia, usually with urinary incontinence.

When not sacrificed, rats in the last stage (+++) died from infections associated with urinary incontinence. However, from the first experiments on, it was found that, beyond stage ±, the lesions always developed progressively. Therefore, stage + was used as the endpoint in the determination of the latent period and the tolerance doses. The rats were subsequently killed for histopathological studies.

The relation between the degree of muscular atrophy and the neurological status depends on the dose and type of radiation. For example, after irradiation with fast neutrons or with high doses of X-rays, the progression in severity of the neurological signs is much more rapid than the development of muscular atrophy (see Chapter IV).

3.4.2 Region C5-T2

In contrast to the radiculoneuropathy developing in the lumbosacral region, the lesions in the cervical region represent a definite myelopathy. Although variation in symptoms depending on the distribution and extent of the lesions inside the irradiated area was observed, the progression of damage was scored according to specific signs of increasing severity. The following grades were distinguished:

± Slight ataxia of the forelegs. Sporadic dragging of feet;

+ Regular dragging of feet with palmar flexion or dragging of extended forelegs. When lifted by the tail, reduced ability to walk on forelegs or to hold unto the edge of the cage;

++ Monoplegia, with usually the leg flexed at the knee joint and the toes clenched;

+++ Both forelegs severely paralyzed, with ataxia of the hind legs in some animals.

In contrast to signs in the lumbosacral region, palpable muscular atrophy does not accompany the developing myelopathy after irradiation of C5-T2, indicating that the primary lesion is not situated in the nerve roots, but in the spinal cord itself.

Most lesions were observed to be progressive, although the rate of development is dose-dependent and also differs markedly for various syndromes (see Chapter V). In determining the latent period and toler-

ance dose levels, stage + was employed as the endpoint and the animals were subsequently killed for histopathological studies.

3.4.3 Region T12-L2

A specific scoring system was not developed for this region because of the small number of animals involved in these experiments. The first signs of neurological damage were slight ataxia and a reduced strength of the hind legs. The tension of the hind leg muscles was strongly reduced. Within a few weeks, these symptoms progressed to severe paresis, while muscular atrophy was minimal in contrast to region L2-L5.

3.5 HISTOPATHOLOGY

Rats were anesthetized with Nembutal and 15 mg heparin was injected into the femoral vein. After about 5 minutes, the thorax was opened and a catheter was inserted through the left ventricle into the aorta and fixed in position with a ligature. The right atrium was then incised to allow drainage of blood and perfusate. Following a rinse with physiological saline for about 1 minute, fixation was started by perfusion with phosphate buffered 10% formalin. Standard clinical infusion sets were used, with bottles at a height of 120-150 cm. Generally, 2 out of 5 rats of the same experimental group were fixed with Bouin's fluid, resulting in minimal tissue shrinkage after processing and in excellent fixation, especially of nuclei. After 15 minutes of perfusion, the spinal column was dissected out and immersed in fixative for at least 2 days.

An 8 cm long portion of the spinal column containing the irradiated part in the center was decalcified in 100 ml of a mixture of 8 N formic acid and 1 N sodium formate in a continuously rotating jar. After dehydration and embedding in paraffin, 6 µm transverse or longitudinal sections were prepared from successive 5 mm blocks of spinal column. Routine staining was performed with hematoxylin-phloxine-saffron. Additional staining methods included luxol fast blue-PAS for normal and degenerating myelin, martius scarlet blue for hemorrhages and fibrin deposits and Van Gieson for elastic fibers.

CHAPTER IV

DOSE-LATENT PERIOD RELATIONSHIPS AND THRESHOLD DOSES: EFFECTS OF INTRINSIC AND EXTRINSIC VARIABLES

4.1 INTRODUCTION

For the assessment of early damage in tissues with rapid cell turnover such as skin, the hemopoietic system and the gastrointestinal tract, quantitative scoring techniques based on repopulation of stem cells have become available (Chapter I). However, these techniques are not applicable to organs, in which cellular turnover occurs at a low rate. In tissues such as the liver, kidney and lung, impairment of function has been assessed by physiological techniques (Hopewell and Berry, 1975; Chauser et al., 1976), while, in a number of radiobiological studies, the death of the animal has been used as an endpoint (Field et al., 1976). The specificity of this endpoint depends on whether the sequences of events leading to death are directly related to damage to a particular organ.

4.1.1 The latent period

For the spinal cord, a specific and reproducible endpoint is the development of paralysis due to impairment of one of its functions - namely, the initiation and coordination of motor activity. By observation of movements of the animal and with simple tests for muscular strength and reflexes, the progression of damage can be assessed by a scoring system for symptoms of increasing severity (Chapter III). A defined stage in the development of damage is then used for the determination of the latent period as a function of the dose. The highest dose at which no paralysis develops is defined as the experimental threshold dose for this effect and it can be derived from dose-latent period curves. The true threshold may be slightly higher than the experimental threshold. Analogous to the concept used in radiotherapy, tolerance doses (TD) are derived from dose-incidence curves and have to be defined on the basis of a fixed percentage of paralyzed rats, e.g., TD_5 or TD_{50} (Chapter VI).

The determination of the latent period is based on the observation of definite neurological symptoms, which are expressions of certain stages in the development of the lesion, while providing no information on the pathological character of that lesion. However, the observation of changes in the length of the latent period might be regarded as a reflection of changes in the kinetics of the development of a particular lesion. This enables a comparison of the effects of extrinsic as well as intrinsic variables on the relationship of the dose of radiation and the length of the latent period. Experiments have been performed on three different regions of the spinal cord, with as intrinsic variables the genetic constitution (involving three inbred strains) or the age and, as extrinsic variables, the type of radiation (high LET versus low LET), dose rate, dose fractionation, the anesthetic agent and the oxygen concentration.

The dose-latent period relationships are mainly presented for experiments with single doses, in order to exclude complicating factors such as repair and repopulation. The effect of the dose rate or dose fractionation on the tolerance level is discussed in Chapter VI.

4.2 GENERAL OBSERVATIONS

Both the irradiated rats and the controls were weighed at regular time intervals. The relative increase or decrease in weight can serve as an indicator of the general condition of the animal and reflects whether damage is present in other organ systems outside the spinal cord during the latent period of the development of paralysis. The extent to which other organs are damaged depends on the region of the vertebral column irradiated and on the dose distribution characteristics of the beam. Since the type and progression of the neurological symptoms are also related to the spinal cord level, the effects observed in different regions are presented separately.

4.2.1 Region C5-T2

In irradiations of the neck area from the dorsal side, a 15 mm segment of the esophagus and trachea are also included in the field. Because of the sharp boundaries of the X-ray beam, tissues directly outside the beam such as the lungs, thyroid and salivary glands receive only a small percentage of the total dose. The decrease in

weight (Figure 4.1) during the first week after irradiation is due to esophageal damage. Total restoration is accomplished within 20 days after irradiation with single doses of up to 45 Gy of X-rays. This is indicated by a rapid increase in weight. The weight curve is subsequently parallel to that for the unirradiated controls as shown in Figure 4.1. Obviously, the X-ray induced early esophageal lesions do not interfere with the later development of spinal cord damage. Signs of tracheal damage were never observed.

With 15 MeV neutrons, 15-20 percent of the dose is deposited in the penumbra region at 20 mm outside the boundary of the main beam, involving large parts of the lungs. A large percentage of the neutron irradiated rats died after 30-40 days from severe lung disease, with the pathological characteristics of a viral or Pneumocystis carinii infection but without signs of radiation pneumonitis. These infections are probably the result of a local decrease in resistance, presumably due to irradiation of the bronchial lymph nodes. The few data obtained from the surviving rats are presented in Chapter VII on the effects of fast neutrons.

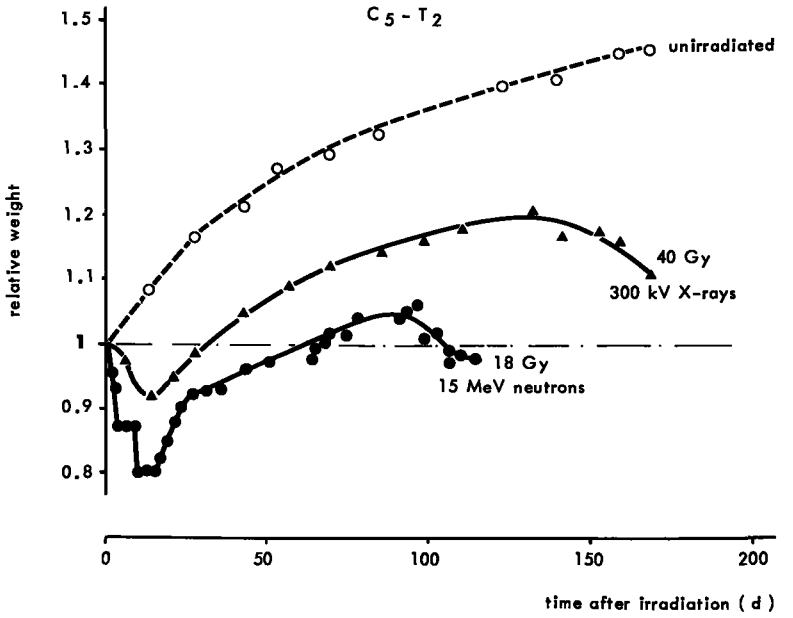

Figure 4.1

Weight relative to weight at day of irradiation of region C5-T2 of 13-week-old male WAG/Rij rats. Symbols represent the mean value for five animals. Standard deviations were less than 3%.

With doses above 19 Gy of X-rays, neurological symptoms develop after a latent period, the length of which is dose dependent (see section 4.3). The symptoms are scored according to the system described in Chapter III. Progression from stage ± to stage ++ or +++ occurs within 2 to 3 weeks (defined as subacute). For the determination of the length of the latent period, stage ± or + was used as the endpoint and the rats were then usually killed for histopathological studies.

After doses in the range of about 17-19 Gy (see section 4.3), differences in progression of symptoms are observed in comparison with doses in excess of 19 Gy. The lesions are mainly characterized by vascular damage, in contrast to the lesions induced at higher doses (Chapter V). The length of the latent period for this vascular syndrome is much longer and shows great variability. The neurological symptoms range from an acute paralysis developing in 1 or 2 days to a chronic progressive type which may take months to develop. In a few rats with slight impairment of motor function, the symptoms were even observed to disappear; this recovery was later confirmed by the observation of scarred lesions in the cord.

4.2.2 Region L2-L5

Irradiation of this region of the vertebral column with X-rays does not lead to damage in other vital organs, with the exception of a small part of the left kidney, which is situated close to the edge of the radiation field. Partial damage in one kidney is not likely to interfere with the health of the animal (Phillips and Ross, 1973). In addition, the latent period for the development of radiation damage in the kidney is approximately of the same magnitude as observed for the spinal cord (Madrazo, 1976; Chauser et al., 1976). The weight curves obtained for rats irradiated with single doses of up to 100 Gy of X-rays do not differ significantly from that for the control rats (Figure 4.2). The curves start to deviate from the control curve shortly before or concurrently with the development of neurological symptoms. During irradiation with single doses in excess of 50 Gy, the skin was surgically retracted in order to avoid severe ulceration and necrosis. As discussed for the cervical region, with 15 MeV neutron irradiation a significant part of the dose is dissipated outside the direct beam. Although with single doses of up to 22 Gy the rats did not die during the latent period, the reduced increase in weight (Figure 4.2) indicated that subclinical damage was present in other organs, probably mainly in the intestinal tract.

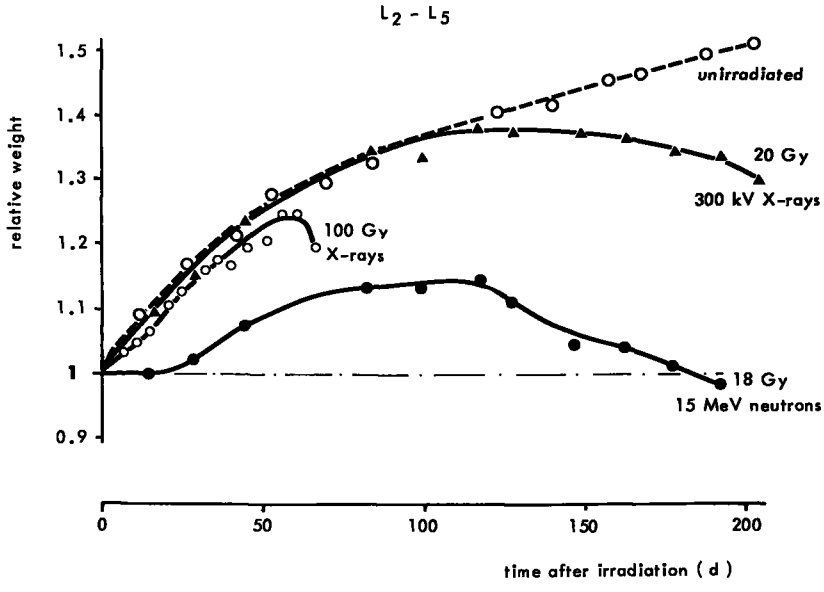

Figure 4.2

Weight relative to weight at day of irradiation of region L2-L5 of 13-week-old male WAG/Rij rats. Symbols represent the mean value for five animals. Standard deviations were less than 3%.

For region L2-L5, the development of muscular atrophy of the hind legs is scored separately from other neurological symptoms, as described in Chapter III. This separate scoring has been employed mainly for rats irradiated with doses of up to 30 Gy of X-rays, in which the development of considerable muscular atrophy (grade 3) precedes the first symptoms of paresis. The muscular atrophy can be attributed to a slowly progressing radiculopathy, i.e., nerve root degeneration, resulting in an increasing number of denervated muscle fibers which subsequently become atrophic. Only in an advanced stage of denervation with involvement of a number of muscle groups is paresis of the hind legs observed. Beyond this stage, the lesion is always progressive and, if not killed, the rats become incontinent and die from urinary tract infection. With doses from 30-60 Gy of X-rays, the radiculopathy develops more rapidly and, at stage + or ++, the muscular atrophy has advanced only to stage 2 or 3. With doses of 80 and 100 Gy of X-rays, the neurological symptoms represent an acute radiculomyelopathy, with paralysis developing within a few days after latent periods of 2 to 3 months, while, because of this short time-course, muscular atrophy is not observed.

After irradiation with doses in the range of approximately 15-19 Gy of X-rays, minor symptoms of denervation, starting at about one year postirradiation, are observed in most rats. This represents a chronic degenerative lesion. These lesions are markedly different from those induced with higher doses and show similarities with age-related changes (see Chapter V).

In approximately 25% of the rats irradiated with doses below 19 Gy, tumors (mostly osteogenic or undifferentiated sarcomas) developed in the irradiated bone or muscle after a latent period of about 1-1½ years. In a number of rats, these tumors caused paralysis by invasion or compression of the spinal cord (Figure 4.3).

4.2.3 Region T12-L2

Because of the totally different types of damage induced in regions C5-T2 and L2-L5, a separate experiment was performed on region T12-L2 with WAG/Rij rats. This region contains the lumbar enlargement of the cord, where the large motor neurons, which are the origin of the nerves running through region L2-L5 to the hind legs, are situated. The weight gain of the rats irradiated on T12-L2 was similar to that of the controls. The development of paralysis was markedly different as compared to L2-L5, with strong ataxia, a rapid impairment in motor function and decreased reactions to sensory stimuli. This indicated the involvement of the spinal cord instead of only the nerve roots as observed for L2-L5.

4.3 DOSE-LATENT PERIOD RELATIONSHIPS

4.3.1 Region L2-L5

The relationship between the dose and the latent period as derived for three strains is presented in Figure 4.4. The most complete curve is obtained for WAG/Rij rats, while experiments with BN and F_1 rats were performed only for selected dose ranges. No attempt was made to determine the threshold dose in the latter strains. With increasing doses of up to 18 Gy, no symptoms of progressive radiculopathy are observed during the lifespan of the rat. Thus, a dose of 18 Gy represents the threshold dose for this syndrome.

Figure 4.3

Spinal cord compression by radiation induced sarcomas.

a. Osteogenic sarcoma in a cervical vertebra, 310 days after 87 Gy X-rays (60 fractions/40 d) (HPS, x 12)

b. Pleomorphic sarcoma invading through foramen of a lumbar vertebra, 430 days after 24 Gy X-rays (2 fractions/1 d) (HPS, x 21)

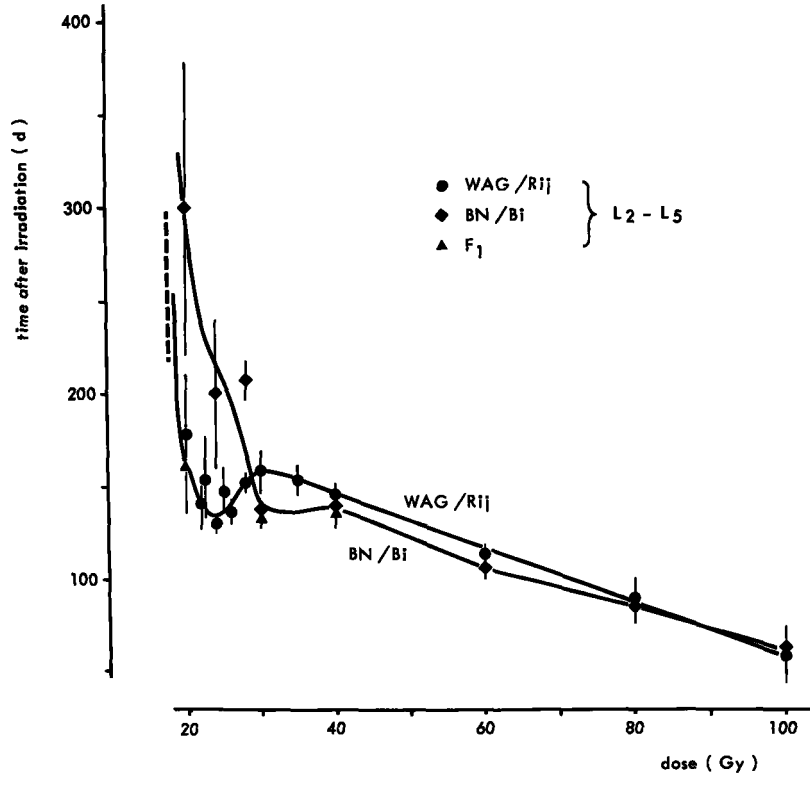

Figure 4.4

Relationship between dose and latent period for the induction of hind leg paresis after irradiation of region L2-L5 of male WAG/Rij, BN/Bi and F1 rats. Each point represents the mean ± standard deviation of at least five animals. The vertical dotted line represents the experimental threshold, the highest dose at which no animals showed signs of paresis.

A large divergence in latent period is observed for doses in the range of 19-21 Gy. This is partly a result of the slow progression of the lesions in this dose range, which leads to some difficulty in the unambiguous estimation of the endpoint. With higher doses, the standard deviation is small. On the basis of the shape of the curve, two parts can be distinguished. The region between 20 and 30 Gy shows a minimum value at about 24 Gy and the latent period is significantly longer at 30 Gy. For BN rats, the precise shape of the curve is determined with less accuracy in this dose region, although it is clearly

different from the WAG/ Rij strain. More information on the pathological basis of this phenomenon is obtained from serial killing experiments, to be presented in Chapter V.

The other part of the curve, between 30 and 100 Gy, is linear within the limits of error and shows a continuous decrease in latent period with increasing dose. In this dose region, the latent periods for WAG/Rij and BN rats are closely similar.

In Figure 4.5, data obtained under three conditions are presented: 1) nembutal anesthesia; 2) nembutal anesthesia with breathing of 95% O_2 + 5% CO_2; 3) inhalation anesthesia with 100% O_2 and halothane . The latent periods and the threshold dose did not differ significantly for either of the conditions.

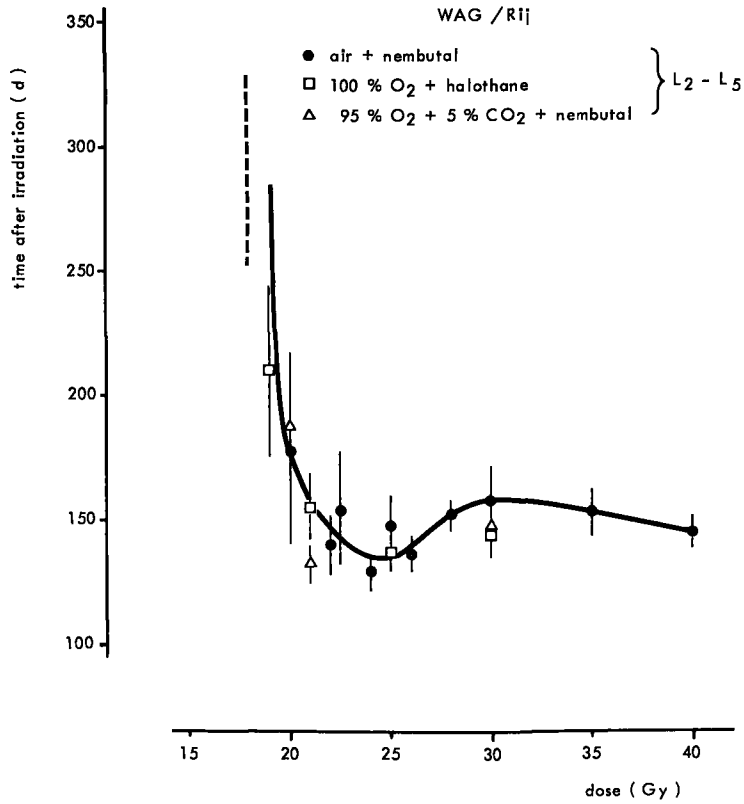

Figure 4.5

Dose-latent period relationships for region L2-L5 of male WAG/Rij rats. Comparison of different anesthetic agents and oxygen concentrations. Further details see Figure 4.4.

In Figure 4.6, the effect of X-rays is compared with that of fast neutrons. The curves differ in two aspects. The threshold dose for neutrons is approximately 3 Gy lower than the value of 19 Gy for X-rays. Secondly the latent periods observed for neutrons are significantly shorter than for X-rays. This latter difference is even greater with fractionated irradiation (see Chapter VII). For X-rays, no significant difference in latent period is observed after fractionated as compared to single doses.

The last variable studied was the influence of the age of the rats at the time of irradiation on the threshold dose level. No shift in threshold dose was observed for rats irradiated at the age of 9 months as compared to irradiated 3-month-old rats.

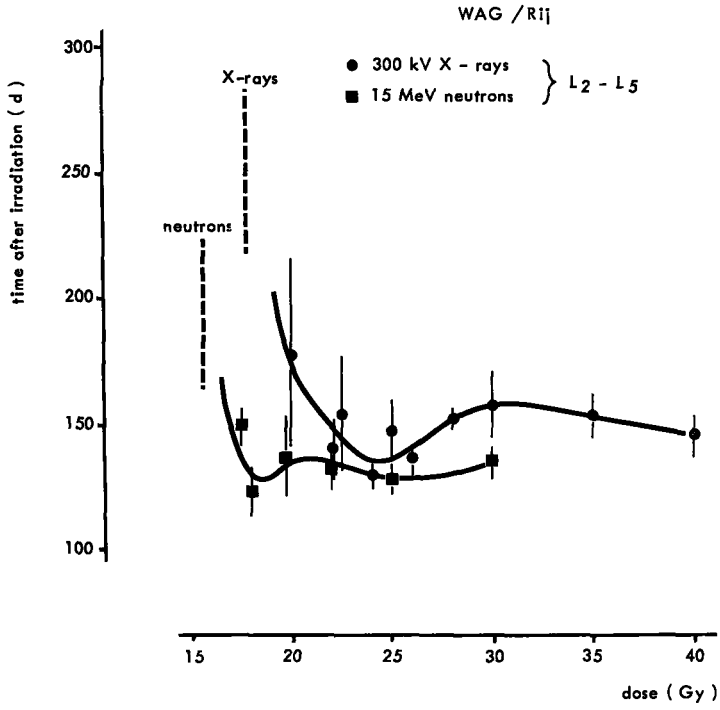

Figure 4.6

Dose-latent period relationships for region L2-L5 of male WAG/Rij rats. Comparison of 300 kV X-rays and 15 MeV neutrons. Further details see Figure 4.4.

4.3.2 Region C5-T2

As mentioned in section 4.2.1 of this chapter, after doses below 20 Gy of X-rays, mainly vascular lesions are induced and these vary greatly in extent and time of onset. Latent periods observed for this syndrome vary from 7 months to more than one and one-half years, which

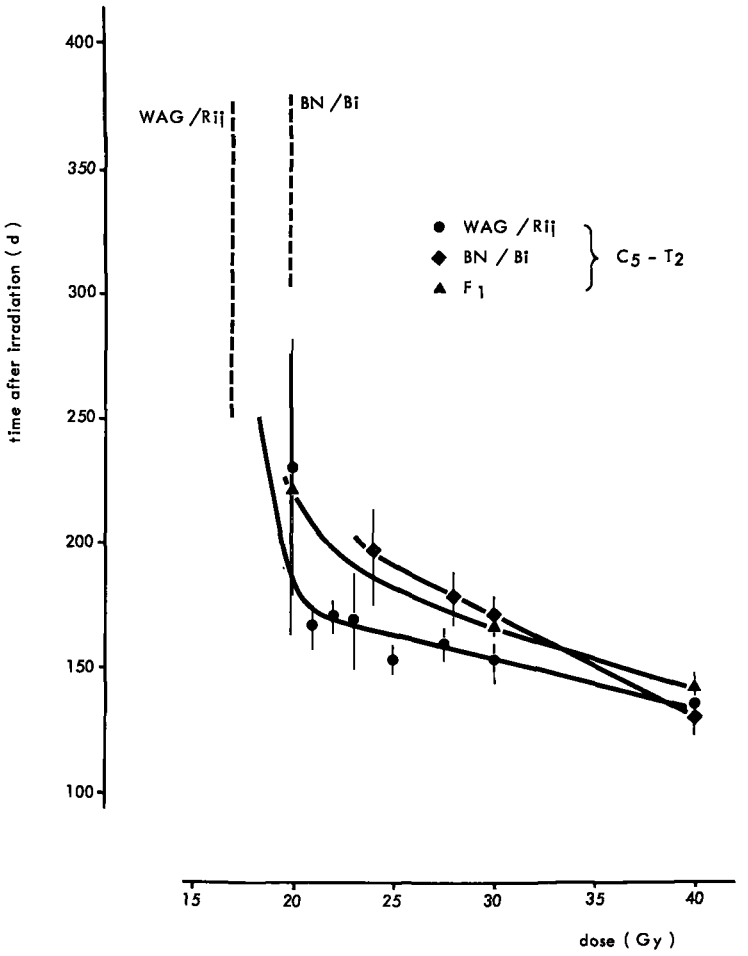

Figure 4.7

Dose-latent period relationships for the induction of foreleg paralysis after irradiation of region C5-T2 of male WAG/Rij, BN/Bi and F1 rats. Further details see Figure 4.4.

is close to the mean life span of the rats. Therefore, the life span might be a limiting factor in the determination of the exact threshold dose for this syndrome. Obviously, a mean latent period cannot be estimated in that dose region in which only a fraction of the rats develop paralysis during their life span. The highest dose at which no paralyzed rats were observed is represented by the dotted lines in Figures 4.7 and 4.8, respectively, for three rat strains and various

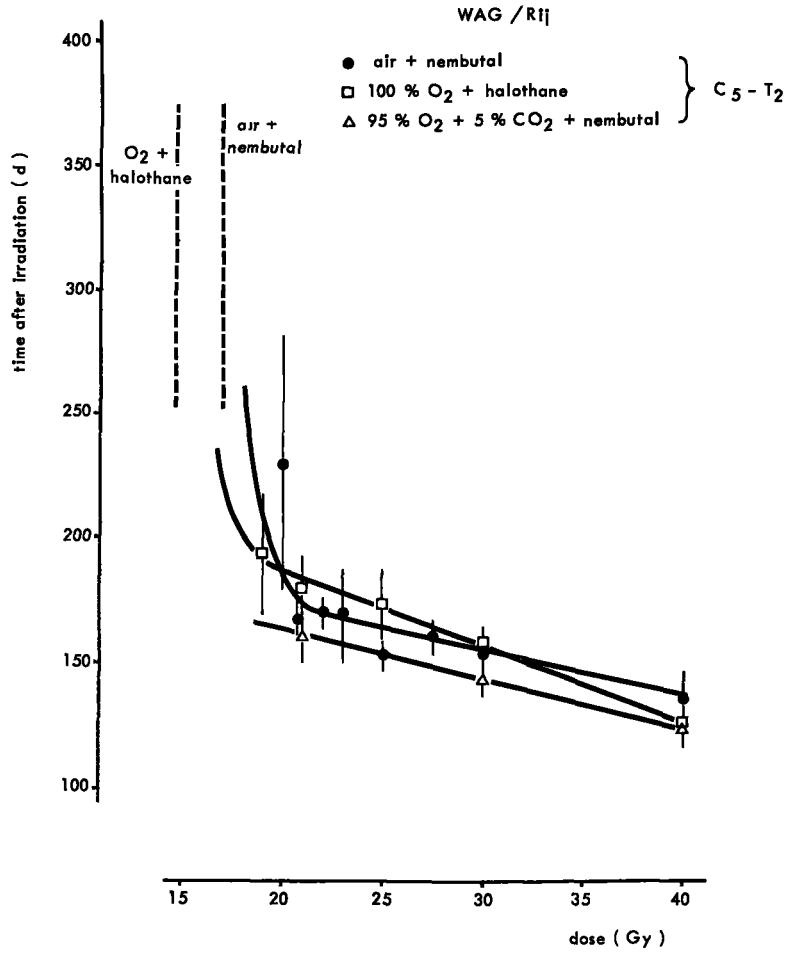

Figure 4.8

Dose-latent period relationships for region C5-T2 of male WAG/Rij rats. Comparison of different anesthetic agents and oxygen concentrations. Further details see Figure 4.4.

experimental conditions. There seems to be a difference in threshold dose between WAG/Rij and BN rats (Figure 4.7), although the limited amount of data precludes a precise estimation. A difference in threshold dose is also observed for different types of anesthesia, suggesting that nembutal anesthesia without additional oxygen provides some protection (threshold 17 Gy) as compared to halothane/oxygen anesthesia (threshold 15 Gy) (Figure 4.8).

Finally, the threshold dose level was studied with respect to the age of the rats at the time of irradiation. A number of 9-month-old rats was irradiated with doses of 15, 17, 19 and 21 Gy of X-rays. None of these rats developed a grade + paralysis within a year after irradiation. However, at more than one year postirradiation, minor symptoms of paresis (grade $\pm$) developed in the rats irradiated with 19 and 21 Gy. The threshold dose for the induction of definite paralysis in rats irradiated at the age of 9 months appears to be higher as compared to rats irradiated at 3 months. However, the threshold for the development of microscopical damage as derived from dose-response curves is observed to be about 17 Gy for both groups (Chapter VI, Table 6.1).

After irradiation of 3-month-old rats with doses above 20 Gy, paralysis develops within 7 months. The histopathological picture of this syndrome is less dominated by vascular lesions (see Chapter V), suggesting the involvement of another type of target cell. The latent period appears to decrease linearly with increasing dose. In this respect, the curves are closely similar to those obtained for the lumbar region, although the minimum in the latent period between 20 and 30 Gy is not observed. Up to 30 Gy, the curve for BN rats has the steepest slope and is significantly different from the curve for WAG/Rij rats, while an intermediate value was obtained for F_1 rats (Figure 4.7). At 40 Gy the latent period is similar for all three strains, with the mean value at about 140 days. Whether at 40 Gy the lines actually cross or run parallel at higher doses cannot be deduced from the present experiments. The differences in latent period obtained for the application of different anesthetics and oxygen levels (Figure 4.8) are not significant. The threshold dose for irradiation under halothane/oxygen anesthesia appears to be lower as compared to irradiation under nembutal anesthesia.

4.3.3 Region T12-L2

Thirty WAG/Rij rats were irradiated under nembutal anesthesia with single doses varying from 20-40 Gy. Although the neurological symptoms observed for this region differ markedly from those observed for L2-L5, the latent period curve seems to have a similar shape (Figure 4.9). However, at 22.5, 25 and 30 Gy, the variability is large and the difference with the latent periods for regions L2-L5 and C5-T2 is not significant. At 40 Gy, the mean latent period for all regions is close to 140 days, with a small standard deviation. Observations on 4 rats which did not show signs of damage within one year after a dose of 20 Gy suggest the threshold to be slightly higher as compared to the other regions.

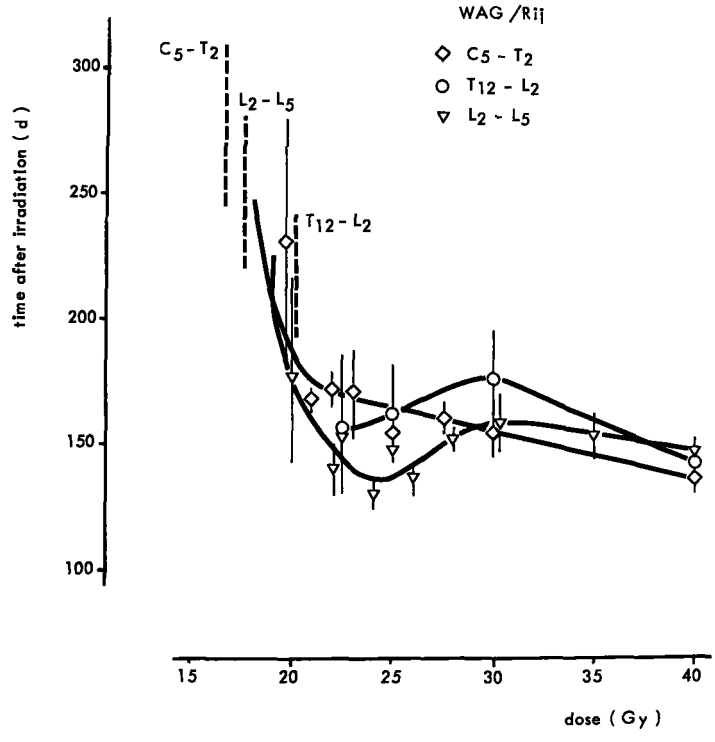

Figure 4.9

Dose-latent period relationships for induction of neurological signs after irradiation of three different regions of the spinal cord of WAG/Rij rats. Further details see Figure 4.4.

4.4 DISCUSSION

From the presentation of the dose-latent period relationships obtained for various conditions, it is evident that a number of variables affect the development of paralysis in the irradiated spinal cord. Some of these variables such as the genetic constitution or the age of the animals, are intrinsic while others are extrinsic, and can be manipulated. The relative importance of the extrinsic factors can only be discriminated from the intrinsic variables in a system which yields reproducible results with a small spread under controlled conditions. In the experiments reported here, these requirements were met by using rat strains which have been inbred for a large number of generations.

Although based on different types of observable lesions, the dose-latent period relationships obtained for three regions of the cord for various strains and conditions have some main characteristics in common. Most curves are linear, at least over a large part of the dose range, and the latent periods are inversely related to the dose. For the linear part, differences in the slope are observed, which probably reflect variations in the kinetics of the underlying processes, but do not reveal their pathological nature. With increasing doses, the curves tend to converge and, at 40 Gy, the latent period is close to 140 days, irrespective the region, the condition or the rat strain.

The specific differences in threshold dose and latent period, as observed in relation to a number of extrinsic or intrinsic variables, are summarized in Table 4.1.

4.4.1 Intrinsic variables

The intrinsic variables studied are the genetic constitution (3 inbred strains) and the age of the rats. Differences in both threshold dose and latent period for three inbred strains clearly illustrates the variability which might be expected to occur in random bred populations (and is also evident in the human population). This is illustrated by the considerable variation in mean latent period observed for different groups of random bred Sprague Dawley rats irradiated with a dose of 40 Gy (Hubbard and Hopewell, 1978). The present results obtained for each of the three strains are well reproducible and show little variation. Obviously, this is of great advantage in analyzing the effects of external variables and for experiments on pathogenesis.

TABLE 4.1

EFFECT OF EXTRINSIC AND INTRINSIC VARIABLES ON LATENT PERIOD AND THRESHOLD DOSE

	C5-T2		L2-L5	
	latent period	threshold dose	latent period	threshold dose
3 strains (WAG/Rij, BN, F1)	< 40 Gy: ++ 40 Gy: -	+	< 30 Gy: ++ > 30 Gy: -	
age (3 m-9 m)		+		-
anesthetic agent/ oxygen level	-	+	-	-
X-rays/neutrons		+	++	++

- : no significant difference
+ : difference indicated (small number of data)
++: significantly different - $p < 0.05$ (multiple Welch S-test)

The effect of the age at the time of irradiation as an intrinsic variable was evaluated for 9-month-old rats in comparison with rats of the standard age of 3 months. Preliminary results obtained for a small number of rats indicated no significant differences in threshold dose for the lumbosacral region. For the cervical region the threshold appears to be higher for the rats irradiated at 9 months (see also Chapter VI).

Important intrinsic variables not studied in the present experiments might be the sex of the animals and the blood pressure. Various authors (Hopewell and Wright, 1970; Asscher and Anson, 1962) have shown that hypertension reduces both the latent period and the threshold dose, although the effect disappeared with doses of 40 Gy. This phenomenon of a decreasing difference in latent period with increasing doses has also been observed in the present experiments with the various rat strains and for the extrinsic variables of anesthetic agent and oxygen level.

4.4.2 Extrinsic variables

The rationale for the experiments under various conditions is given in Chapter III. They were performed to evaluate the effect of

anesthesia, especially on the occurrence of a radiobiologically significant reduction in the oxygen-supply of the spinal cord. Table 4.1 shows that no differences were observed for either region with respect to the latent period or for the threshold dose for L2-L5, but a decrease in threshold dose for C5-T2 was observed under halothane-oxygen conditions. For C5-T2, the threshold dose is mainly associated with late vascular damage, in contrast to damage to the lumbar region. Whether the decrease in threshold for this syndrome in the cervical region is due to the higher oxygen tension or to a sensitization by halothane cannot be deduced from our experiments. On the other hand, the higher threshold for nembutal anesthesia could result from a locally decreased oxygen tension. Barbiturates are known to reduce the systemic blood pressure (Johnson et al., 1976) and to cause cerebral vasoconstriction and a reduced cerebral blood flow (Michenfelder et al., 1976). Unfortunately, the doses used for the nembutal/oxygen combination were not low enough to estimate a threshold dose. For the human spinal cord, the threshold dose seems to be decreased after irradiation in hyperbaric oxygen (Van den Brenk et al., 1968; Coy and Dolman, 1971). Although based on a small number of cases, these data tend to indicate that the target cells for the development of late damage in the normal, unanesthetized cord might not be optimally oxygenated. Atmospheric or hyperbaric oxygen has been reported to shorten the latent period for cord damage in rats (Asbell and Kramer, 1971), but the effect disappeared with doses above 35 Gy. In these studies, no attempt was made to estimate the threshold dose and a wide spread in latency was observed at all dose levels, probably as a result of the use of a random bred rat strain.

The other extrinsic variable studied is the LET of the radiation. In comparison with X-rays, damage by fast neutrons is associated with a significant decrease in threshold dose and in latent period for region L2-L5. The threshold dose was also decreased in the few rats which survived the cervical irradiation with neutrons.

The decreased latent period for fast neutrons does not seem merely to be the result of a shift of the total curve along the dose-axis. A specific difference in the effect of fast neutrons on the kinetics of development of damage is indicated by the very short latent periods encountered especially after fractionated irradiation, even with doses which only slightly exceed the threshold. In addition to the short latent periods, a qualitative difference could also be observed. The development of paralysis is very rapid; within a few weeks after the first symptoms, the rats irradiated on region L2-L5 are completely paraplegic. With X-rays, this rapid progression is observed only with

high single doses in excess of 60 Gy. The relevance of these observations for the use of fast neutrons in radiotherapy and the evaluation of RBE values will be discussed in Chapter VII.

In conclusion, both extrinsic and intrinsic variables affect the kinetics of development of damage, as reflected by differences in dose-latent period curves. A general phenomenon seems to be that with higher doses, starting at 35-40 Gy, the differences disappear. The changes in threshold dose, mainly observed for the cervical region, are of direct importance for the tolerance of the spinal cord. From the present results, it can be concluded that, in the evaluation of the various factors which influence the tolerance, experiments have to be carried out with inbred strains and under controlled conditions, in order to minimize the variations inherent in the system.

CHAPTER V

THE PATHOGENESIS OF VARIOUS TYPES OF LESIONS: THE DEPENDENCE ON DOSE, TIME AND REGION OF SPINAL CORD

5.1 INTRODUCTION

In most studies concerning the mechanisms of development of radiation damage in various tissues, especially with respect to late effects, a fundamental question is what cell type is primarily involved. For the CNS, two main theories pertaining to the pathogenesis of radiation encephalopathy or myelopathy have been proposed. In one theory, damage to the glial cell population is regarded as the primary stage in the development of the lesions; in the other theory, the vascular system is thought to be the primary target. Late functional damage to the CNS is probably not due to direct effects on the neurons. In the adult animal neurons do not divide and consequently cell reproductive death does not occur. Ultrastructural changes have been observed in neurons predominantly after high single doses of 40 and 60 Gy (Reyners personal communication).

In most reports on human radiation myelopathy, it has been concluded that the lesions were of vascular origin (Jellinger and Sturm, 1971). A minority of the investigators regarded the vascular lesions as secondary to the white matter necrosis (Burns et al., 1972). The latter explanation was confirmed by a number of experimental studies which led to the conclusion that white matter necrosis as observed in radiation myelopathy is primarily due to damage to the oligodendroglial cells (Innes and Carsten, 1962; Bradley et al., 1977; Mastaglia et al., 1976). However, all except one of the reports have neglected the possibility that the histopathological changes might depend on the dose level. Most authors used only one fixed single dose and this was twice as high as the threshold for the induction of paralysis. Hopewell (1970), in a study on the rat brain, used various doses and suggested that the sudden death occurring after 20-30 Gy was due to vascular damage, while glial cell depletion led to white matter necrosis after doses of 30-40 Gy.

In the present experiments, anatomically different regions of the rat spinal cord were irradiated with a wide range of doses, including the threshold dose. After neurological signs developed, the rats were

deeply anesthetized and killed by perfusion of buffered formalin or Bouins fluid through the aorta. Perfusion-fixation is a prerequisite in neuropathological studies for obtaining adequately fixed material and reproducible results. The spinal column was dissected out and decalcified. By this procedure, the irradiated part was easily identified in the histological sections, because the bone marrow had become permanently depleted as a result of the irradiation.

In a number of experiments, rats were killed at regular intervals after irradiation to study the pathogenesis of the lesions. An advantage in these experiments is the reproducibility of the latent period within a narrow range at a particular dose level. This allows derivation of information on the approximate time scale of the progression of a lesion from observations on individual rats killed before the development of paralysis.

Unless specified, the lesions described in this chapter were observed in WAG/Rij rats irradiated at the age of 3 months with single doses of X-rays under nembutal anesthesia. Different types of lesions were observed. These will be described with respect to the spinal cord region and the dose range over which the main aspects of the lesions did not change.

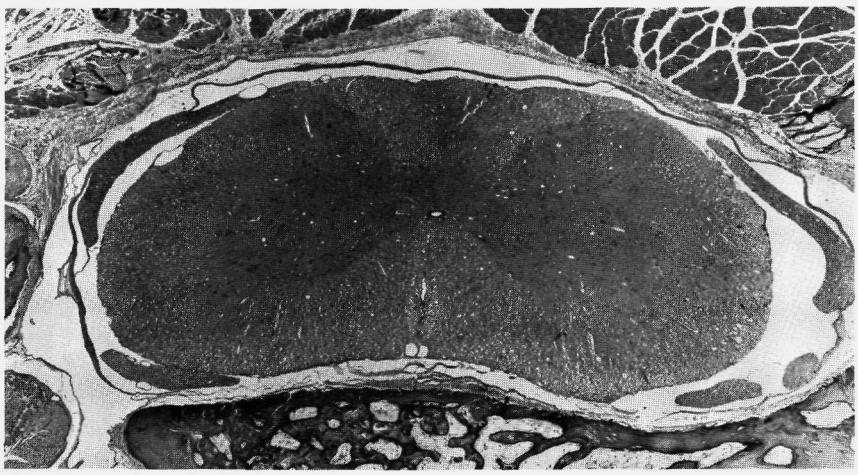

Figure 5.1

Cervical cord, 160 days after 22 Gy. No damage observed in the cord of this rat. The bone marrow is replaced by fibrotic tissue and fat cells (HPS, x 22).

5.2 RESULTS

5.2.1 Region C5-T2 (cervical cord)

a. Demyelination and necrosis of the white matter

Over the dose range of 20-40 Gy, the latent period of the neurological signs was shown to be inversely related to the dose (Figure 4.7) and varied from 7-4 months. Serial killing experiments were performed after irradiation with doses of 22 Gy and 40 Gy.

Histopathological changes after 22 Gy

Starting at 120 days postirradiation and successively at 10-day intervals, groups of 4 rats were killed. The mean latent period at this dose level is 170 ± 7 days. No abnormalities were observed in the spinal cord or nerve roots for up to 150 days postirradiation. At 160 days postirradiation, two rats were normal (Figure 5.1); one showed a few demyelinated foci in segment C6 (Figure 5.2). One rat that did not exhibit neurological signs, showed an area of extensive demyelination and necrosis in the lateral white matter of segment C6 (Figure 5.3a).The demyelinated focus contained a large number of swollen axons, while very few nuclei were seen. The number of glial cells was slightly increased at the border of the lesions. Vascular damage was restricted to a few dilated capillaries showing minute hemorrhages. Macrophages were not observed. Three other rats started to show neurological signs at 160 days postirradiation and were killed at day 166 with signs varying from stage ± to ++ (see 3.4.2). The observed lesions were all basically similar to those observed in a large number of other rats killed after development of paralysis. The major aspect was demyelination progressing into necrosis (Figure 5.3b). The lesions were irregularly distributed over the white matter of the irradiated segments, with a predilection for the lateral and ventral columns. There was a slight glial reaction, with hypertrophic astrocytes, around most necrotic areas. Occasionally, astrocytes were seen in mitosis. While most of the lesions showed only a moderate cellular reaction, a necrotic area with lipid macrophages ("foam cells" or "gitter cells") was observed in a number of cases

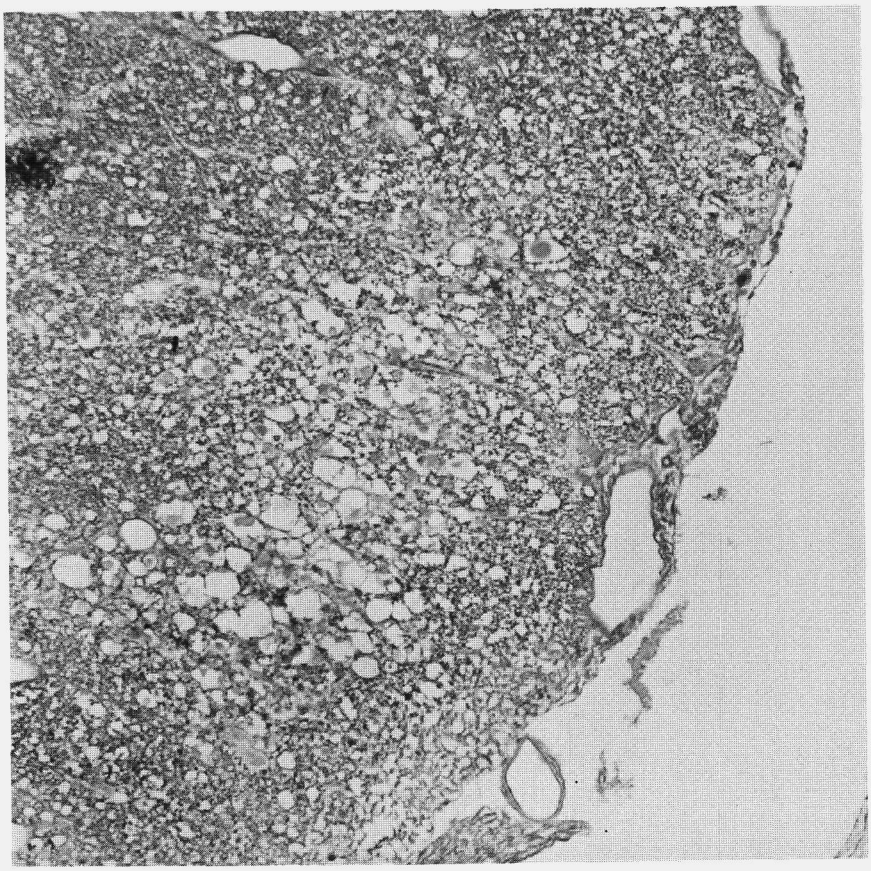

Figure 5.2

Cervical cord, 160 days after 22 Gy. Area with swollen axons and disappearance of the myelin sheaths (demyelination) in the lateral white matter of segment C6 (LFB-PAS, x 185).

(Figure 5.4). The greatest concentrations of these lipid macrophages were found near the borders of the irradiated area, predominantly in the dorsal columns of the white matter. Vascular damage consisted of dilated blood vessels and small fresh hemorrhages which varied in extent and number. A small number of granulocytes was usually observed around the dilated vessels in a necrotic area. Only in a few cases was perivascular cuffing with mononuclear cells observed. Fibrinoid degeneration of arteriolar walls with partial occlusion of the lumen, which is generally observed in the

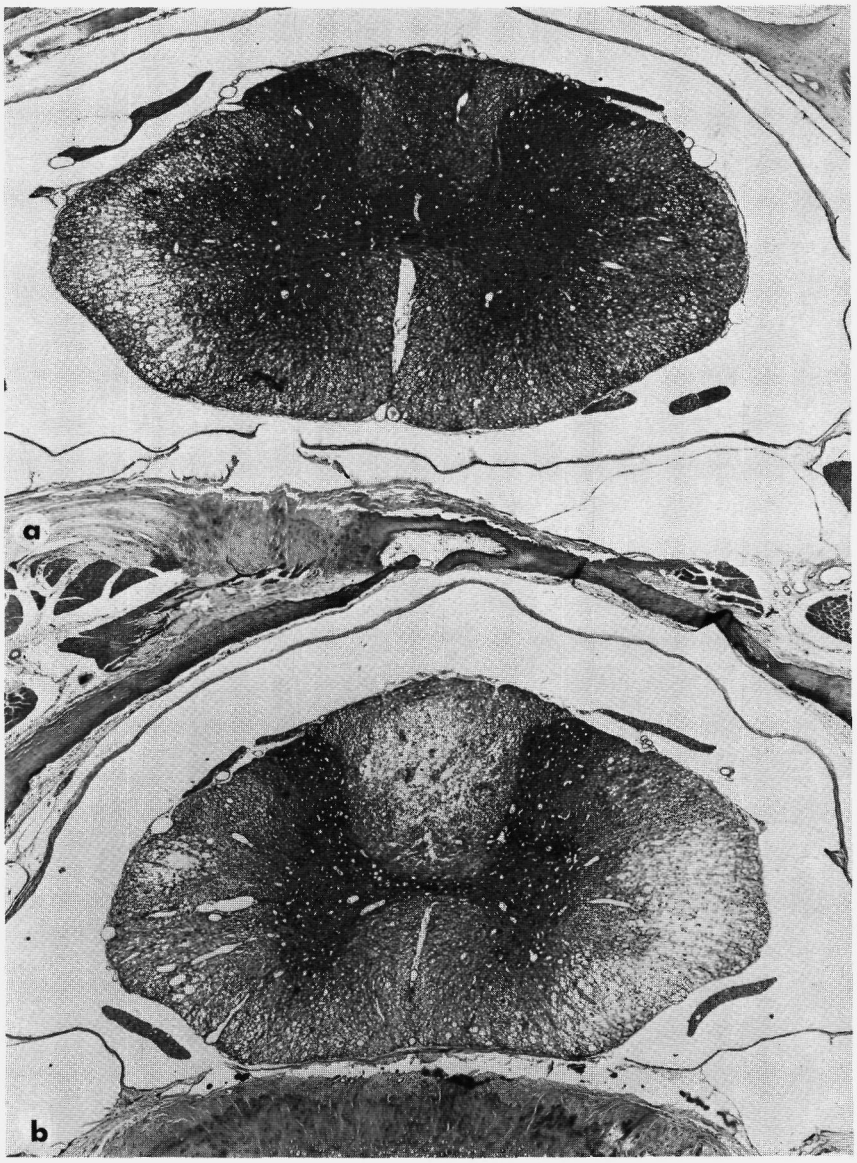

Figure 5.3

a. Beginning white matter necrosis, restricted to segment C6, in rat with no neurological signs (160 days after 22 Gy).
b. Extensive demyelination and necrosis, randomly distributed throughout the white matter of the irradiated area, 170 days after 21 Gy. First neurological signs at 165 days (HPS, x 29).

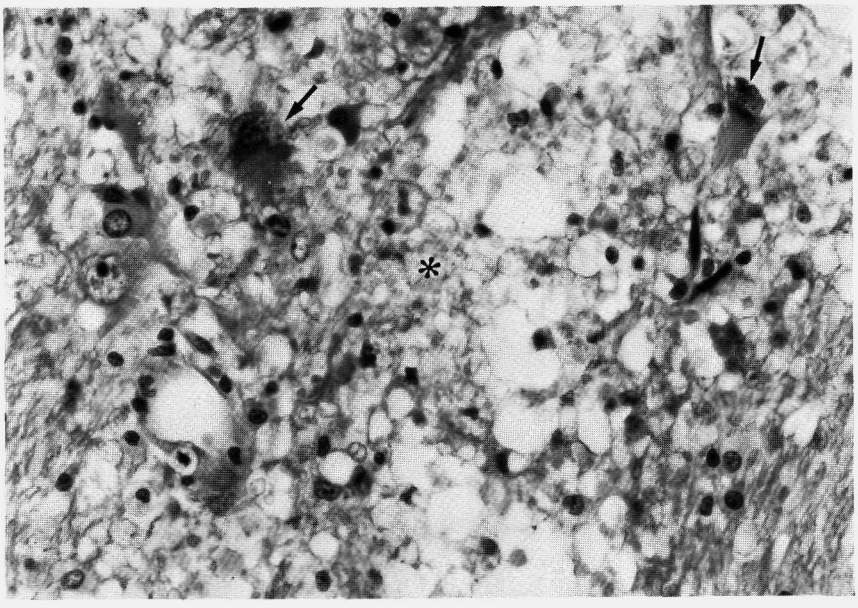

Figure 5.4

Cervical cord, 185 days after 27.5 Gy (2 F/56 d). Detail of necrotic area in dorsal white matter, with lipid macrophages (*) and giant astrocytes (➹) (HPS, x 320).

vertebral muscles from about 6 months after irradiation, does not occur in the spinal cord. Petechiae without inflammatory reactions or ischemic changes were also observed in the gray matter. Other changes in the gray matter were mainly restricted to an increase in glial cells, especially around the ventral horn motor neurons, probably as a reaction to retrograde changes. No changes were observed in nerve roots and spinal ganglia.

In the cervical cord of BN rats irradiated with 22 Gy, no histological changes were observed at 160 days postirradiation, which was the longest time interval used in the serial killing experiment. This result was later explained by the longer latent period observed for BN rats as compared with WAG/Rij rats at this dose level (Figure 4.7). The spinal cord of BN rats with paralysis showed lesions which were essentially the same as those in WAG/Rij rats.

Histopathological changes after 40 Gy

At this dose level, the latent period is 137 ± 11 days. Up to 120 days postirradiation, no changes were observed. At 130 days postirradiation, two rats were killed, one in stage ± and the other with paralysis of fore and hind legs (stage +++). In the latter animal, the white matter of several segments in the irradiated area was totally necrotic, with minor infarction of the gray matter. Two other rats with only slight neurological signs when killed at 140 days postirradiation showed focal areas of demyelination and necrosis in the white matter comparable to the lesions described after 22 Gy (Figure 5.5). As compared to this lower dose level, the vascular damage appeared to be more severe, with a larger number of fresh hemorrhages in both the gray and white matter. There was no damage in nerve roots and ganglia. Observations in BN rats were identical to those in WAG/Rij rats.

A large number of rats irradiated with single doses in the range of 20-40 Gy or in the equivalent range with fractionated doses (Chapter VI) and killed after development of paralysis all

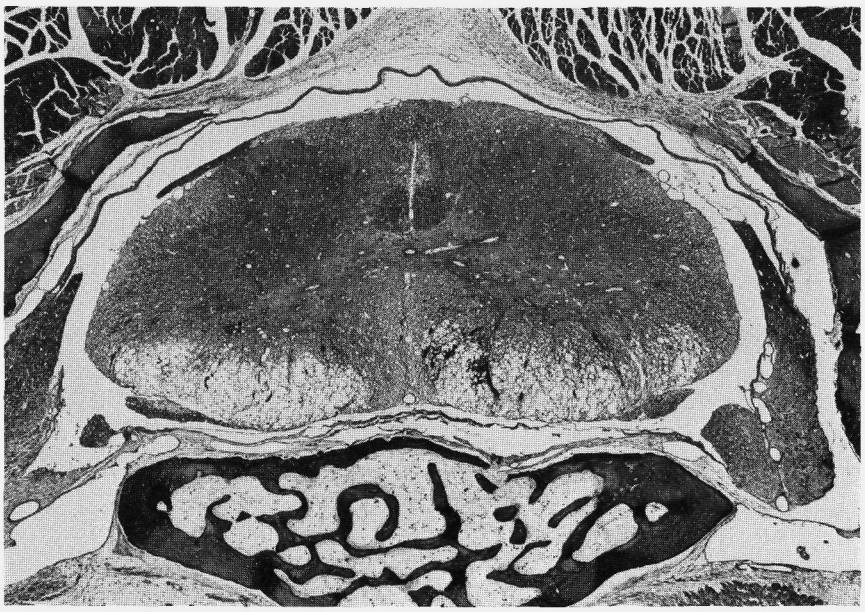

Figure 5.5

Cervical cord, 140 days after 40 Gy. Necrosis and focal hemorrhages in ventral white matter. No damage in nerve roots (HPS, x 22).

showed the above described white matter necrosis. The hemorrhagic component of the lesions appeared to become more prominent with increasing doses, but was always of recent origin. Furthermore, it can be concluded from the results of the serial killing experiments that the progression from the first microscopically discernible demyelinated foci into extensive white matter necrosis occurs in less than 10 days.

b. Late vascular damage

As shown in the previous section, demyelination and white matter necrosis is a general finding in rats developing paralysis within 4-7 months after single doses of 20-40 Gy on the cervical cord. Over a small dose range of about 17-20 Gy of X-rays, lesions develop after much longer latent periods, up to the end of the lifespan of the rats. Histologically, these lesions consist of vascular damage and are markedly different from the type characterized by white matter necrosis. The vascular damage varies from capillary proliferation and dilatation in neurologically normal rats to massive hemorrhage in acutely paralyzed rats. Between these extreme stages, a series of lesions are observed, which differ in various aspects such as extent and distribution of the lesions as such, the hemorrhagic component, glial and inflammatory reactions, etc. Based on these aspects, three main categories of vascular damage are arbitrarily distinguished.

Type 1. (Figure 5.6a,b). Increased capillary density, in both white and gray matter. A number of capillaries or venules are dilated (telangiectasis). In some cases, microthrombi and petechial hemorrhages in combination with a moderate gliosis are present. The reactive cells are mainly hypertrophic astrocytes and small round macrophages. Lesions of this type are observed in rats which do not show paralytic signs and are killed approximately at the end of their lifespan.

Type 2. (Figure 5.7a,b) Extensive telangiectasia with focal hemorrhage and fibrin deposits. In addition to a strong reaction by endogenous cell types (astrocytes, microglial cells) or hematogenous monocytic infiltrates, inflammation with neutrophilic leukocytes is observed, especially in cases with extensive fibrin deposits and hemorrhages. In areas with a strong cellular reaction, other cell types of interest are monstrous astrocytes with large nuclei and macrophages laden with erythrocytes or hemosiderin pigment.

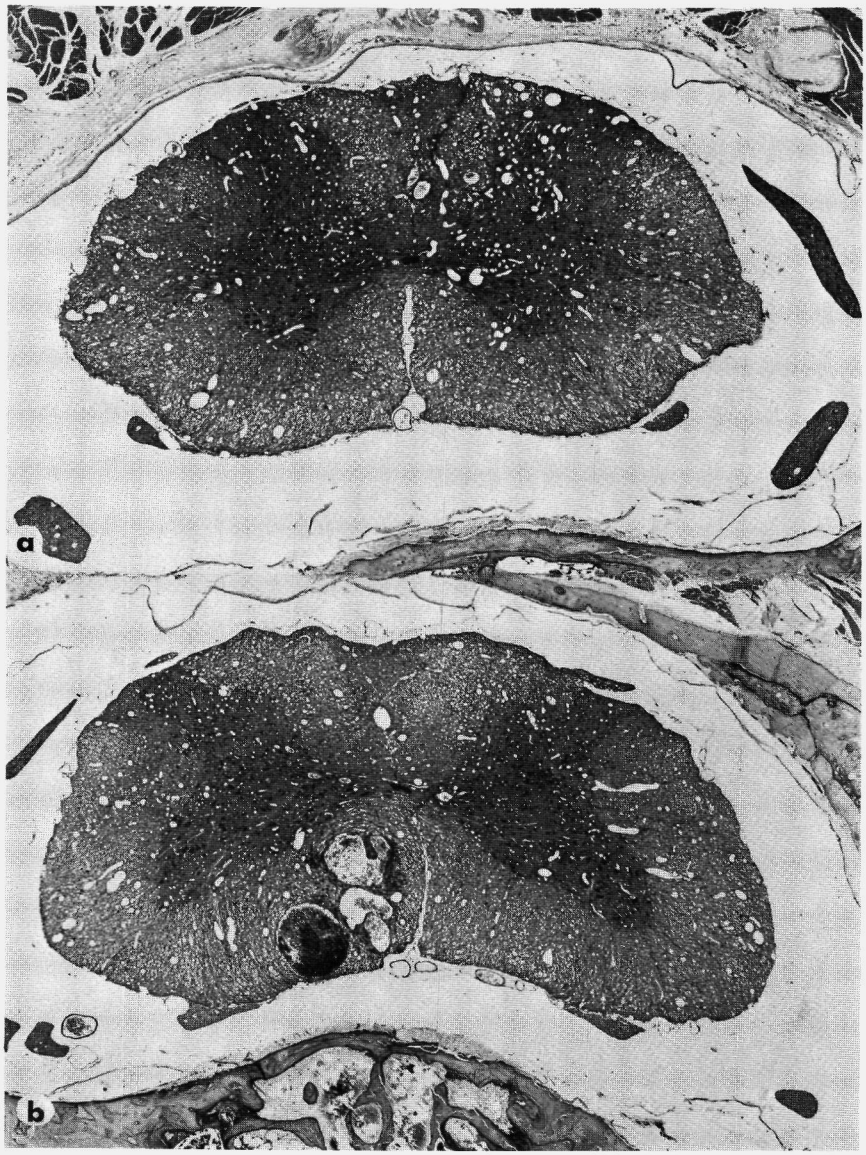

Figure 5.6

Cervical cord, vascular damage type 1, 370 days after 26 Gy (2 F/1 d).
a. Dilatation and increased density of capillaries. Compare with Figure 5.1 (HPS, x 26)
b. Telangiectasia in ventral white matter (HPS, x 26)

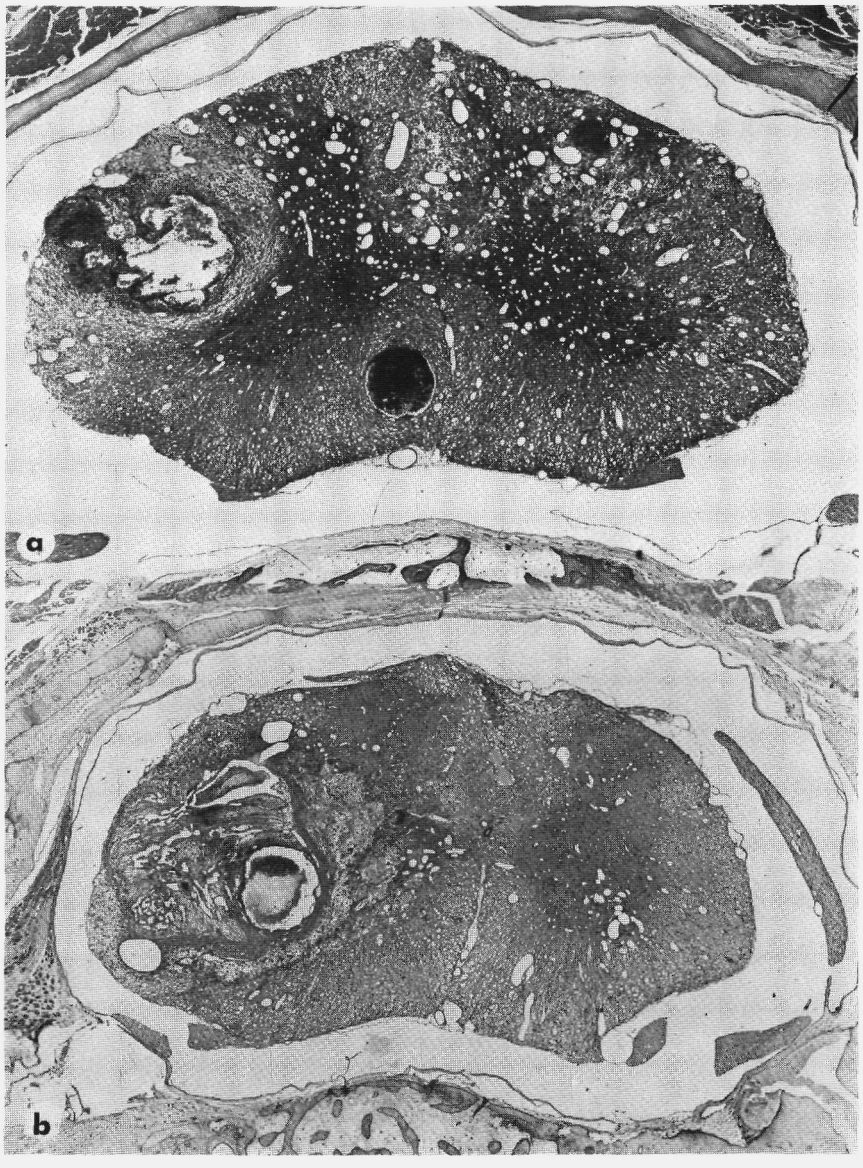

Figure 5.7

Cervical cord, vascular damage type 2. Extensive telangiectasia with hemorrhage and fibrin deposits. Strong glial reaction and infiltration with monocytes and neutrophilic leukocytes.
a. 340 days after 17 Gy (halothane/O_2) (HPS, x 27)
b. 345 days after 26 Gy (2 F/1 d) (HPS, x 22)

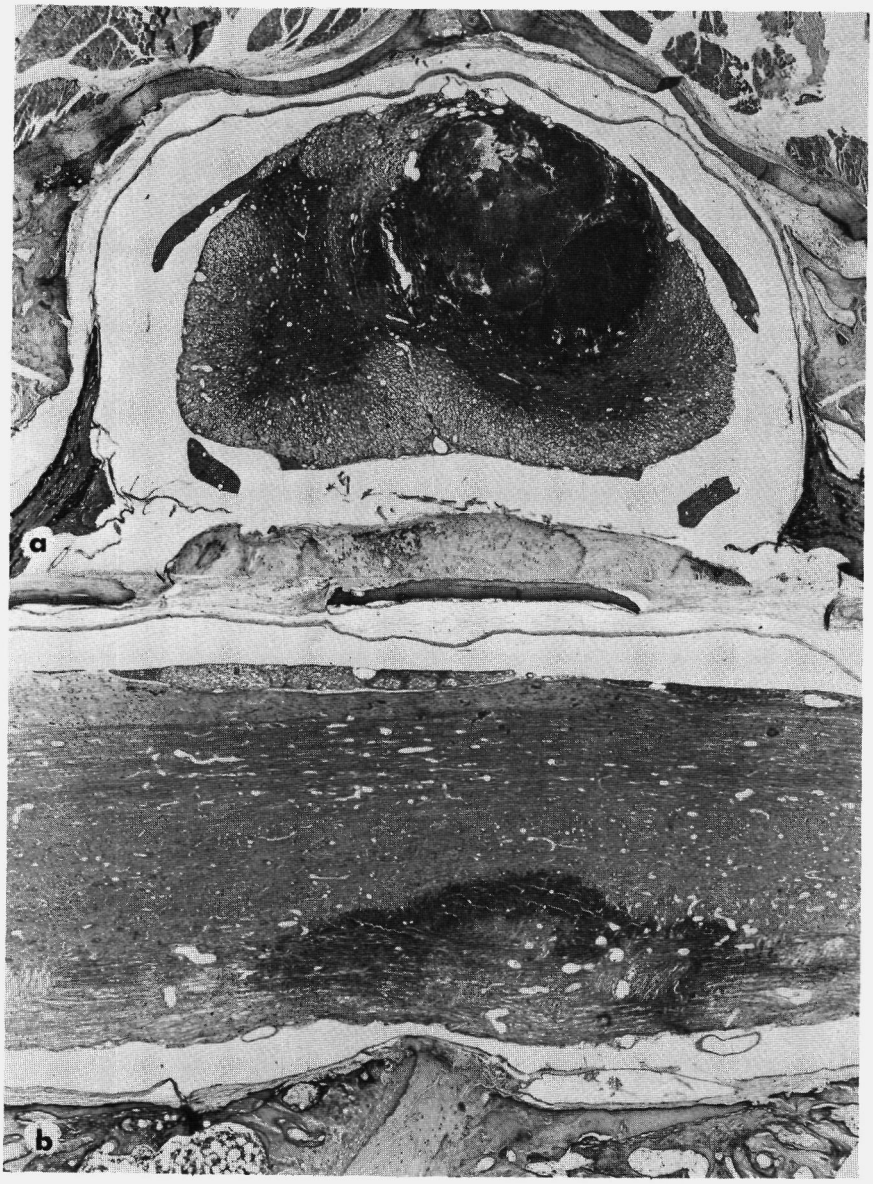

Figure 5.8

Cervical cord, vascular damage type 3. Acute hemorrhage with compression of surrounding tissue.

a. 221 days after 50 Gy (10 F/11 d). Large hemorrhage, extending over several cord segments (HPS, x 29)

b. 435 days after 15 Gy (halothane/O_2). Longitudinal section, showing relatively small hemorrhage in ventral part of the cord (HPS, x 22).

Lesions of this type represent a slowly progressive chronic process of vascular damage. The distribution varies from small foci to involvement of a number of cord segments over a large area. This is reflected in a large variability of neurological damage; some rats show no signs at all, while others have a slight or more severe paralysis which is unilateral in most cases.

Type 3. (Figure 5.8a,b) Instead of the slowly progressing chronic lesions, a large hemorrhage extending over a number of cord segments may develop acutely. This leads to sudden paralysis due to compression of the surrounding tissue. Depending on the time course of the process, a cellular reaction is absent or moderate. Most of the type 1 and type 2 lesions are observed at more than one year after irradiation. This is in contrast to the extensive hemorrhages (type 3), whereby 6 out of 9 developed in the period of 220-350 days postirradiation. A detailed analysis of the time-dose relationships and threshold doses for the various types of damage is presented in Chapter VI.

5.2.2 Region L2-L5 (lumbosacral cord and cauda equina)

a. Progressive necrotizing radiculopathy

The lesions observed in the lumbosacral cord and the cauda equina are completely different from those observed in the cervical region. The threshold dose for the induction of paresis is about 19 Gy and, up to a single dose of 60 Gy, the lesions are basically similar. However, with increasing doses, the latent period decreases and the progression of neurological signs is more rapid (see Figure 4.4). The pathogenesis of the lesions observed over the dose range of 20-60 Gy has been studied in serial killing experiments on WAG/Rij and BN rats at various dose levels. The main features of the lesions are demyelination and necrosis of the nerve roots, without damage to the spinal cord itself. As illustrated in Figure 5.9, the lesions develop in a centrifugal way in most cases. Starting from the center of the root, there is a completely acellular necrotic area, with only the former lining of the myelinated nerve fibers consisting of neurilemmal sheath material remaining. At the periphery of this area, a number of mostly pyknotic Schwann cell nuclei is present. The outer region of the nerve root appears to be completely normal. When the lesion progresses, the necrotic center expands; however, even in advanced

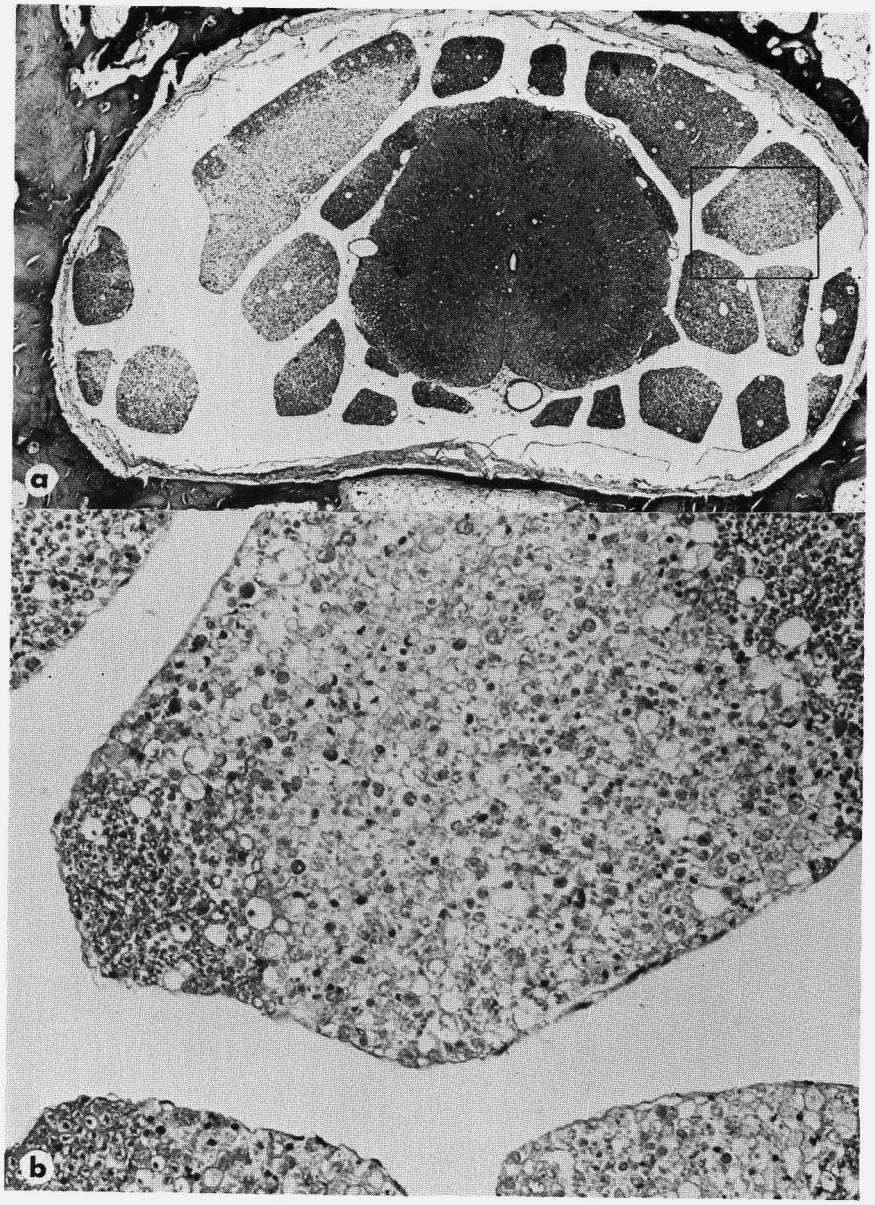

Figure 5.9

Lumbosacral cord, 140 days after 22.5 Gy.
a. Demyelination and necrosis of the nerve roots without damage in the spinal cord. The bone marrow is depleted and replaced by fat cells (HPS, x 25)
b. Detail of nerve root. The center is necrotic, while at the periphery a normal structure is observed (x 185).

cases, a small outer zone of normal myelinated fibers is usually still present (Figure 5.10). During development of the nerve root necrosis, vascular damage is inconspicuous and is restricted to a few arterioles which show thickening of their walls. The most striking observation for region L2-L5 is that, even in paralyzed rats irradiated with doses of up to 60 Gy, the spinal cord and the spinal ganglia show no degeneration, while the nerve roots are totally necrotic.

Secondary degenerative changes are observed outside the irradiated area. In the dorsal nerve roots in the rostral direction, the myelin sheaths are fragmented and phagocytized by Schwann cells or macrophages, which are greatly increased in number. This ascending secondary degeneration is observed to continue in the dorsal columns of the white matter. At the same level (rostral from the irradiated region) retrograde degeneration was indicated by a severe gliosis in the area of the ventral horn motor neurons. Caudal from the irradiated region, Wallerian degeneration of the ventral roots down into the peripheral nerves was observed.

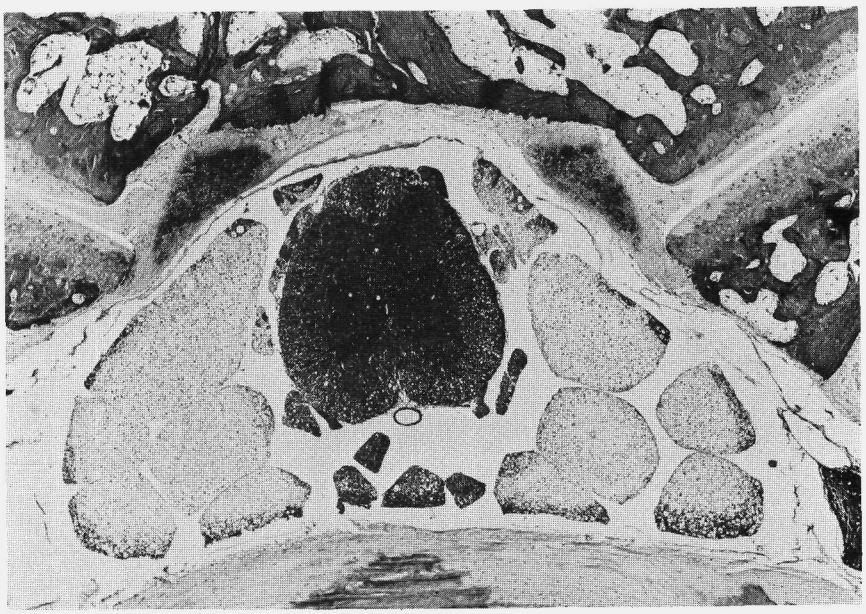

Figure 5.10

Lumbosacral cord, 170 days after 22 Gy. Nerve roots almost totally necrotic, while cord appears normal (HPS, x 29).

To compare the pathogenesis of the lesions for different dose levels in a quantitative way, the successive stages in the development of the nerve root lesions were classified into various grades:

- : Normal, or a slight increase in the number of Schwann cells.
± : Phagocytic and proliferative activity of Schwann cells. A small number of nerve fibers shows demyelination. Myelin sheaths are locally swollen, resulting in a large space around the axon (intramyelinic edema) (Figure 5.11).
+ : Extensive demyelination, with increasing space between the individual fibers. Focal honeycomb-like structures consistin of residual basement membrane material are observed. In these structures, a central axon may still be present. The number of nuclei in these foci is sharply reduced.
++ : Larger necrotic areas comprising 5-50% of the nerve fibers in the roots on transverse section.
+++: More than 50% of the nerve fibers in the roots are necrotic.

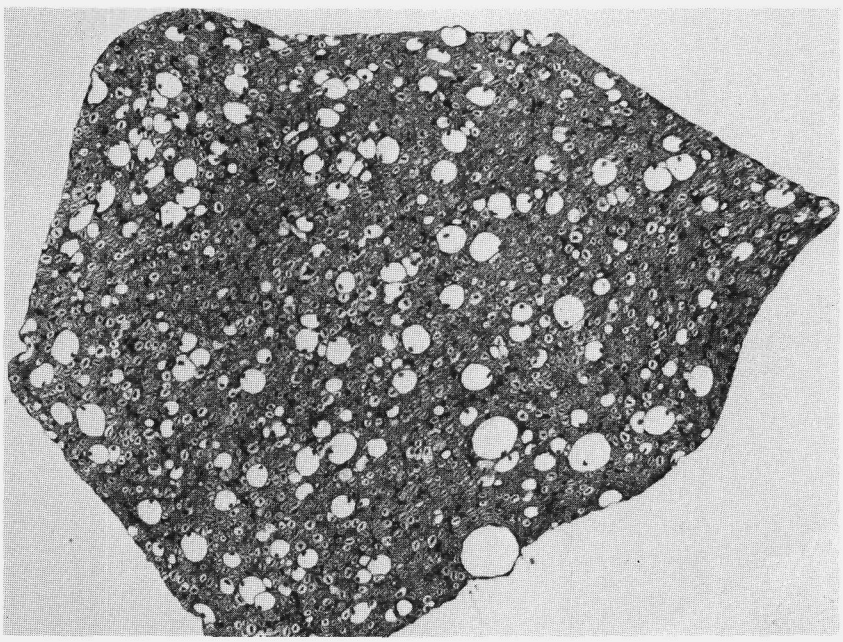

Figure 5.11

Dorsal lumbar root, 60 days after 40 Gy. A large number of fibers show swelling of myelin sheaths (HPS, x 140).

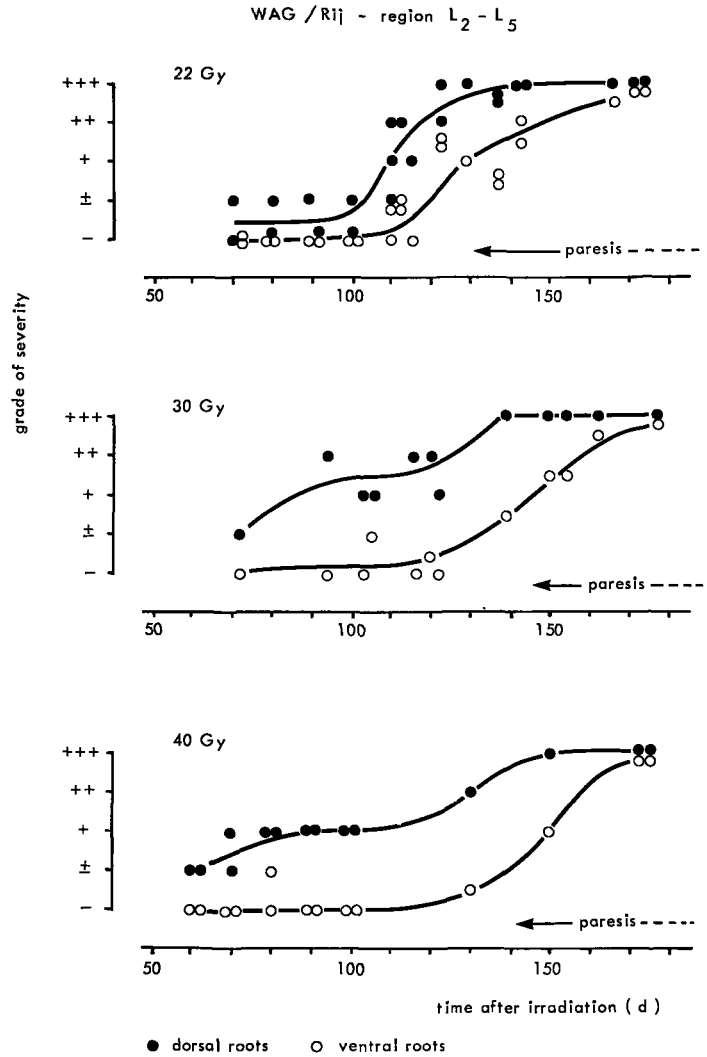

Figure 5.12

Relation between the development of lumbar root necrosis and the observation of paresis in WAG/Rij rats. The grade of severity of the lesions is plotted versus the time after irradiation. Each point represents the score for the dorsal or ventral roots of one animal.

An analysis of the development of nerve root necrosis in WAG/Rij and BN rats is presented in Figures 5.12 and 5.13, respectively. For each animal, the lesions were scored for the ventral and dorsal roots separately and an estimate of the grade of severity was made on the basis of 4 or 5 transverse sections from the irradiated area.

For WAG/Rij rats, the development of nerve root damage (radiculopathy) was studied at three dose levels: 22, 30 and 40 Gy (Figure 5.12). The dorsal roots are affected earlier and more severely than are the ventral roots after all doses. With increasing doses, the latent period for the first signs of dorsal root degeneration (±) appears to become shorter. However, the progression from grade ± to +++ occurs in about 20 days with a dose of 22 Gy, as opposed to 60-70 days with 30 and 40 Gy. For the ventral roots, no significant difference in progression of damage for the three dose levels is found.

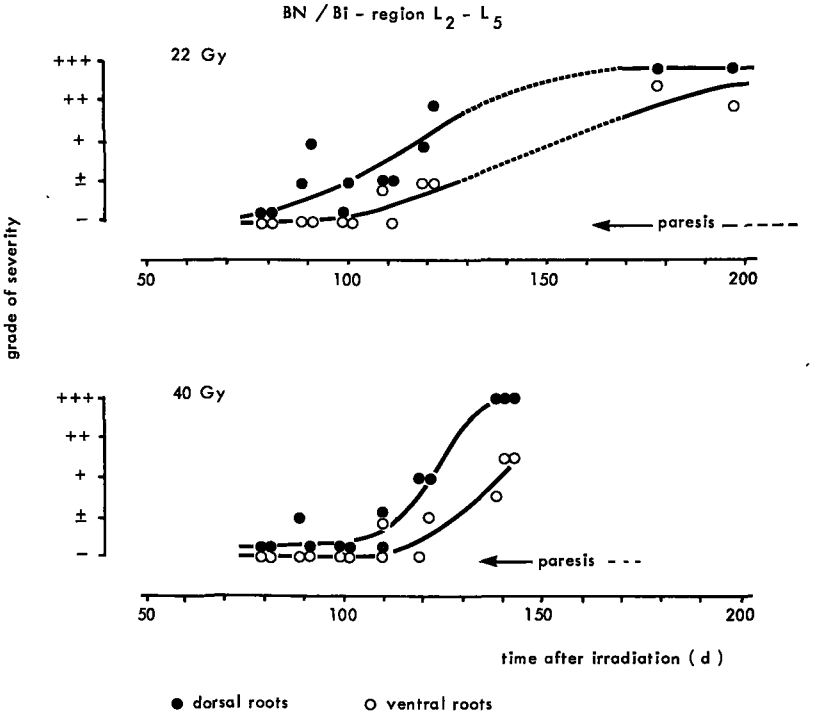

Figure 5.13

Relation between the development of lumbar root necrosis and the observation of paresis in BN/Bi rats. Further details see Figure 5.12.

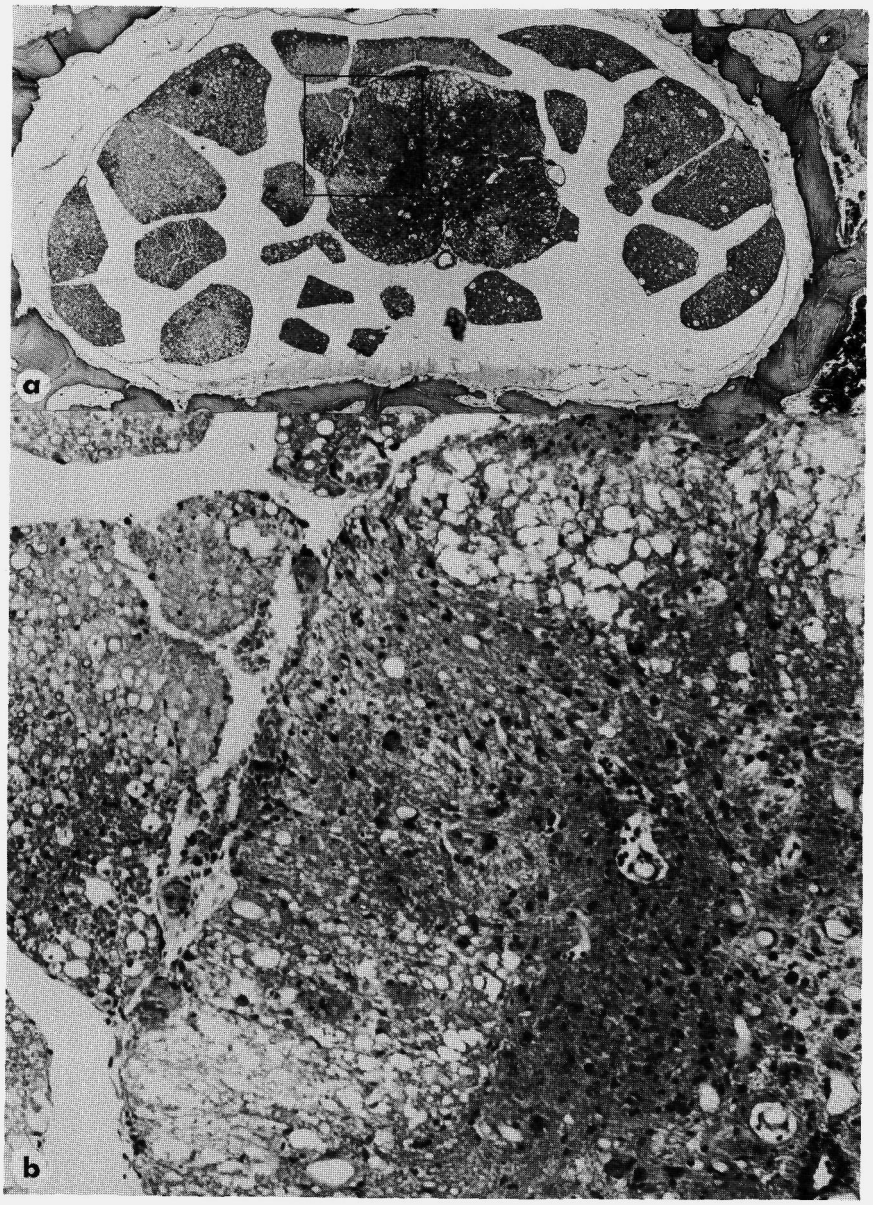

Figure 5.14

a. Lumbosacral cord, 66 days after 100 Gy. Severe necrosis of cord and nerve roots (HPS, x 29)
b. Detail (HPS, x 185)

The development of nerve root damage in BN rats was studied after irradiation with doses of 22 and 40 Gy (Figure 5.13). The observed pattern differs from that observed in WAG/Rij rats. After a dose of 22 Gy, the development from grade ± to +++ occurs in about 60-80 days, while this period is about 30 days with 40 Gy. A constant finding in both rat strains is the early and more severe damage in the dorsal roots as compared to the ventral roots. In Figures 5.12 and 5.13, the occurrence of the first signs of paresis is indicated for each dose level, showing the consistent correlation with the histological grade of damage in the dorsal (+++) and ventral roots (+ or ++).

To study a possible change in pathogenesis with increasing dose, a few groups of WAG/Rij and BN rats were irradiated with single doses of 80 and 100 Gy. In addition to severe nerve root necrosis of a similar type as described above for lower doses, moderate to severe spinal cord damage was observed. Both white and gray matter showed disseminated necrosis, hemorrhages and edema (Figure 5.14). Even with these high doses, the dorsal root ganglia showed remarkably few degenerative changes.

b. Chronic nerve root degeneration and hypertrophic neuropathy

When doses below the threshold (about 19 Gy) for the induction of progressive necrotizing radiculopathy were applied to WAG/Rij rats, paralysis did not occur within the first year after irradiation. However, histopathological changes were definitely discernable after doses as low as 15 Gy and were different from the nerve root necrosis observed at higher doses. The lesions consisted of degenerative and proliferative changes in the nerve roots, with the ventral roots being more severely affected. The first sign of demyelination of the ventral roots of the cauda equina was found at about 250 days postirradiation. Ventral root degeneration was more generalized, with proliferation of Schwann cells in one or more ventral roots after 300-350 days. The degree of proliferation showed a wide variation and was used to distinguish different stages of root damage. Three stages were arbitrarily designated:

I. (Figure 5.15) Demyelination of mainly ventral roots with later involvement of the dorsal roots. A common finding was a thin swollen myelin sheath with the axon still present. Macrophages containing PAS-positive material were observed near to and within myelin sheaths. In the more severe stages, the number of Schwann cells was greatly increased.

Figure 5.15

a. Lumbosacral cord, 427 days after 15+6 Gy (112 d interval). Chronic nerve root degeneration stage I (HPS, x 25)
b. Detail of ventral root with degenerating and swollen myelin sheaths and an increased number of Schwann cells (HPS, x 330)

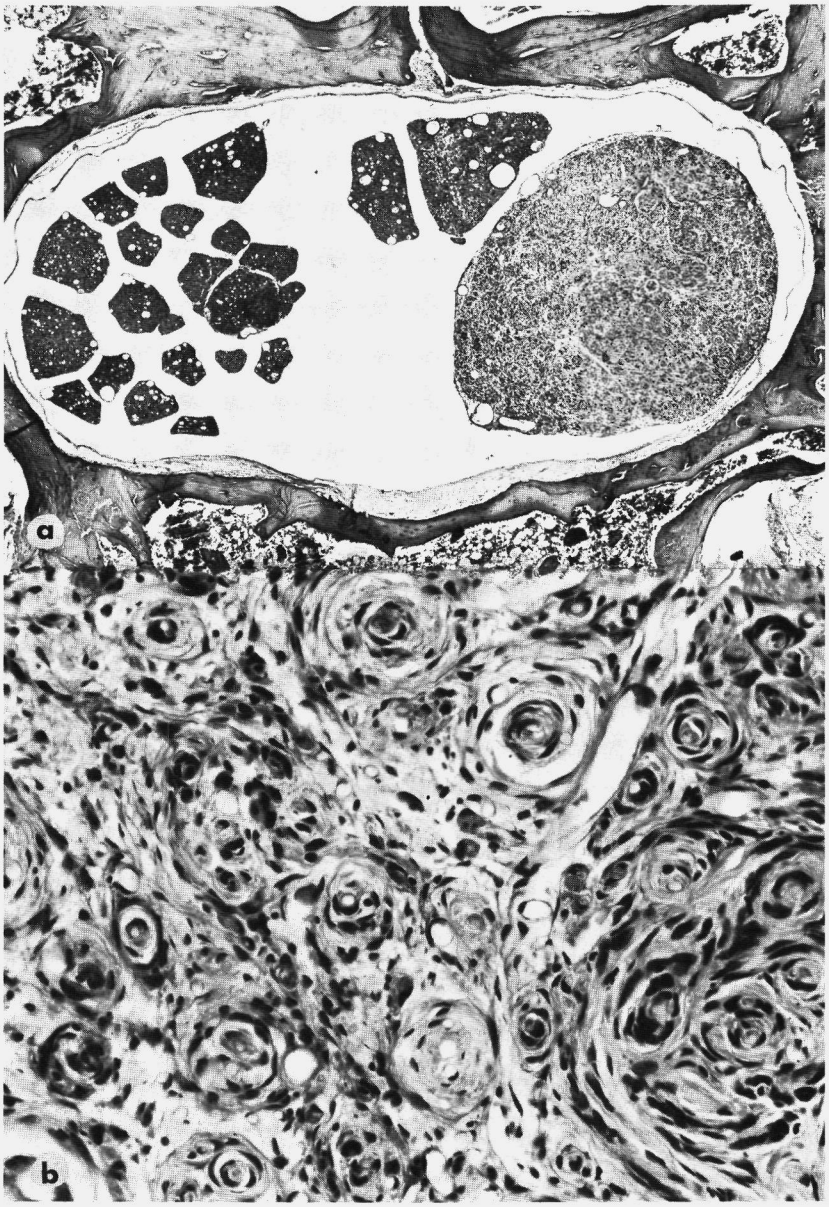

Figure 5.16

a. Lumbosacral cord, 562 days after 15+6 Gy (84 d interval), showing large neurofibroma (HPS, x 25)

b. Detail of ventral root with neurofibroma showing onion bulb structure (HPS, x 330)

II. (Figure 5.16) Severe hyperplasia of Schwann cells with local thickening of nerve roots. The proliferated cells were generally arranged in concentric layers or so-called onion bulbs. A thinly myelinated or demyelinated axon was present in a number of these structures. Redundant myelin was formed in some nerve roots. In the most extensive lesions, the locally thickened nerve root occupied nearly half of the space of the spinal canal. Because of their local, noninvasive character, the latter lesions are regarded as benign neurofibromas.

III. (Figure 5.17) Malignant proliferative lesions, with aspects of Schwannomas. In contrast to stage II lesions, infiltrative growth in other roots and in the spinal cord was observed. The onion bulb growth pattern was not present in these tumors.

The distinction between stage I and stage II lesions was not sharply defined. The presence of some small concentric whorls of Schwann cells ("onion bulbs") was regarded as stage I.

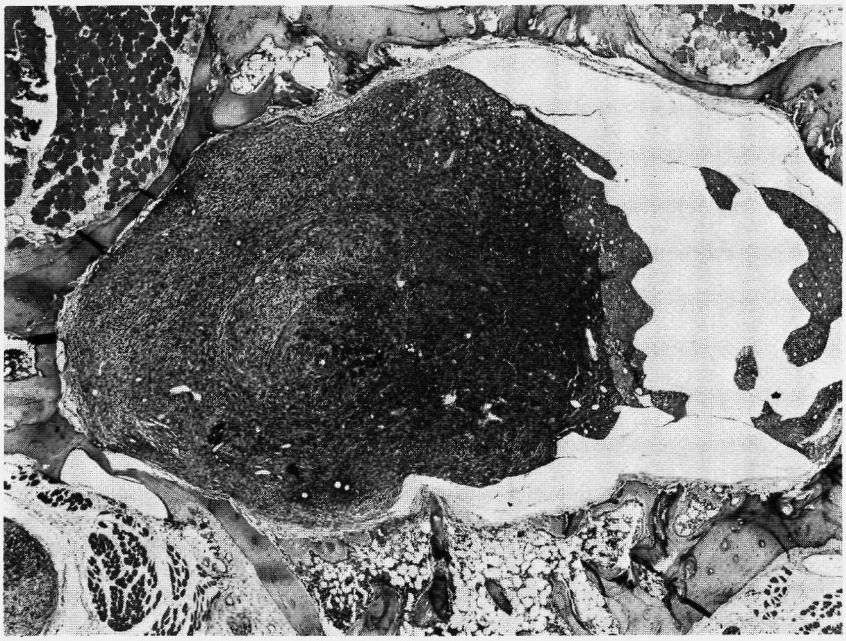

Figure 5.17

Malignant Schwannoma in lumbosacral cord, 438 days after 24 Gy (2 F/1 d) (HPS, x 25)

A distribution of the three stages at 100-day intervals is shown in Table 5.1. Ventral root lesions were observed in all irradiated rats at more than 300 days postirradiation. Distinct proliferation of Schwann cells started at about one year postirradiation, with a sharp increase in the development of stage II lesions at older ages. Rats with stage I or stage II lesions did not show obvious paresis, but a mild degree of muscular atrophy in the hind legs reflected a chronic denervation in the older age groups.

The presence of neoplastic lesions (stage III) was evidenced by the development of paralysis due to invasion of the spinal cord or severe destruction of the roots. These stage III lesions include only the tumors of neural origin and not those originating in the surrounding irradiated bone or muscle tissue. The latter tumors developed in approximately 25% of the animals which survived for more than one year postirradiation (see Figure 4.3).

Degenerative changes in the roots in the cauda equina were also observed in aging unirradiated WAG/Rij rats (Burek, 1978). The earliest signs of lumbosacral ventral root degeneration were observed at ages of 550-600 days. The main aspect of the lesion was demyelination with local swelling of myelin sheaths and well-preserved axons. Macrophages were found in and outside the myelin sheath. At ages of 600-800 days, the degeneration of the ventral roots was more generalized and the dorsal roots were also involved. In two rats aged 800 days, slight focal proliferation of Schwann cells was observed. Schwannomas were not observed in the aging control rats.

Table 5.1.

DEGENERATIVE AND PROLIFERATIVE CHANGES IN VENTRAL ROOTS OF THE IRRADIATED LUMBOSACRAL SPINAL CORD
(dose range 15-19 Gy)

Days post-irradiation	200-300	300-400	400-500	500-600	Total number
Number of rats	10	41	59	80	190
Stage I	40% (4)	90.2% (37)	86.4% (51)	73.8% (59)	79.5% (151)
II	-	7.3% (3)	8.5% (5)	25.0% (20)	14.8% (28)
III	-	2.5% (1)	5.1% (3)	1.2% (1)	2.6% (5)

5.2.3 Region T12-L2: a transitional area

Because of the strong contrast between the histopathological pattern observed in the cervical and the lumbosacral cord, an additional region T12-L2 was studied. This region contains a large part of the lumbar spinal cord and overlaps slightly with region L2-L5. Thirty WAG/Rij rats were irradiated with single doses varying from 20-40 Gy. Serial killing experiments were not performed and all rats were killed after development of paralysis.

At the level of T12/T13 with doses up to 25 Gy, the damage to the cord consisted of focal demyelination of the ventral root zone, with astrocytosis and moderate monocytic infiltration. The dorsal funiculus of the white matter showed extensive secondary degeneration of the fasciculus gracilis. Both the white matter and the nerve roots showed extensive necrosis after doses of 30 and 40 Gy (Figure 5.18). Numerous lipid macrophages were present in the necrotic cavities in the white matter. In severe cases, the necrosis extended into the ventral gray horns with the large motor neurons. In the next segment in the caudal

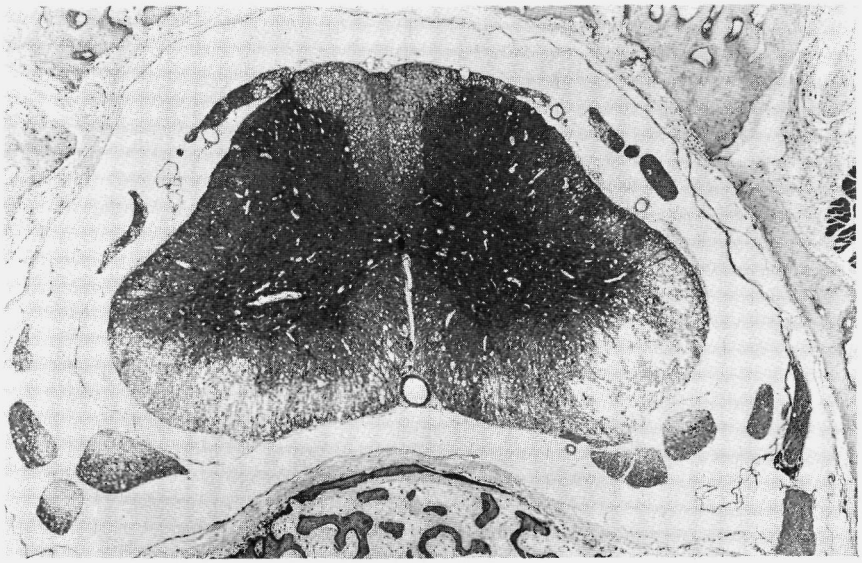

Figure 5.18

Lumbar cord, 195 days after 30 Gy on region T12-L2. Necrosis of ventrolateral white matter and of ventral nerve roots (HPS, x 24).

direction (Tl3/Ll), damage in the spinal cord after doses of 30 and 40 Gy was restricted to small demyelinated or necrotic foci in the root entry zones, while no damage was observed at the level of segment Ll/L2. However, the severe nerve root necrosis at this level was identical to the lesions described for L2-L5. Apparently, vertebral level Tl2/Tl3 (cord segments L3-L5) represents the caudal border for the development of predominantly white matter necrosis, while the lesions are restricted to the nerve roots in lower segments.

5.3 DISCUSSION

5.3.1 General

One of the basic questions of the present studies is which cell types are primarily involved in the development of damage. From the histopathological results summarized in Fig. 5.19, it is evident that fundamentally different types of lesions are observed depending on the dose, time after irradiation and region of the cord irradiated. This suggests the involvement of different target cells. Damage to the

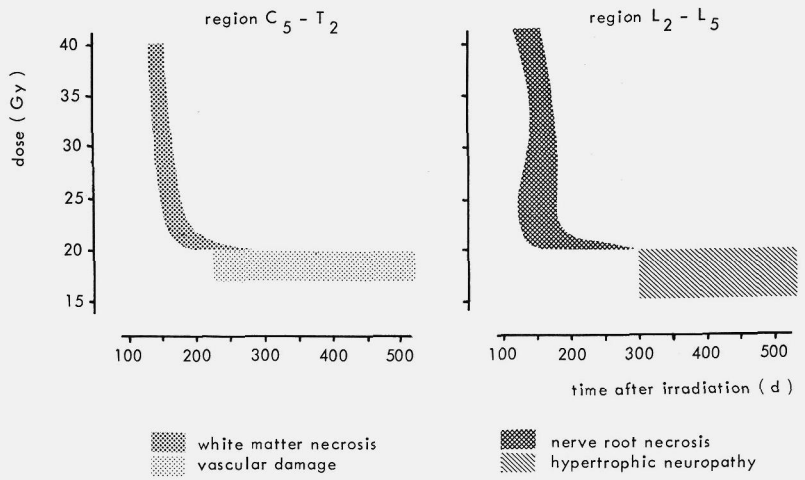

Figure 5.19

Time-dose relationships for the different types of lesions observed after irradiation of region C5-T2 and L2-L5.

neurons, astrocytes and microglial cells is not thought to be directly related to the development of the lesions. Neuronal chromatolysis was observed only in cases of severe gray matter infarction or found to be due to secondary retrograde degeneration. Although damage to astrocytes might play a role in the initiation of the radiation induced cord lesions, this could not be determined from the light microscopic observations. However, both astrocytes and microglial cells were observed to be involved in secondary cellular reactions.

Each of the three remaining cell types, the oligodendrocytes, Schwann cells and vascular endothelium, is assumed to be primarily involved in one or more specific types of lesions. The occurrence of different lesions and their dependence on the dose range and the time after irradiation suggests the presence of different dose-effect relationships for the induction of damage in the target cells (see Chapter VI). In addition to this dependence on dose and time, there appears to be a remarkable difference in susceptibility for each cell type related to the location in the spinal cord.

In the lumbosacral region, the main lesion for doses above 20 Gy is nerve root necrosis, which is primarily associated with Schwann cell damage. A different, chronic type of root lesion, also attributed to Schwann cells, is observed for doses in the range of about 15-20 Gy.

With doses of up to 40 Gy, no nerve root damage occurs in the cervical region and the predominant lesion observed over the dose range of 20-40 Gy is white matter demyelination and necrosis. This indicates primarily damage to oligodendrocytes. Over a small range of about 17-20 Gy, lesions of an indisputable vascular origin arise after long latent periods ranging from 7 months postirradiation to the end of the normal life span. The various types of lesions which are distinctly characterized will be discussed separately, with emphasis on the possible pathogenesis.

5.3.2 Cervical cord - white matter necrosis

With doses above 20 Gy, the lesions consist primarily of foci of demyelination which develop into necrosis of the white matter. This type of damage and its predilection for the white matter has been described for both the spinal cord and the brain for several species, but most extensively in rats (Innes and Carsten, 1962; Hopewell, 1975; Bradley et al., 1977; van der Kogel, 1977), rabbits (Scholz et al., 1962; Berg and Lindgren, 1958) and monkeys (Innes and Carsten, 1962;

Caveness et al., 1974). In the described serial killing experiments, it was observed that the first changes consisted of focal demyelination and the swelling of axons. The glial nuclei in these areas disappeared and necrosis rapidly developed. This sequence of events indicates the presence of a primarily demyelinating lesion, with the oligodendrocyte as the affected cell type. Several authors have recently elaborated on the role of the oligodendrocyte in the pathogenesis and the kinetics of this type of damage. After irradiation of the rat cervical spinal cord with 40 Gy of X-rays, Hubbard (1977) observed a reduction in the number of oligodendrocytes after one month. Control values were again reached within two months, but the cell density once more showed a steady decrease after three months. It was suggested that the white matter necrosis is due primarily to the loss of oligodendrocytes, while the slow turnover rate of these cells accounts for the delayed onset of necrosis. More insight into the degenerative process affecting the myelin sheath has been obtained by Mastaglia et al. (1976). The development of damage in individual myelinated nerve fibers was quantitatively assessed by teasing the fibers apart and by electron microscopic examination of cord sections at various time intervals after irradiation. As early as two weeks after irradiation with single doses of 5-60 Gy of X-rays, myelin breakdown was observed; this was followed by signs of remyelination after two months. No vascular damage was observed. It was concluded that the changes were suggestive of oligodendrocyte malfunction. Two important unsolved questions are: 1) what is the relationship between the random degeneration of myelinated fibers observed over the whole range of 5-60 Gy and the occurrence of necrosis, which has a well defined threshold of about 20 Gy; 2) does the remyelination occur upon replacement of the damaged oligodendrocytes by newly produced cells or upon some delayed type of intracellular repair? Results of experiments with increasing time intervals between two fractions (see Chapter VI) show the occurrence of a wave of recovery starting sometime between two and four months after irradiation. This time sequence is in agreement with the above-mentioned studies and seems to indicate that repopulation takes place. A constant finding in the present study is the increased number of glial cells at the borders of the demyelinated areas. In part, these cells are reactive astrocytes which occasionally show mitotic figures, but a number of them are likely to be newly produced oligodendrocytes. The capacity of oligodendrocytes in adult animals to proliferate locally and replace destroyed cells has recently been reported for an experimental demyelinating disease in mice (Herndon et al., 1977).

Combining the various experimental results leads to the following hypotheses concerning the sequence of events. Within a few weeks post-irradiation, accumulation of degenerated myelin sheaths and a depletion of the oligodendrocyte population induces a proliferative response. The proliferative phase is followed by regeneration of the myelin sheath after 2-3 months. Although this repair phase seems to occur with doses as high as 40-60 Gy, the recovery does not prevent the later breakdown of the tissue, which is preceded by a second wave of disappearance of oligodendrocytes above a critical level of 20 Gy.

The relative contribution of vascular damage to the development of white matter necrosis is difficult to assess. White matter necrosis observed in paralyzed rats is accompanied by recent petechial hemorrhages which are distributed randomly in gray and white matter, usually distant from the necrotic areas. These hemorrhages, which are indicative of local rupture of the capillary wall, become more conspicious with increasing doses. In general, vascular damage in the cervical cord appears to be restricted to capillaries and venules. Characteristic changes in arteries and arterioles such as hyaline degeneration of the wall and narrowing of the lumen by fibrin deposits were rarely observed.

5.3.3 Cervical cord - late vascular damage

Over a small dose range of approximately 17-20 Gy, vascular damage is specifically observed from about 7 months postirradiation up to the end of the life span of the rats (about 18 months postirradiation). A general aspect of these lesions is an increased density of capillaries and the occurrence of telangiectasias (severely dilated capillaries). A similar phenomenon has been observed in the rat brain (Reinhold and Hopewell, 1979) 1.5-2 years after a dose of 20 Gy. In the brain of rabbits irradiated with 21 and 23 Gy, telangiectasia was observed from 6 months postirradiation (Hassler and Movin, 1966).

The capillary proliferation might be a regenerative response in an attempt to compensate for a decreasing permeability of the endothelium for nutrients and oxygen due, e.g., to an increase in the thickness of the basal lamina (McDonald and Hayes, 1967). Capillary dilatation resulting in stretching of the endothelial cells might render the capillary wall more susceptible to rupture. This stage of proliferation and dilatation, defined as type 1, is thought to be the basis for the development of the chronic (type 2) and acute (type 3) vascular lesions; the possible pathway is presented in Fig. 5.20. However, the

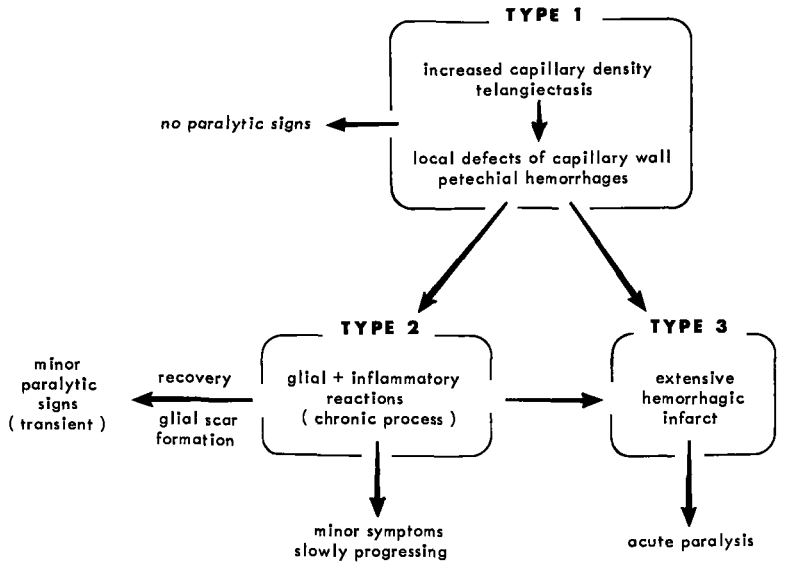

Figure 5.20

Pathogenesis of late vascular damage in the cervical cord. Possible pathways and relations between various types.

observation of type 1 lesions even at 18 months postirradiation suggests that these lesions do not always progress into the more severe stages.

These vascular lesions are markedly different from and do not lead to the characteristic white matter necrosis which is observed with doses above 20 Gy and a latent period of less than 7 months. This supports the conclusion that white matter necrosis and late vascular damage have a separate pathogenetic mechanism.

5.3.4 Lumbosacral cord - progressive radiculopathy

The major characteristic of the lesions induced in the lumbosacral region with doses of up to 60 Gy is progressive demyelination and necrosis of the nerve roots, with little observable damage of the cord. Schwann cells and myelin sheaths appear to be affected rather than the axons. This striking difference with lesions induced in the

cervical region (Van der Kogel and Barendsen, 1974) has been recently confirmed in various rat strains (Bradley et al., 1977; White and Hornsey, 1978). Histologically, lesions were observed to develop during one to two months before the animal showed neurological signs. The peculiar shape of the dose-latent period curve for WAG/Rij rats (Fig. 4-4) with doses between 20 and 30 Gy obviously reflects a difference in the kinetics of the development of damage. For a dose of 22 Gy, the progression of damage is significantly more rapid than for 30 and 40 Gy. This phenomenon seems to be strain dependent. It is not observed in BN rats and is therefore not regarded as an important aspect in the pathogenesis of the root damage.

Little vascular damage is seen in the lumbosacral cord, at least with doses up to 60 Gy (single doses). Thickening of the arteriolar wall or a focal hemorrhage is occasionally observed in the nerve roots. No equivalents of the various types of vascular damage as described for the cervical cord are found in the lumbosacral region. Only after extremely high doses of 80 and 100 Gy is a spectrum of changes including severe edema and hemorrhages observed in the lumbosacral cord. Obviously, the complete breakdown of the tissue with these high doses is difficult to attribute to one cell type.

5.3.5 Comparison of regional differences: white matter necrosis versus nerve root necrosis

The occurrence of completely different types of lesions at two levels of the spinal cord leads to the question of whether an explanation can be given on the basis of present knowledge. Theoretically, the differences might have their origin in a local variation in cellular turnover (Hubbard, 1977). No experimental data are presently available to support this hypothesis. Furthermore, it seems unlikely that both the Schwann cell and the glial cell populations show such abrupt changes in regional kinetics as are required to account for the marked differences. Therefore, it is thought to be more realistic to inquire whether the origin of the regional variability can be found by comparing similarities and differences between the two regions. Although the cervical and the lumbosacral regions are similar with respect to their cellular architecture, some important quantitative differences exist; these might in some way contain the clue to the marked differences in reactions.

In the cervical region, the cord of the rat has a diameter of about 4 mm, 75% of which is white matter (Waibl, 1973). The capillary

supply of the white matter is relatively poor as compared to that of the gray matter (Tveten, 1976). The nerve roots have a length of about 1 mm, which implies that only 1-3 Schwann cells per nerve fiber are irradiated (see Chapter II). The root diameter is 150-500 μ.

In the lumbosacral region, the cord diameter decreases from about 2 mm (at L2) to 0.5 mm (at L5), with only 30% consisting of white matter. The vascular supply to the lumbosacral cord is reported to be much better, with extensive intramedullary arterial anastomoses. This was thought to be an explanation for the preservation of the lumbosacral cord and the presence of severe lesions in the higher cord regions after clamping of the aorta (Tveten and Loken, 1975). The nerve roots in this area comprise 50-70% of the total space and are closely packed together. It is not known how the circulation in this bundle of roots compares to that in the isolated cervical and thoracic roots. These quantitative structural differences might be relevant to the pathogenesis.

At the time of irradiation, local differences in oxygen tension do not seem to be a basis for the regional variability in reactions. No shift in type of lesions is observed after irradiation under 100% oxygen conditions, although the threshold dose for the cervical region is decreased (Chapter VI). If the capillary permeability decreases after irradiation, this should have consequences for a region with a poor blood supply, especially when diffusion from the surrounding cerebrospinal fluid is not likely to be compensatory. This might explain the generally observed presence of a well preserved outer zone of nerve fibers around a necrotic bundle of roots (Figs. 5.9, 5.10). In addition, the existence of a common causative factor in the pathogenesis of the cervical white matter necrosis and the lumbosacral progressive nerve root necrosis is suggested by similarities in dose-effect relationships (Chapter VI), threshold dose and dose-latent period relationships (Chapter IV). Despite the different cell types involved in the two types of lesions, demyelination is a common characteristic. In experiments on the spinal cord white matter (Mastaglia et al., 1976) and in preliminary experiments on rat lumbar nerve roots, damage to the myelin sheath has been observed as early as 2 weeks after irradiation. This suggests a direct effect on the myelin membrane instead of damage expressed after cell division. Although no vascular damage is observed even at an ultrastructural level, changes in vascular permeability might play a role by interference with the normal myelin metabolism. Further experiments must be performed to determine the relevance of these early changes in the sequence of events which lead to the development of the late effects.

5.3.6 Chronic nerve root degeneration and hypertrophic neuropathy

For doses below 19 Gy (the threshold for the induction of progressive radiculopathy), a striking regional difference in damage is again observed. An equivalent to the late vascular damage in the cervical cord is not observed in the lumbosacral region. Over a dose range of approximately 15-19 Gy, a chronic degeneration of the roots in the cauda equina is observed, the characteristics of which are markedly different from the progressive nerve root necrosis seen after higher doses. In most rats, the lesions were accompanied by only minor neurological signs. Demyelination mainly of the ventral roots was observed to start 8-10 months postirradiation. Different grades of proliferation were observed. These varied from small foci with an increased number of Schwann cells (about 11 months postirradiation) to intense proliferation with swelling of the roots. The latter lesions were characterized by specific patterns, with concentric layers of Schwann cells in an "onion bulb" configuration as described for hypertrophic neuropathy and neurofibromas (Thomas et al., 1975). The greatest percentage and the most extensive lesions of this type are found in the oldest age group of more than 20 months. Probably, the proliferative changes divided into stage I and stage II (Table 5.1) represent a continuous series of stages of a slowly progressive lesion. This would be in accordance with the present views on hypertrophic neuropathy, which is considered a nonspecific lesion resulting from continuous proliferation of Schwann cells in the course of a chronic demyelinating process (reviewed by Thomas et al., 1975).

The distribution of malignant proliferative changes over the age groups, scored as stage III (Table 5.1), seems to be random. This is in contrast to the stage II lesions which increase in number with increasing age. Morphologically, the tumors do not show the concentric arrangements of Schwann cells which are characteristic for the benign lesions. These observations seem to indicate that the pathogenesis of the malignant Schwannomas is different from that of the other proliferative lesions scored as stage I and stage II (Table 5.1).

In aging unirradiated rats, degeneration of primarily the ventral nerve roots of the cauda equina was found at 18-20 months. The type of degeneration is very similar to the early less severe lesions of stage I in the irradiated rats. The proliferation of Schwann cells which is observed to occur abundantly in the ventral roots of irradiated rats was found only in the two oldest unirradiated rats (27 months). Age-related changes in peripheral nerves and spinal roots have been described in various species: rats (Berg et al., 1962; Gilmore, 1972;

Burek et al., 1976), dogs (Griffiths and Duncan, 1975) and man (Corbin and Gardner, 1937). Gilmore (1972) found the demyelination of ventral roots in unirradiated rats to start at the same age of 18-20 months as in the aging rats of the present study. However, in that paper, no differences in lesions and in age of onset were found between unirradiated rats and those irradiated on the spinal cord at 3 days of age. In the present study, demyelination of the ventral roots was observed at the age of 11-12 months in rats irradiated on the spinal cord with doses in the range of 15-19 Gy at the age of 3 months. Thus, a reduction in the age of onset of nerve root degeneration by almost 6 months is observed after irradiation of the adult spinal cord.

The pathogenesis of the lesions described (stage I and stage II), taking into consideration the differences between the late reactions after irradiation of neonatal and adult spinal cord, could be as follows. In the neonatal cord and nerve roots, there is active myelination and proliferation of Schwann cells. Irradiation of such a proliferating system is expected to lead to an early manifestation of damage due to death of cells during or after mitosis. If sufficient cells survive, repopulation occurs and the damage will be repaired. This general radiobiological mechanism probably operates in the neonatal spinal cord as well. Gilmore (1966) and Beal and Hall (1974) reported a rapid demyelination and a temporary delay in the formation of myelin, followed by remyelination, after irradiation of the neonatal spinal cord. In the adult animal, Schwann cells do not proliferate or only at a very low rate. Mitotic cell death as an effect of irradiation will become manifest only when the cells are stimulated to divide by some other form of injury. This has been shown by Cavanagh (1968) in peripheral nerves of rats. Based on results of the present study, it could be assumed that this latent radiation damage might interfere with or accelerate a pathological process associated with normal aging. The resulting demyelination could be a stimulus for other Schwann cells to divide and a number of unsuccessful attempts at remyelination might lead to the observed lesions.

5.3.7 Comparison of the histopathology of human and rat radiation myelopathy

Various types of distinct lesions have been described for the rat spinal cord in this Chapter. In man, radiation myelopathy can be classified into several major syndromes based on distinct clinical or pathological characteristics. The question arises as to whether the

different syndromes in man are comparable with the lesions observed in rats. Therefore, the human syndromes will be discussed and their pathogenesis compared with the experimental results.

1. Transient radiation myelopathy.

This type is characterized by sensory disturbances (Lhermitte's sign of electrical paresthesia) which develop after a short latent period of about 3 months and symptoms disappear in most patients within a few months. Usually, later persistent myelopathy of another type does not develop. This syndrome has been reported for both the spinal cord (Jones, 1964; Dynes and Smedal, 1960) and the brain (Rider, 1963). Partly because of neurological similarities with known demyelinating disorders such as multiple sclerosis, these authors suggested the occurrence of demyelination followed by recovery. Although transient sensory disturbances are not likely to be detected in rats, recent experiments on the rat spinal cord (Mastaglia et al., 1976) showed demyelination after 2-3 months; this was followed by subsequent recovery (see section 5.3.2).

2. Disseminated demyelination or "early" delayed radiation myelopathy

The small number of patients reported to exhibit this syndrome (Jellinger and Sturm, 1971; Lampert and Davis, 1964; Rider, 1963) showed demyelination, swelling of axons, a diminished number of oligodendrocytes and no vascular changes. A more severe stage of this reactivity is probably represented by the occurrence of coagulative necrosis of the white matter (Burns et al., 1972). Both the histopathological aspects and the short latent periods (about 3-6 months) suggest a similarity with the white matter necrosis type of lesions observed in the rat cervical spinal cord.

3. Chronic progressive myelopathy.

This syndrome is the most common in patients with latent periods varying from 6 months up to about 4 years. In most cases, the origin of the lesions was thought to be primarily vascular, with telangiectasia as a constant finding (reviewed by Jellinger and Sturm, 1971; Palmer, 1972). The histopathology and the variable latent period show a striking similarity with late vascular damage (type 2) observed in the present studies.

4. Acutely developing paraplegia or quadriplegia.

This syndrome is rarely observed in man (Boden, 1950) and is thought to be the result of hemorrhagic infarction, although a patho-

logical description is not found in the literature. In the present experimental studies, this syndrome is probably represented by late vascular damage type 3 (acute hemorrhagic infarction) which was observed in a total of 9 rats.

A common aspect of the lesions observed in the cervical and thoracic cord in man is the normal appearance of the nerve roots and spinal ganglia, even in the presence of severe cord necrosis Jellinger and Sturm, 1971; Kristensson et al., 1967). This was attributed to a difference in radiosensitivity between Schwann cells and glial cells. In the studies reported here, a similar resistance of the nerve roots was found in the cervical region, but a reverse effect was seen in the lumbosacral region. The presence of such a regional variability in damage is also indicated for the human spinal cord by the occurrence of a specific syndrome in the lumbar cord (see below).

5. Lower motor neuron syndrome.

This syndrome represents damage to the anterior horn cells and/or their axons and occurs specifically after irradiation of the lumbosacral spinal cord and cauda equina. In all patients showing this syndrome, the main symptoms are flaccid paraparesis and muscular atrophy, without sensory disturbances (Greenfield and Stark, 1948; Gänshirt, 1975; Sadowsky et al., 1976; Kristensen et al., 1977). Primary damage to the cell bodies or the proximal fibers of the motor neurons was favored as the mechanism, in the absence of a histopathological description. At first sight, this syndrome is in accordance with the muscular atrophy and paresis observed in the lumbosacral irradiated rats. However, histological examination reveals that the progressive radiculopathy affects both the dorsal and the ventral roots and this is expected to result in sensory as well as motor disturbances. It is also possible that the human syndrome is more closely related to the chronic nerve root degeneration which affects mainly the ventral roots in rats.

Despite the presence of some minor differences between the lesions observed in rats and man, the general characteristics of the various lesions are largely similar in both species. This suggests the operation of common mechanisms for the induction of damage, which also emphasizes the suitability of the rat as an animal model for predictions of similar effects in man.

CHAPTER VI

SPINAL CORD TOLERANCE: TIME-DOSE-ISOEFFECT RELATIONSHIPS

6.1 INTRODUCTION

One of the most important factors determining the success of clinical radiotherapy is the tolerance of critical dose limiting normal tissues. In this chapter, the tolerance of the spinal cord and its dependence on dose fractionation, dose-rate and overall treatment time will be discussed. In addition, the effect of various factors, e.g., the type of anesthetic agent, oxygen concentration and the age of the rats at the time of irradiation will be analyzed for responses to single doses.

In clinical considerations, tolerance levels are determined by the probability of development of permanent neurological damage in a small percentage of patients (Chapter I), irrespective of the length of the latent period or the type of syndrome. It was shown in the previous chapter that, despite the presence of neurologically similar symptoms, the pathological mechanisms involved in the development of late damage can be different. This suggested the involvement of different cell types as target cells. In this chapter, dose-effect relationships for specific types of lesions will be analyzed, in order to provide more insight into the mechanisms of development of damage and into the dependence on various factors.

From the isoeffect relationships obtained from experiments with multiple fractions and varying overall times, the repair processes and proliferative regeneration could be analyzed. An advantage in these experiments, in contrast to those on rapidly proliferating tissues, is that proliferation of possible target cells in the spinal cord is minimal under normal conditions. Thus, for relatively short overall times, recovery can be attributed to cellular repair processes.

The expression of some types of lesions in tissues can be assumed to be related to a requirement of a fixed critical percentage of surviving target cells for integrity and function of the tissue. By comparison of the effectiveness of various fractionation schemes with doses that all result in the same level of tissue damage, various characteristics of so-called isoeffect curves can be calculated. For survival of cells, these parameters include the ratio of the initial

to final slope or the extent of the initial exponential region of the survival curves. These characteristics allow predictions about the therapeutic gain for specific fractionation schemes, provided that some of these characteristics are also known for tumors.

6.2 RESULTS

6.2.1 Cervical cord

In the cervical cord, the threshold for the occurrence of paralytic symptoms during the lifespan of the rats corresponds to vascular lesions types 2 and 3 . As discussed in Chapter V, the type 1 vascular lesion is regarded as a stage from which potentially type 2 or 3 lesions may develop. In a series of experiments designed to establish tolerance doses, a number of rats which had to be killed because of severe respiratory disease were subsequently classified as having type 1 lesions. As a consequence, the lack of a long follow-up for this group of rats represents a factor of uncertainty in establishing definite tolerance levels. Nevertheless, when rats in an experimental group develop no lesions of any type within one year after irradiation, the applied dose is regarded as being below the threshold level.

In addition to their histological characteristics, the two main categories of damage, i.e., white matter necrosis and vascular damage, can be distinguished on the basis of the time of development, with the point of transition at about 7 months postirradiation. Thus, by separation in time, dose-response curves representing a specific lesion, presumably due to damage to a specific target cell, can be constructed.

In Figure 6.1, dose response curves for single dose and two-fraction experiments are shown. Some of the curves were constructed by computer probit analysis and are accompanied by the 95% confidence intervals, but sigmoid curves were fitted by eye for the data which did not fulfill the requirements for probit analysis. The slopes of most of the dose-response curves are rather steep, indicating that a small increase over a tolerated dose results in a considerable percentage of paralyzed rats. As illustrated in Figure 6.1, two series of dose-response curves could be derived. The curves in A represent the induction of paralysis due to white matter necrosis, which occurs within 7 months postirradiation, while the curves in B represent the induction of neurological signs due to vascular damage type 2 or 3. In the ex-

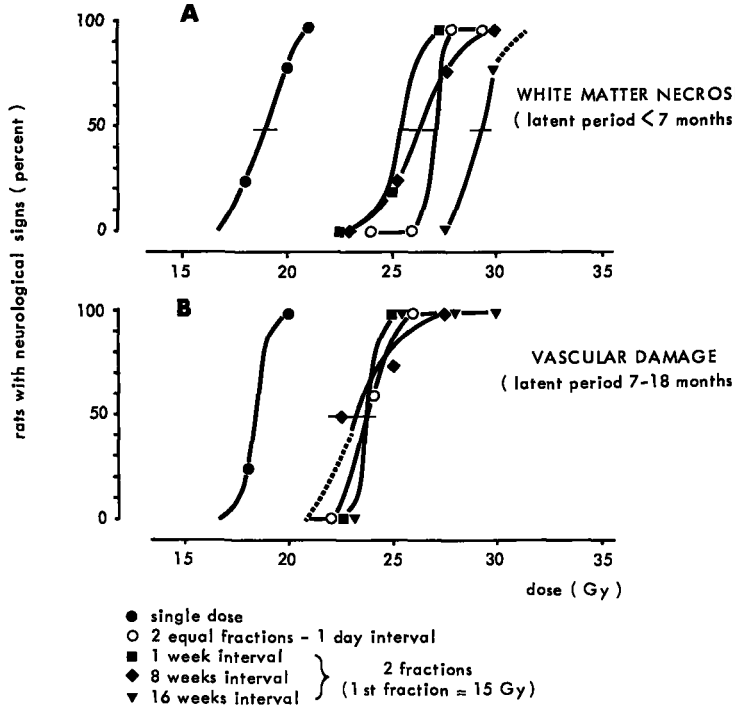

Figure 6.1

Dose-response curves for two different syndromes in the cervical cord of WAG/Rij rats. For the curves fitted by probit analysis the 95% confidence limits are shown, other curves are fitted by eye.

periments with single doses and two equal fractions, dose response curves were also constructed for all vascular types, thus including the type 1 lesions which are only observable at the microscopical level. Ideally, absolute tolerance levels have to be based on the latter curves, which represent the lowest doses at which the animals are at risk for developing paralytic signs during their lifespan. Unfortunately, the data in a number of experiments do not allow the construction of complete dose-response curves for vascular damage. In these experiments, threshold doses are approximated by using the mean values between the highest dose at which no vascular damage is observed for at least 1 year postirradiation and the lowest dose at which vascular damage is observed. For those animals developing paralysis at one year or more postirradiation, it is especially important to determine the histological type of damage, because the neurological signs may also be due to invasion and compression of the cord by tumors induced in the irradiated surrounding vertebrae and muscular tissue.

TABLE 6.1.

ISOEFFECT AND THRESHOLD DOSES FOR THE INDUCTION OF SPECIFIC TYPES OF DAMAGE IN THE CERVICAL CORD

Experiment	Time	white matter necrosis (ED_{50})	vascular damage type 2/3* (ED_{50})	vascular damage all types** (ED_{50})	threshold
single dose	-	19 ± 0.5 Gy	18.5 ± 1.7 Gy	17.8±0.5 Gy	17 Gy
2 f	4 h	25.5	22.3 ± 0.5	20.8±0.7	20
2 f	1 d	27	24	23	23
5 f	4 d	37.8	-	-	32.5
10 f	11 d	55	-	-	45
30 f***	40 d	$>$ 80	-	-	$>$80
60 f***	40 d	$>$108	-	-	96
2 f	7 d	25.5	24	-	$<$ 22.5
(1st = 15 Gy)	56 d	26.1 ± 0.9	22.8 ± 2.8	-	$<$ 22.5
	112 d	29	24	-	$<$ 22.5
single dose (halothane/O_2)	-	16.9 ± 0.5	16 ± 0.6	-	$<$ 15
single dose (9-months old rats)	-	$>$21	19.8 ± 1.2	17 ±0.8	16.5

ED_{50} values with 95% confidence limits derived from computer probit analysis, other ED_{50} values from dose response curves fitted by eye. Threshold doses represent the mean value of the lowest dose at which vascular damage of any type is observed and the highest dose with no vascular damage within at least one year after irradiation.
* in general accompanied by neurological symptoms;
** including type 1, which is damage at a microscopical level;
***anesthesia: 1% ethrane/99% O_2. For the 60 fractions: 2 fractions/day with 6 h interval.

From the dose-response curves, isoeffect doses can be obtained, e.g., the ED_{50}, defined as the dose at which 50 percent of a group of rats develop paralysis or a histologically defined specific type of damage (Table 6.1). In Figure 6.2, the ED_{50} values for the induction of paralysis due to white matter necrosis are plotted versus the number of fractions of equal magnitude on a double logarithmic scale (curve 1). A straight line is fitted by least square analysis for 1-10 fractions, yielding a slope of 0.46 (correlation coefficient 0.996). At the highest doses applied in the experiments with 30 and 60 fractions, 80 and 108 Gy, respectively, no paralysis was observed at one year postirradiation.

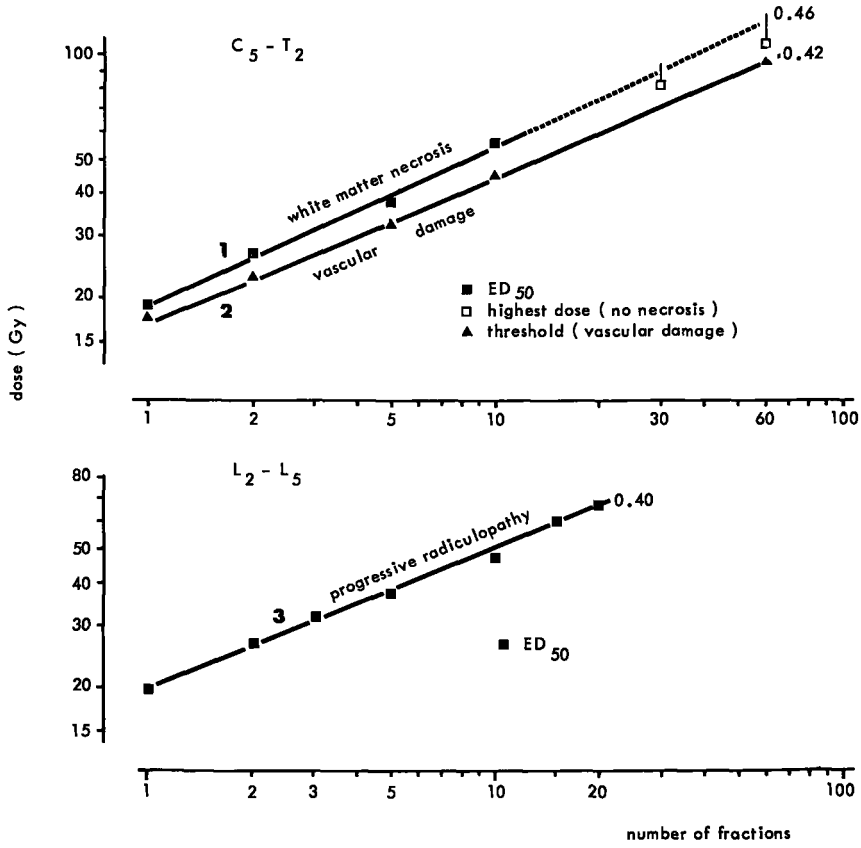

Figure 6.2

Isoeffect curves for the induction of different syndromes in the cervical and lumbosacral cord of WAG/Rij rats. The ED_{50} (curves 1 and 3) or threshold dose (curve 2) is plotted versus the number of fractions.

For the vascular damage, only for single dose and two-fraction experiments complete dose-response curves could be constructed from which ED_{50} values could be obtained. Therefore, in order to derive isoeffect lines, "approximated threshold doses" have also been plotted and a straight line which has a slope of 0.42 (correlation coefficient 0.999), is fitted for these approximate threshold doses. This curve 2 thus represents the minimal tolerance level below which no rats of the WAG/Rij strain are expected to develop any type of damage during their

lifespan. It shows that these values are lower than the ED_{50} data for white matter necrosis.

The influence of the overall time was estimated in split dose experiments with various time intervals. With intervals of up to 56 days, there is no significant difference in the ED_{50} for white matter necrosis. However, in the experiment with an interval of 112 days, significant additional recovery, equivalent to an extra dose of about 3 Gy was observed. This increase in ED_{50} is not evident for the induction of late vascular damage (Type 2/3). From the split-dose experiments with time intervals of 7 days and longer, a "threshold dose" could not be determined.

It is important to note that in a series of experiments with single doses, the responses are definitely affected by the anesthesia or the oxygen concentration. In the single dose experiments employing 1% halothane/99% O_2 for anesthesia, the ED_{50} values were decreased by 2-2.5 Gy. In the 30 and 60 fraction experiments, anesthesia was performed with 1% ethrane/99% O_2. The sensitizing effect is suggested to be minimal in these experiments, because the ED_{50} values are at most 5-10% below the extrapolated ED_{50} curve (curve 1, Figure 6.2).

The single dose response of 9-month-old rats shows an increase in ED_{50} of at least 2 Gy for the white matter necrosis syndrome, but threshold values for vascular damage are not different from those obtained for rats irradiated at the age of 3 months (see Table 6.1).

6.2.2 Lumbosacral cord (L2-L5)

The effect observed in this region of the cord, i.e., the development of muscular atrophy of the hind legs followed by paresis, is due to a progressive necrotizing nerve root degeneration (radiculopathy). Similar to the cervical white matter necrosis, the latent period at threshold dose levels is about 6-7 months. The chronic type of nerve root degeneration observed after irradiation with doses below the threshold for progressive necrotizing radiculopathy, results in only a mild muscular atrophy of the hind legs in most cases. The development of severe paralysis sometimes observed a year or longer after irradiation generally is due to the development of a tumor (see Figure 4.3). Thus, in contrast to the cervical cord, with increasing time intervals beyond 8-9 months postirradiation, the significant shift in dose response curves due to vascular damage does not occur for the lumbosacral cord. In Figure 6.3, dose-response curves most of which were constructed by probit analysis, are presented. For those experiments

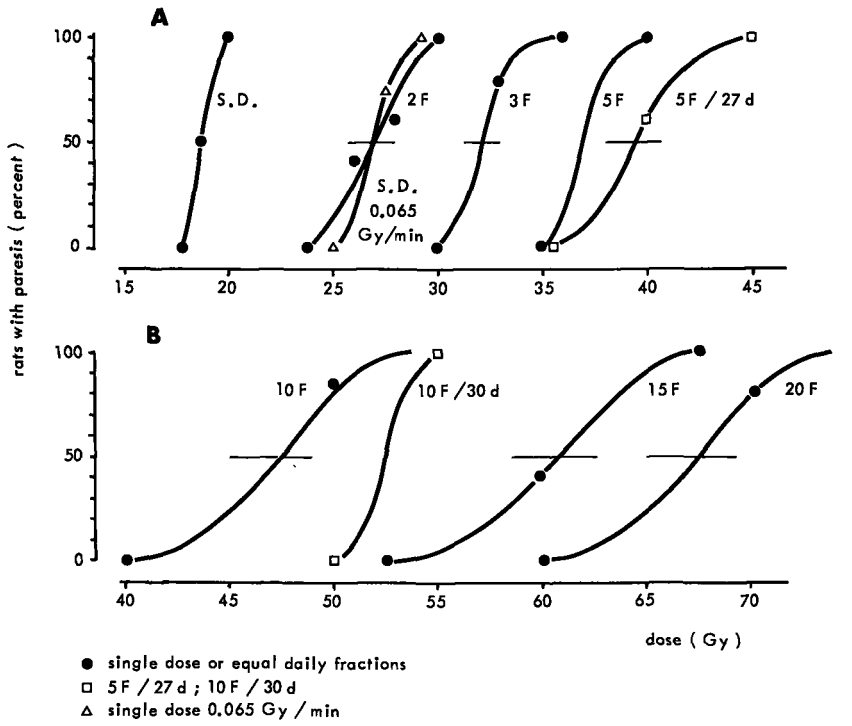

Figure 6.3

Dose-response curves for induction of hind leg paresis after irradiation of region L2-L5 of WAG/Rij rats.
A: Single dose, 2, 3 and 5 fractions
B: 10, 15 and 20 fractions.
For the curves fitted by probit analysis the 95% confidence limits are shown, other curves are fitted by eye.

yielding only a 0 percent and a 100 percent isoeffect dose, sigmoid curves were fitted by eye. Especially in the experiments with 10 or more fractions the dose increments are relatively large, which limits the precision of the estimation of the slope of the curves. The ED_{50} values derived from these curves (Table 6.2) are plotted versus the number of fractions on a double logarithmic scale for those experiments employing equal daily fractions (curve 3, Figure 6.2). The slope of the line, fitted by least square analysis, is 0.40 $\pm$ 0.015.

The relative contribution of time dependent recovery was estimated in split-dose experiments with increasing time intervals and in experiments using 5 fractions in 27 days and 10 fractions in 30 days. The

TABLE 6.2.

ISOEFFECT DOSES FOR THE INDUCTION OF PROGRESSIVE RADICULOPATHY IN THE LUMBOSACRAL CORD

Experiment	Time	ED_{50} (Gy)
single dose	± 10 min	19.5
single dose	± 8 h	26.9 ± 0.6
single dose (halothane/O_2)	± 10 min	19
2 f	1 d	27 ± 1
3 f	2 d	32.1 ± 0.7
5 f	4 d	36.8
5 f	27 d	39.4 ± 1.2
10 f	11 d	47.7 ± 1.3
10 f	30 d	52.3
15 f	18 d	60.4 ± 2
20 f	25 d	67.1 ± 2
2 f	1 d	25.6 ± 0.75
2 f	6 d	25.1 ± 0.5
2 f	27 d	± 27
2 f	55 d	> 27

lst = 15 Gy

95% confidence limits are indicated for data derived by computer probit analysis

results indicate that, in contrast to the cervical cord, some additional recovery starting between 1 week and 4 weeks postirradiation takes place. Unfortunately, an exact estimation of the dose equivalent for this type of recovery cannot be obtained from the present split dose experiments, because, with an interval of 55 days and more, the maximal applied dose was found to be below the threshold. Further experiments will be required to clarify this effect.

It is finally of interest to note that an increase in ED_{50} of about 35 percent was obtained when single doses were applied at a low dose rate of 0.065 Gy/min instead of 3 Gy/min.

6.3 DISCUSSION

6.3.1 Quantitative evaluation of fractionation effects

The present results with fractionated irradiation show that the spinal cord has a large capacity for repair of subeffective damage. Several concepts have been employed to describe the effect of frac-

tionation of doses and repair in intervals quantitatively. Most of these concepts are based on survival curve characteristics. In some cases, however, the deductions have been made on the basis of idealized survival curves. One of these concepts is the recovered dose. The average recovery per fractionation interval, expressed as radiation dose recovered, can be calculated as $(D_N - D_1)/(N-1)$, where D_1 and D_N are the isoeffect dose, applied as a single dose or in N fractions, respectively. This concept raises several problems but it will be used only for the possibility to compare different systems. The relative recovery per fractionation interval expressed as dose recovered/dose per fraction increases with an increasing number of fractions from about 55-60 percent for two fractions of 13.5 Gy up to 75 percent for 20 fractions of 3.35 Gy (L2-L5) and up to about 85% for 60 fractions of 1.8 Gy (C5-T2). When compared to other normal tissues, these values are among the highest reported (see review by Withers, 1975).

Assuming that the repair phenomena observed in vivo have characteristics in common with those in vitro, a measure for the width of the shoulder of a cell survival curve, or D_Q, is represented by the value of $D_2 - D_1$. Each of the two dose fractions has to be large enough to reduce survival well below the shoulder in order to obtain the maximum value of D_Q. In the present experiments, this requirement might not have been fully met in the split dose experiments employing a fixed first dose of 15 Gy. As can be seen in Tables 6.1 and 6.2, the resulting ED_{50} from these experiments is, for both regions of the cord, somewhat lower than that obtained from the experiments employing two equal fractions. This indicates the presence of a wide shoulder, which is in general a characteristic of organized tissues.

As discussed in Chapter V, the various types of lesions observed in the spinal cord are assumed to be the result of damage to specific target cells. For cervical white matter necrosis and lumbar radiculopathy, the $D_2 - D_1$ (or D_Q) values are, at the ED_{50} levels, 8 Gy and 7.5 Gy, respectively, and these cannot be considered as significantly different. For late cervical vascular damage, however, the value of $D_2 - D_1$ is significantly lower, namely 5.5 Gy. That this lower $D_2 - D_1$ value does not necessarily predict a greatly reduced repair capacity with multiple small fractions is reflected by the slope of 0.42 of the curve for vascular damage as compared with 0.46 for the white matter necrosis.

For the spinal cord, the recovery during the fractionation intervals must be largely attributed to intracellular repair phenomena, because nearly all of the target cells suggested to be involved are in a noncycling or G_0 stage (see Chapter II). This is obviously an advan-

tage in studies on the repair capacity of cells in vivo, since the results obtained for relatively short overall times are not expected to be complicated by redistribution of cells over the division cycle and by proliferation (repopulation).

6.3.2 Isosurvival curve characteristics as derived from organized tissue responses

An important fundamental problem which is also of interest to the radiotherapist is whether there is a limit to the amount of cellular recovery with decreasing doses per fraction. Employing a scoring system for human skin desquamation, Dutreix et al. (1973) reported that, for doses below 2 Gy per fraction, no further increase in the tolerated total dose was observed with a further decrease in the dose per fraction. This conclusion was reached by determination of the dose increment which had to be added when each single daily dose was replaced by two equal doses per day with 8 h intervals. In several animal tissues, a similar phenomenon was observed with small doses per fraction (reviewed by Field and Hornsey, 1977).

The effect of fractionation can be studied in more detail by analysis of isosurvival characteristics. To construct survival curves from tissue responses, it has to be assumed that isoeffect doses derived from experiments with a varying number of fractions reflect a similar level of survival of the target cells. Based on microdosimetric concepts (Kellerer and Rossi, 1972) and on biological data gathered from the literature (Chadwick and Leenhouts, 1973), it has been suggested that cell survival curves for doses smaller than 5 Gy are well approximated by an equation of the form:

$$S = e^{-(a_1 D + a_2 D^2)} \qquad (1)$$

In this equation, S is the surviving fraction, D the dose per fraction and a_1 and a_2 are constants representing the probability of single hit and two hit lethal events, respectively. In this model, the initial part of the survival curve will be exponential, due to irreparable single hit events. With increasing dose, the curve will start to bend downward because of additional cell killing due to accumulation of sublethal events, representing the two-hit component. As a consequence, the effect of decreasing the doses per fraction will be lost when the size of the dose per fraction is within the region where cell survival is dominated by irreparable single hit events.

A method by which an estimate of the relative contribution of a linear and a quadratic component of cell survival in organized tissues in vivo can be made has been described by Douglas and Fowler (1976). Multifractionation experiments on mouse skin were performed during short overall times of 8 days or less to keep the contribution of repopulation at a minimum. Using a defined isoeffect level of desquamation, a linear relationship was found between the reciprocal of the isoeffect dose and the dose per fraction. The resulting straight line could be described by the equation:

$$\frac{1}{D_N} = a + bD \qquad (2)$$

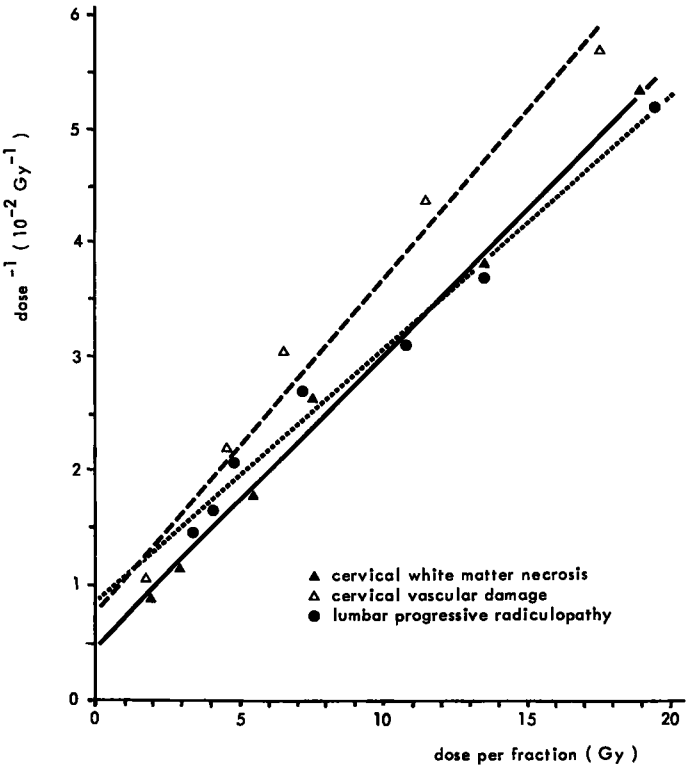

Figure 6.4

Relationship between reciprocal of the isoeffect dose for different syndromes and the dose per fraction.
Straight lines are fitted by regression analysis. Values of the intercept and slope of the curves are shown in Table 6.3.

where D is the dose per fraction, D_N the total isoeffect dose, $\underline{a}$ is the intercept and $\underline{b}$ the slope of the line. The intercept and the slope were shown to be proportional to, respectively, a_1 and a_2 in equation (1). In our experiments, isoeffect doses have been obtained for damage to the lumbosacral cord for up to 20 fractions and for damage to the cervical cord for up to 60 fractions (Table 6.1 and 6.2). For the 30 and 60 fraction experiments on the cervical cord, the ED_{50} is probably not much below the extrapolated values of, respectively, 90 and 120 Gy (see Figure 6.2) and are, for the present calculations, conservatively approximated at 85 Gy (30f) and 110 Gy (60f). This is supported by the observation of Hornsey and White (1979) on the lumbar cord, showing an ED_{50} for 60 fractions of 112 $\pm$ 10 Gy. In Figure 6.4, the reciprocal of the ED_{50} values and threshold doses for vascular lesions have been plotted versus the dose per fraction. Regression analysis showed that the data are not incompatible with straight lines, the characteristics of which are presented in Table 6.3. The inverse of intercept $\underline{a}$ represents the maximally tolerated dose for an infinite number of small fractions or for continuous irradiation at a low dose rate. The values of 118 $\pm$ 15 Gy (lumbar), 130 $\pm$ 40 Gy (cervical threshold) and 210 $\pm$ 30 Gy (cervical white matter necrosis) are much higher than the reported 75.8 Gy for mouse skin (Douglas and Fowler, 1976). The ratio $(\frac{a}{b})$ of the parameters derived from the intercept and the slope of the curve is the dose at which $a_1 = a_2 D$ in equation (1), i.e., the dose at which the linear term is equal to the quadratic term. The obtained values of 3.9, 2.8 and 1.9 Gy indicate that only at very low doses of about 0.2-0.4 Gy per fraction will the contribution of the quadratic term be less than 0.1 of the contribution of the linear term and accumulation

TABLE 6.3.

ISOSURVIVAL CURVE CHARACTERISTICS

	$a(10^{-2}\ Gy^{-1})$	$b(10^{-3}\ Gy^{-2})$	$\frac{1}{a}$ (Gy)	$\frac{a}{b}$ (Gy)
cervical white matter necrosis	0.47 $\pm$ 0.07	2.5 $\pm$ 0.1	210 $\pm$ 30	1.9 $\pm$ 0.4
cervical vascular damage (threshold doses)	0.77 $\pm$ 0.24	2.8 $\pm$ 0.23	130 $\pm$ 40	2.8 $\pm$ 1
lumbar progressive radiculopathy	0.85 $\pm$ 0.11	2.2 $\pm$ 0.16	118 $\pm$ 15	3.9 $\pm$ 0.8

of reparable sublethal events can be considered to be negligible at smaller doses.

Another generally used method for comparing isosurvival characteristics of tissues is based on the ratio of the initial to the final slope. As illustrated in Figure 6.5 (from Field and Hornsey, 1977), the final slope is proportional to D_1-D_Q. Similarly, the initial slope is proportional to D_N for $N \longrightarrow \infty$, which is the inverse of intercept a from equation (2). The slope ratio is then derived from $(D_1-D_Q)/D_N$. For the three specific types of damage in the spinal cord, these ratios are between 0.05 and 0.1. Thus, the initial slopes are 10-20 times less steep than the final slopes. These values are higher than those obtained for other normal tissues and tumors, where the ratios are between 0.1 and 0.4 (reviewed by Elkind, 1976).

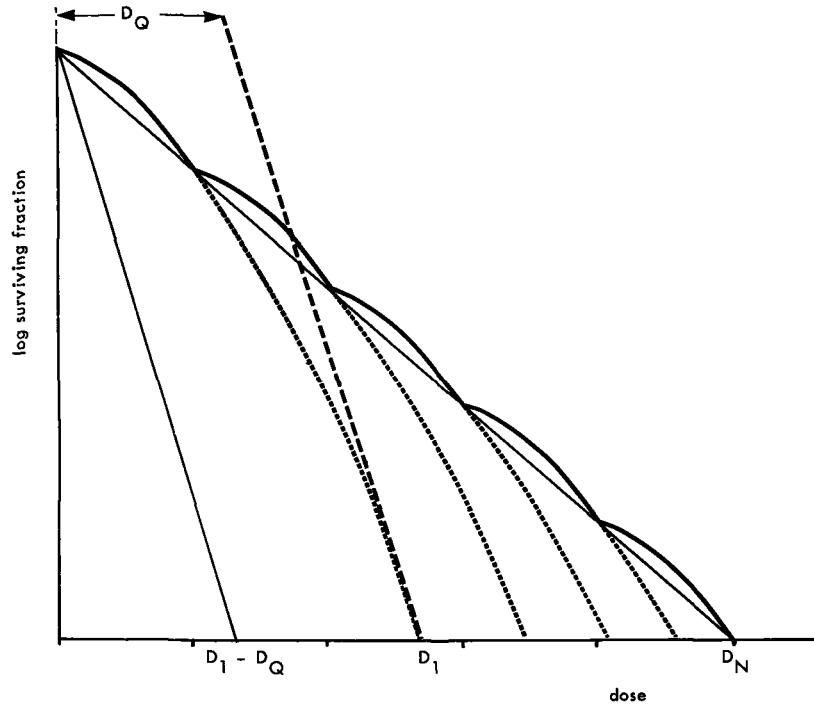

Figure 6.5

Hypothetical survival curves for single doses and N fractions, reaching the same level of damage with dose D_1 and D_N, respectively. The ratio of the final slope of the survival curve to the intercept slope up to the dose per fraction D_N/N is given by $(D_1-D_Q)/D_N$ (from Field and Hornsey, 1977).

On the basis of a single experiment, the reliability of extrapolation of the obtained curves to low doses per fraction cannot be estimated. It can be tentatively concluded, however, that, with an increasing number of fractions, the tolerance of the spinal cord is expected to reach a maximum value at much larger doses as compared to a number of other normal tissues. This might be exploited clinically to increase the therapeutic ratio in those treatments where the CNS is the main dose limiting tissue.

6.3.3 *Repair kinetics over one day*

Some insight into the kinetics of the repair mechanisms can be obtained by using the method of Liversage (1969). With this method, the biological effects of high-dose-rate fractionated irradiation in N fractions are predicted on the basis of data obtained for continuous irradiation during $\underline{t}$ hours. For each value of $\underline{t}$, one value of N can be calculated for the condition that the same total dose is required for equal effects. Liversage developed the formula which is based on the assumption that sublethal damage shows an exponential fading with a half-life τ :

$$N = \frac{\mu t}{2\left[1-\frac{1}{\mu t}(1-e^{-\mu t})\right]} \quad ; (\mu = 0.693/\tau) \qquad (3)$$

A value for τ of 1-2 hours was derived from studies in monocellular cultures and rapid renewal systems (Liversage, 1969). In the present experiments on effects of irradiation on region L2-L5 of the rat spinal cord employing a dose rate of 0.065 Gy/min, the ED_{50} is 26.9 Gy (Table 6.2). It can be seen that this value corresponds with N=2 after high dose rate fractionated irradiation. Fitting these data in the formula results in a value for τ of 2 hours. This value also seems to be similar for the cervical cord. For the two-fraction experiment with an interval of exactly 4 hours, the D_2-D_1 value for the various types of damage is 70-80 percent of the D_2-D_1 value determined for an interval of about 24 h. This agrees with the 4 hour period being about twice the half-time for repair of sublethal damage. These observations in the lumbar and cervical cord indicate that at least the kinetics of this type of repair are similar in tissues with a high as compared to a low turnover rate of cells.

6.3.4 Time dependent recovery over long intervals: repopulation or slow repair?

In experiments carried out to investigate the shape of isosurvival curves in vivo, care has to be taken to exclude as much as possible the effect of proliferation. Therefore, these experiments employing a large number of fractions on rapid renewal tissues such as skin and intestine were performed in overall times of a week or less (Douglas and Fowler, 1976; Withers, 1975). For the usual clinical treatment periods of 6-8 weeks, repopulation may account for a significant part of the tolerance of the rapid renewal systems. From observations on human skin, Dutreix et al. (1973) even concluded that, at doses per fraction smaller than 2 Gy, the increase in tolerance observed is mainly due to repopulation.

For nonrenewal or conditional renewal systems such as the liver, kidney, lung and CNS, proliferation might be expected to have a limited influence for short overall times. The most simple method to separate the relative contribution of sublethal damage repair from time-dependent recovery is to use various time intervals in split dose experiments. In the cervical cord (white matter necrosis syndrome), with intervals of up to 56 days, no additional recovery increasing the tolerance above that for a 1 day interval was observed. Thus, the significant additional recovery observed for a 112 day interval started somewhere between 56 days and 112 days (compare Table 6.1). Although no estimate can be made concerning the kinetics of this type of recovery, the results indicate that repopulation takes place. Accumulation of tissue damage due to mitotic death of cells which normally have a slow turnover, could provide a stimulus for proliferation at a certain stage. This explanation is supported by the cell kinetic data of Hubbard (1977). As discussed in more detail in Chapter V, this author found an increase in oligodendrocytes at two months postirradiation. Thus, for the cervical white matter necrosis syndrome, there is a good correlation between histological, cell kinetic and radiobiological data. It appears, however, that the additional recovery, which is probably attributable to a specific target cell, does not influence the tolerance of the cervical cord. Due to the occurrence of vascular damage as late as 1 1/2 year postirradiation, the effect of additional recovery is totally lost. Apparently, time-dependent recovery does not occur in the vascular type of damage, at least for intervals of up to 112 days.

For the lumbosacral radiculopathy, different kinetics of time-dependent recovery seems to be involved. In split-dose experiments, ad-

ditional recovery was observed to start rather early, somewhere between 1 and 4 weeks. This indicates a rapid reaction of normally slowly proliferating Schwann cells. The high regeneration capacity of Schwann cells after various types of injury has been widely documented (see Chapter II). Recent experiments on the pathogenesis of lumbar radiculopathy have shown that degeneration of separate myelin segments (each segment represents one Schwann cell) starts as early as two weeks after irradiation. This could be a stimulus for the regeneration starting relatively early.

It is also worthwhile to consider whether a correlation exists with "slow repair" as has been reported by Field et al. (1976) for split dose irradiation of the mouse lung. However, the latter type of repair started immediately upon irradiation and was attributed to an intracellular process similar to, but much slower than, the "Elkind-type" of repair of sublethal damage. In the present experiments, in both the cervical and the lumbosacral cord, additional recovery is observed to start after a delay period and this favors the involvement of repopulation. This is supported by recent observations on the lumbar cord by White and Hornsey (1978), who found a delay between 15 and 32 days before additional recovery started. In addition, Masuda et al. (1977) observed no increase in tolerance of the rat thoracic cord for a time interval of 15 days between two fractions, as compared to a one day interval. In the kidney, a delayed wave of proliferation probably accounts for the strong increase in tolerance observed to start between 18 and 39 days after a first dose (Hopewell, 1977, personal communication).

It can be concluded that the delayed type of recovery observed in the spinal cord indicates the occurrence of repopulation and this recovery is different from the "slow repair" observed for mouse lung.

6.3.5 Isoeffect formulas

Isoeffect formulas are used in clinical radiotherapy to determine normal tissue tolerance for a given fractionation scheme in comparison with a standard scheme. These formulas represent a relationship between the tolerance dose and the number of fractions and the overall time for a defined biological effect, e.g., 5 percent incidence of late effects. The most generally used formula is the one proposed by Ellis (1968). Ellis made several assumptions for his derivation. The basis for his formula was the slope of 0.33 of an isoeffect curve for skin desquamation. From this exponent, a time factor was derived by

subtraction of an exponent of 0.22 obtained from an isoeffect curve for cure of squamous carcinoma, assuming that a time factor does not apply for a tumor. After correction of the exponent for the number of fractions from 0.22 to 0.24, the resulting formula was $D = NSD \times N^{0.24} \times T^{0.11}$ (see also Chapter I). It was further assumed that this formula represents general connective tissue tolerance in the whole body. Although the separation in time related and fractionation related factors is in itself a valuable contribution to a better understanding of time-dose relationships in radiotherapy, the derivation of the exponents in the Ellis formula, especially of the time factor, are at least disputable. Since the total exponent of 0.33 was derived from isoeffect doses for skin tolerance, it is not surprising that the formula is of practical value in radiotherapy when skin is the dose limiting tissue and for treatments whereby doses per fraction and overall times are usually coupled ($N = 5/7\ T$). However, it is highly questionable whether the formula is also valid for the prediction of late skin reactions (Berry et al., 1974) or for the prediction of tolerance of other tissues.

From the preceding parts of this discussion, it has become clear that a fixed exponent for both the N and T factors is highly unlikely to be generally applicable. A constant exponent for the N factor representing intracellular repair during fractionation intervals implies a continuous rise in tolerance with an increasing number of fractions. It has been shown in section 6.3.2 that, with the presence of an initial exponential region on the survival curve, the isoeffect dose will reach a maximum value with an increasing number of fractions and the N exponent will become zero. The dose per fraction that is small enough for repair to be at its maximum value, differs for various tissues as discussed in 6.3.2. These considerations show that a constant N exponent will result in an overestimation of the repair capacity at high values of N, which is tissue dependent. As calculated in a previous paragraph, this value is expected to be greater for the spinal cord as compared to the skin. In practice, the leveling off of an isoeffect curve due to the limit in repair capacity might be masked by increased proliferation. In the original Ellis formula, the latter process is represented by the factor $T^{0.11}$, which assumes a constant rate of regeneration from the start of treatment. However, the time of onset and the rate of repopulation varies considerably from tissue to tissue. In a rapid renewal tissue such as the skin, it has been shown that proliferation is minimal during the first days, while the rate increases with increasing damage during fractionated treatment (Denekamp, 1973). In split-dose experiments on the pig kidney, a tissue which normally

has a slow turnover of cells, a T exponent was estimated to be zero during an initial period of 18 days (Hopewell, 1977, personal communication). Additional recovery occurring between 19 and 39 days was suggested to be equivalent to about $T^{0.3}$. A similar trend was observed for multiple fractions for the rabbit kidney (Caldwell, 1975).

From the present experiments on the cervical spinal cord, it could be concluded that tolerance doses are based on the occurrence of late vascular damage. The slope of the log-log plot of threshold doses versus the number of fractions is 0.42. This value represents the sum of the exponents for T (overall time) and N (number of fractions) in a formula of the type $D \sim N^{\alpha} \cdot T^{\beta}$.
From the results of split dose experiments with varying time intervals, it can be concluded that $\beta = 0$, at least for an interval of up to 112 days. Therefore, an applicable isoeffect formula for tolerance of the cervical cord would be:

$$D \sim N^{0.42} \quad \text{(for N = 1-60)}.$$

In the lumbosacral cord, tolerance is based on the occurrence of progressive radiculopathy for which some early repopulation appears to occur. For treatment periods of up to 30 days, the time during which all multiple fractionation experiments were carried out, the value of a time correction factor is estimated to be approximately $T^{0.02}$. With a slope of the isoeffect curve of 0.40, the formula would be:

$$D \sim N^{0.38} \cdot T^{0.02} \quad \text{(for N = 1-20; T} \leqslant \text{30 days)}.$$

It can be concluded that isoeffect formulas can be of practical value, but only for the tissues and conditions for which they are derived. The indiscriminate use of one formula for all tissues at risk is expected to impede the development of radiotherapy and might even be dangerous to patients.

6.3.6 Rat spinal cord tolerance: the value for predictions in man

After the discussion of the more fundamental aspects of repair, repopulation and isoeffect formulas, the clinically most relevant question which remains to be considered is the value of the isoeffect relationships obtained for the rat in relation to the human spinal cord tolerance. As described in the previous chapters, there appear to be considerable similarities between the rat and human spinal cord with regard to latent periods and pathological syndromes.

It cannot be expected that tolerance levels as derived for the rat are applicable to the human spinal cord in absolute value. In the rat, all values can be considered to be derived for one individual, because of the great extent of inbreeding in the strain of animals used. In man, a substantial individual variation can be expected, which can be increased by factors such as high blood pressure, atherosclerosis, use of chemotherapeutic agents, etc. Nevertheless, in view of the aforementioned other similarities, the rat spinal cord may be assumed to be a good model for the establishment of time-dose relationships relevant to man. The tolerance levels as reported for the human spinal cord will be discussed briefly below and compared with the present data obtained for the rat.

The first reported tolerance level for the human spinal cord (Boden, 1950) was based on the log-log plot relating the biologically effective dose and the overall time similar to that for skin erythema and skin carcinoma (Strandqvist, 1944). A curve with a slope of about 0.26 was shifted along the vertical dose axis so that all cases with myelopathy were situated above the curve. Some 10 years later, Pallis et al. (1961) proposed a further shift of the curve to lower dose values, because of a few additional cases which occurred at doses below the level suggested by Boden (1950). The first real change in approach to the tolerance of the human spinal cord was made by Atkins and Tretter (1966). These authors suggested the number of fractions to be more relevant than the overall time and showed that the curve with a slope of 0.26 as previously generally used overestimates the tolerance at a small number of fractions but underestimates it at 20 or more fractions. Regression analysis of their cases suggested a slope of 0.38 for a log-log plot of dose versus number of fractions. This exponent was thought to reflect mainly the effect of fractionation. Phillips and Buschke (1969) also concluded that the tolerance of the spinal cord appeared to increase with the number of fractions more rapidly than the isoeffect curves for skin tolerance. The same conclusion was reached in a later report (Wara et al., 1975) including more cases.

Thus, both clinical and experimental data indicate that the tolerance of the spinal cord is much more dependent on the number of fractions than on the overall time. This is also the conclusion of a recent review by Lambert (1978). Although this characteristic of spinal cord tolerance has been recognized for a long time (Atkins and Tretter, 1966), most reports do not contain detailed information on the number of fractions, dose per fraction, etc. As a result, the number of reported cases from which a dose-isoeffect relationship can be

derived is limited. An exact determination of human spinal cord tolerance is further complicated by factors such as the irradiated volume, different sensitivity of the cervical and thoracic cord, difficult determination of cord dose and poor survival of patients at risk. Nevertheless, a crude estimate of cord tolerance can be made by combining data from adequate reports, together covering a wide range of fraction numbers. In Figure 6.6, these doses are plotted versus the number of fractions. A straight line is fitted in such a way that most cases of myelopathy are situated above this line over a range of 2-60 fractions and irrespective of the overall time of treatment. Most weight is given to those data providing information on the incidence. The extrapolation of a straight line down to a few fractions is justified by the experimental results and is also supported by the cluster of cases at 19 Gy/two fractions. The accurately documented cases reported by Reinhold et al. (1976) are all well above the proposed curve. The latter authors concluded on the basis of statistical analysis that the treatment time of the patients who developed myelopathy (42 days) was significantly longer than of the patients who did not develop this

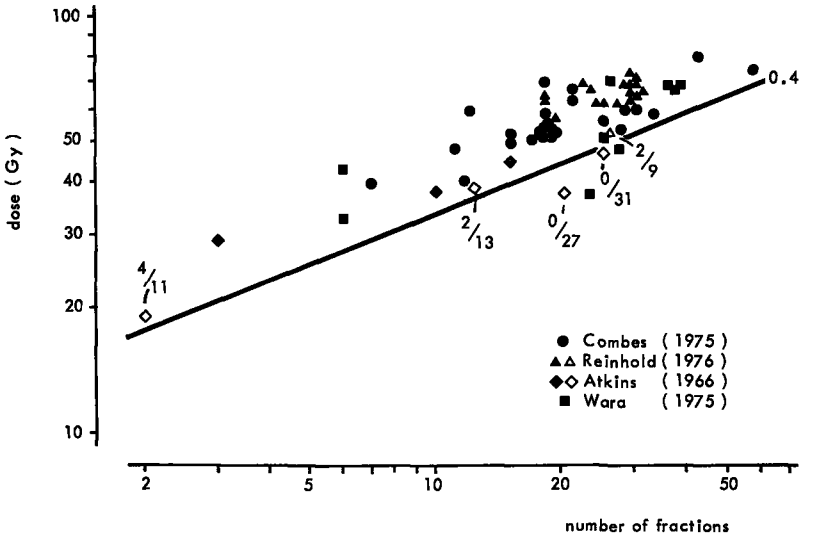

Figure 6.6

Tolerance dose curve for the human spinal cord as a function of the number of fractions. Closed symbols represent individual cases of radiation myelopathy in human patients. Open symbols represent the incidence of myelopathy in relation to dose and fraction number for patients who survived at least one year after irradiation.

complication (37 days) after essentially the same treatment. However, in view of the present experimental results and other clinical reports, it appears highly unlikely that this 5 day difference in overall treatment time has any biological significance.

In conclusion, the isoeffect curve constructed for clinical data (Figure 6.6) suggests a similarity with the experimental results obtained in rats. An isoeffect formula relating a tolerated dose to the number of fractions would be $D = NSD \times N^{0.4}$, while, for the usual treatment period of about 6 weeks, the time factor is negligible. Although more and accurate clinical data are required, this formula is expected to be a better guide for calculating tolerance doses for the spinal cord as compared to the original Ellis formula.

CHAPTER VII

EFFECTS OF 15 MeV NEUTRONS

7.1 INTRODUCTION

The tolerance of different regions of the spinal cord and the various pathological mechanisms involved in the development of late damage have been discussed in the previous chapters. It was concluded from studies on fractionated treatments that the spinal cord has a large capacity for repair of subeffective damage, which is completed within a few hours after irradiation. These results were obtained with X-rays, a low LET type of radiation. An important question is to what extent this repair capacity is also observed when irradiation is carried out with fast neutrons.

Much attention has been given during the past decade to the possibility of using fast neutrons in radiotherapy. At the time of the first clinical trial of fast neutrons by Stone et al. in Berkeley (USA) (1940), little was known about the radiobiological mechanisms involved in cell death and tissue reactions. The use of neutrons was quickly abandoned as excessive late normal tissue damage was observed.

About 20 years ago, the phenomenon of accumulation and repair of sublethal damage was demonstrated for mammalian cells in culture (Elkind and Sutton, 1959). This was soon followed by the observation of Barendsen et al. (1960) that, with increasing LET, the accumulation of sublethal damage decreased (see Figure 1.1). The reduced shoulder on a cell survival curve and the reduced OER observed with high LET radiation (see Chapter I) indicated the potential usefulness of fast neutrons in radiotherapy. One of the decisive factors is whether the RBE for effects on tumors is higher than for effects on the surrounding normal tissues, especially at clinically relevant doses.

The first experience in treatments of patients was the development of excessive late necrosis, which led to the conclusion that the RBE for late effects is greater than the RBE for acute normal tissue damage (Stone, 1948). This difference was later shown not to exist for reactions of the skin of pigs, mice and rats (reviewed by Field, 1976). This observation gave the confidence to again initiate the use of neutrons in the Hammersmith Hospital in London. However, there is still some controversy, since recent experiments on pig skin (Withers

et al., 1977) and mouse intestine (Geraci et al., 1977) indicate that the RBE for late damage is greater than that for acute effects with doses per fraction similar to those used clinically.

In the current clinical trials with fast neutrons, the largest group of tumors treated are those situated in the head and neck regions. These locations are favorable for these trials because the relatively poor depth dose characteristics of neutrons as compared to high energy X-rays or gamma rays and because the immobility of most neutron producing machines are less disadvantageous. For these locations, the brain and spinal cord are among the most important dose limiting tissues, especially with regard to the late effects. After the treatment of brain tumors, both Catterall (quoted by Field, 1977) and Parker et al. (1976) reported the development of dementia, which was not explained by tumor growth or brain necrosis as observed with X-rays. The occurrence of brain damage has recently been observed in a number of centers in the U.S.A. and in Europe and the primary pathological lesion seems to be extensive demyelination (Proc. Third meeting on Fundamental and Practical Aspects of the Application of Fast Neutrons and other High LET Particles in Clinical Radiotherapy, 1978, The Hague). In patients treated for neck tumors, myelopathy developed with doses which were expected to be within safe limits (Ornitz et al., 1977). Because of this experience, the RBE for central nervous system has been increased to 4 in a number of centers, from the general value of 3 which had been used in clinical practice for damage to most normal tissues.

The RBE values used for various normal tissues in clinical trials were initially derived by extrapolation from experimental results obtained with single doses or a few large fractions. RBE values of neutrons for damage to the spinal cord have been reported to be close to 1 for large single doses (Geraci et al., 1974) and 1.7 for five fractions (van der Kogel and Barendsen, 1974). These values are not different from values obtained for acute reactions in other tissues. In this chapter, the results obtained with single doses and 5 fractions of 15 MeV monoenergetic neutrons on the lumbosacral cord will be compared with those from experiments employing an increasing number of daily fractions of about 0.9 Gy. Data obtained from irradiations of the cervical cord with a single dose or 5 fractions are limited, because most rats did not survive long enough to develop cord damage.

The irradiation procedures and dosimetric aspects have been described in Chapter III.

7.2 RESULTS

7.2.1 Histopathology

a. Progressive necrotizing radiculopathy (L2-L5); latent period, < 6 months postirradiation.

The types of lesions observed in the lumbosacral cord after irradiation with 15 MeV neutrons are basically the same as those induced with X-rays. The first type is a progressive necrotizing radiculopathy resulting in muscular atrophy and paresis within 3 to 5 months after irradiation, depending on dose and fractionation scheme. The dose-latent period relationship for single doses is presented in Figure 4.6. With an increasing number of fractions, the latent period decreases. After a dose of 25 Gy, the mean latent period is 128 $\pm$ 6 (single dose), 105 $\pm$ 4 days (5 fractions) and 98 $\pm$ 4 days (29 fractions), all relative to the first day of irradiation.

Because only a small number of rats was available for serial killing experiments on the pathogenesis, the progression through the various stages of nerve root degeneration could not be analyzed in as much detail as for X-rays (see Chapter V). Some insights into the development of the lesions could be obtained from 9 rats killed before the occurrence of paralytic signs. After irradiation with doses of 16.5-20 Gy (single doses) and 20.5-25 Gy (5 fractions), the first signs of damage (stage $\pm$, as defined in 5.2.2.a) were observed at 90 and 70 days postirradiation, respectively. The progression from stage $\pm$ to +++ (nearly complete necrosis) took place in about 30 days for both groups, while differences between dorsal and ventral roots were not significant. As observed with X-rays, the development of necrosis starts in the center and progresses towards the outside of the roots, an outer rim of which usually remains well preserved.

b. Chronic nerve root degeneration (L2-L5)

Rats surviving more than 6 months postirradiation do not develop the extensive necrosis of both dorsal and ventral roots. In the present experiments with single doses as low as 10 Gy, all of the rats surviving the "acute" type of damage did develop the chronic root lesions with a varying degree of severity. This type of damage mainly affects the ventral roots and consists of demyelination and extensive proliferation of Schwann cells, presumably as an attempt at regeneration (Chapter V). In comparison with the

X-ray induced chronic degeneration (with doses of X-rays between ± 15 and 19 Gy), the chronic lesions induced with neutrons are generally more severe, including focal necrosis. This is reflected in some animals by a slowly progressing muscular atrophy and paresis starting from 6-10 months postirradiation, even after a single dose as low as 10 Gy. The formation of "onion bulbs" which cause local swelling of the roots as observed with X-irradiation has not been noted in the neutron irradiated rats.

Late vascular damage seems to be more pronounced with neutrons as compared to X-rays in the lumbosacral cord. Hemorrhagic infarction of the cord occurred in 4 out of 17 rats surviving for more than a year postirradiation.

c. Cervical cord

Most rats irradiated on the neck area with a circular beam of 25 mm diameter died after 30-40 days from severe pneumonia (see Chapter IV, 4.2.1). After a single dose of 13.5 Gy of 15 MeV neutrons, two animals developed paralysis at 187 and 197 days postirradiation. The lesions consisted of demyelination and necrosis of the lateral and ventral columns of the white matter, similar to the damage induced with X-ray doses above 20 Gy. Two other rats from the group that received 13.5 Gy of 15 MeV neutrons survived 224 and 246 days with no neurological or histological damage observable in the spinal cord. From the group irradiated with 18 Gy of neutrons, the last animal died at 161 days postirradiation without observable damage to the spinal cord. Of all groups irradiated with 5 fractions, only 3 rats survived for more than 100 days (namely, 178, 178 and 193 days), all after irradiation with 5 x 3.6 Gy. No changes were observed in the spinal cord of these rats.

7.2.2 Dose-effect relationships and the relative biological effectiveness

Similar to the X-irradiated lumbosacral spinal cord, two phases in the development of damage can be distinguished: a rapidly progressing "early" phase occurring within 5 months and a chronic degenerative phase. With X-rays, the chronic type of damage hardly influences the derivation of tolerance levels, because, in most rats, it is neurologically undetectable or results in mild muscular atrophy. With neutrons, the chronic type of lesion results in some animals in paresis

which can only be discriminated from the early acute type on the basis of the latent period. In the present experiments, dose-effect relationships could be analyzed only for the acute damage, because, even at the lowest doses applied (10 Gy), some rats developed paresis due to chronic degeneration.

In Figure 7.1, dose response curves are shown for single dose and 5 fraction experiments. The curves were constructed by computer probit analysis and the 95% confidence intervals are given. For calculation of the RBE of 15 MeV neutrons, the equivalent X-ray curves are also plotted, as presented in Chapter VI.

From the experiments with a varying number of fractions with a fixed dose of 0.865 Gy (N + γ), a dose-response curve cannot be constructed. Only in the lowest dose group (19.9 Gy/23 fractions), had 2

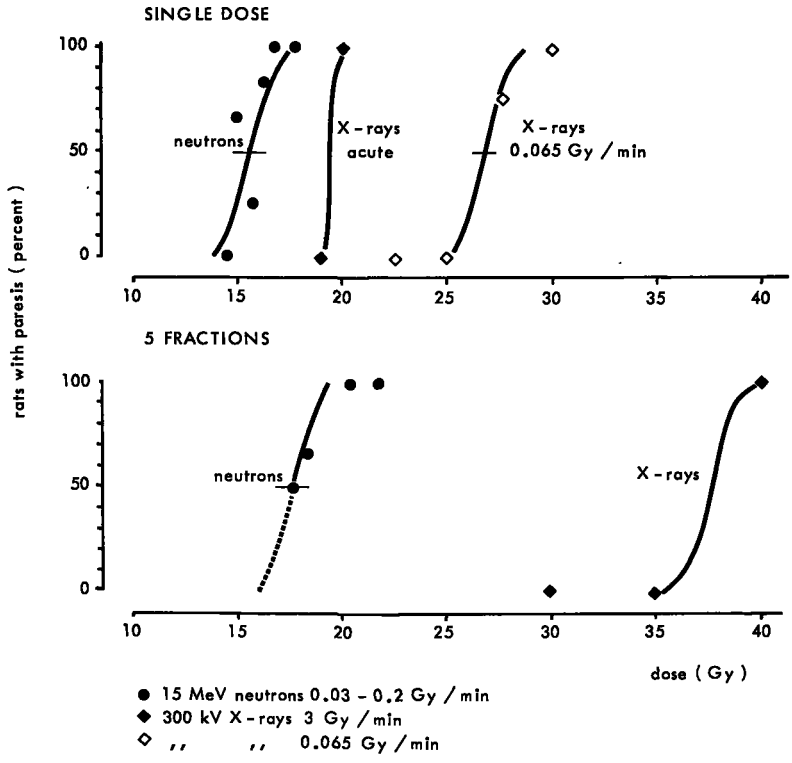

Figure 7.1

Dose-response curves for induction of lumbar progressive radiculopathy with 300 kV X-rays or 15 MeV neutrons. Horizontal bars represent the 95% confidence interval for the curves fitted by probit analysis, other curves fitted by eye.

out of 4 rats not developed the progressive necrotizing radiculopathy within a period of six months postirradiation. The two other animals from this group and all of those irradiated with higher doses (from 21.6 Gy/25 fractions up to 25 Gy/29 fractions) developed paresis within 4 months from the first day of irradiation. The two remaining rats irradiated with 19.9 Gy in 23 fractions were killed after 200 and 230 days with minor paresis. Histologically, the damage observed in these two animals consisted of demyelination and small areas of necrosis in dorsal and ventral roots. The lesions in the ventral roots were the most severe and were accompanied by proliferation of Schwann cells. This type of damage can be regarded as intermediate between the acute progressive and the chronic type. When the shift in histological type of damage observed with 19.9 Gy in 23 fractions is correlated with the results of the other neutron and X-ray experiments, this dose can be estimated to be within the 50-100% incidence range.

The ED_{50} values obtained from the dose response curves and from the experiment with 23 fractions or more are presented in Table 7.1.

TABLE 7.1

DOSES REQUIRED TO INDUCE PROGRESSIVE RADICULOPATHY (L2-L5) AND THE RBE OF 15 MeV NEUTRONS

	ED_{50} (Gy)		RBE
	neutrons	X-rays	
single dose	15.7 ± 0.7	19.5 ± 0.5 (3 Gy/min)	1.2
	-	26.9 ± 0.6 (0.065 Gy/min)	1.7
5 fractions	17.7 ± 0.75	37.5	2.1
23 fractions	19 ± 0.75	70	3.7

In Figure 7.2, the ED_{50} values for the induction of progressive necrotizing radiculopathy with 15 MeV neutrons and 300 kV X-rays are plotted versus the number of fractions on a double logarithmic scale. It can be seen that only a slight increase in ED_{50} is obtained when a neutron dose is administered in 23 fractions instead of in 5 fractions. As a consequence of the strong repair capacity of the spinal cord for X-ray induced subeffective damage, the RBE increases significantly with decreasing dose per fraction and reaches a value of 3.7 for a dose of 0.9 Gy (N + γ) of neutrons.

For the cervical spinal cord, RBE values can only be estimated tentatively. With a single dose of 13.5 Gy, two out of four rats developed paralysis due to white matter necrosis, indicating an ED_{50} of about 13.5 Gy and an RBE of 1.4 for the "acute" type of damage in the cervical cord. With 18 Gy in 5 fractions, no rats surviving 6 months postirradiation showed paralysis, yielding an upper limit to the RBE value equal to 2.1. No rats survived more than 250 days and no vascular damage was observed within that period.

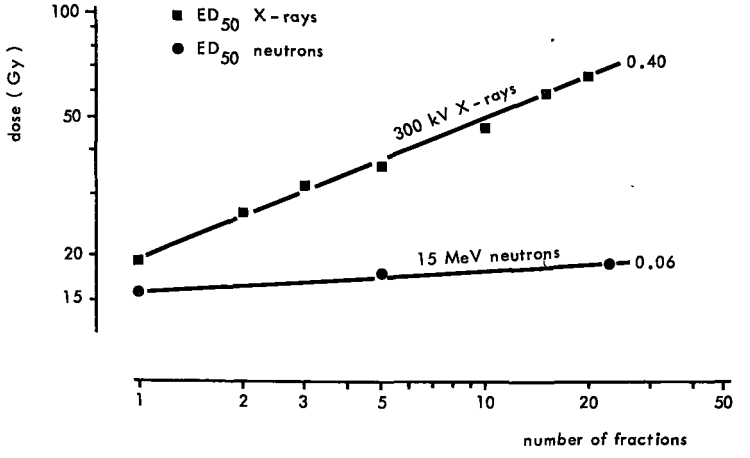

Figure 7.2

Isoeffect curves for induction of lumbar progressive radiculopathy. The ED_{50} is plotted versus the number of fractions.

7.3 DISCUSSION

7.3.1 Factors determining the effectiveness of neutrons relative to X-rays

Different factors have been shown to influence the greater effectiveness of fast neutrons as compared to X-rays for damage in different systems, e.g., cells in culture, skin or intestine. With acute single doses, the main factors are the increased damage that is not dependent on accumulation of subeffective damage and the presence of hypoxic cells. With fractionated treatments, additional factors which might be different for neutrons as compared to X-rays are the capacity for repair of subeffective damage, changes in cell cycle distribution and in repopulation.

a. Oxygen Enhancement Ratio (OER)

While hypoxia is not thought to play a role in most normal tissues (with cartilage and the CNS as possible exceptions) in the normal unanesthetized animal, this condition might be induced by the often unavoidable anesthesia in a number of experimental conditions. This has been reported, e.g., for rodent tails (Hendry, 1976), rat skin (Field and Bewley, 1974), and mouse esophagus (Phillips et al., 1974). In the previous chapter it was shown that irradiation of rats breathing 99% O_2 did not result in a significantly reduced ED_{50} for lumbar progressive radiculopathy, which is attributed to damage to Schwann cells. This indicates that hypoxia is unlikely to be an important factor in these experiments. Thus, the RBE of 1.24 observed for the latter effect is suggested to be due to increased damage that is not dependent on accumulation of subeffective damage or a reduced D_0 value.

For the cervical cord, the presence of a given degree of hypoxia in the white matter is suggested by the decrease in ED_{50} from 19 Gy to 17 Gy when rats were irradiated while breathing 99% O_2 during treatment. Thus, the higher RBE of 1.4 observed for cervical white matter necrosis could be attributed in part to the presence of hypoxia.

b. Dose rate

A factor which does not play a role with single doses delivered at a high dose rate is the repair of subeffective damage. However, in the present experiments, the effective neutron dose rate was only about 0.05 Gy/min. With this dose rate, a substan-

tial repair of subeffective damage can occur during irradiation, as illustrated by the results of the X-ray experiments carried out at a low dose rate. The ED_{50} obtained with X-rays at a dose rate of 0.065 Gy/min is increased by almost 40% relative to acute single doses (Table 7.1). It can be assumed that most of the probably small amount of repairable subeffective damage induced during the neutron irradiations does not accumulate but is repaired during the treatment.

c. Effect of fractionation on acute and late responses

More insight into the influence of the repair capacity is obtained from fractionated irradiation. As can be derived from Figure 7.2, the ED_{50} for fractionated treatments shows only a slight increase with an increasing number of fractions, as expressed by a slope of 0.06 of the isoeffect curve. The relative recovery expressed as the dose recovered/dose per fraction is 14% and 18% for 5 and 23 fractions, respectively. For late damage in the mouse lung (Hornsey et al., 1975) and for rat tail necrosis (Hendry et al., 1976) after neutron irradiation, it has been reported that the total tolerated dose is not increased by reducing the dose per fraction. For both the lung and the tail, maximal repair was observed with two fractions and further fractionation with larger numbers of fractions had no effect. Although no maximum was observed for the effect of fractionation for the spinal cord, it can be concluded that, for these late effects, the relative recovered dose is in the range of 10-20% of the total dose.

The influence of repair appears to be greater for early reactions in tissues such as the skin and intestine as compared with reactions of the lung, spinal cord and tail. In a recent report on early and late effects in mouse small intestine (Geraci et al., 1977), it was concluded that a significant sparing effect of fractionation was observed for both early and late effects with X-rays as well as with neutrons. However, when the percent recovered dose per fraction is calculated from their data, the difference between acute and late damage is quite significant. For acute damage after neutron irradiation, the recovery increases from 27% (two fractions) to 46% (five fractions) and for late damage only from 10% (two fractions) to 15% (five fractions). With X-rays, the percent recovered dose is similar for acute and late damage, namely, about 60% with five fractions.

This phenomenon of a greater reduction in the repair capacity for late effects as compared to acute effects after neutron irra-

diation, appears to support the observation that RBE values tend to be greater for late effects as compared to acute effects with doses per fraction of less than 2 Gy of neutrons.

d. Repopulation

The general observation that the RBE increases with decreasing dose per fraction can be explained on the basis of cell survival curve characteristics which vary with LET (see 7.3.2). However, this does not explain a difference between early and late effects. In addition to the differences in repair, repopulation could play a role in treatment times of several weeks. For the early effects occurring in tissues with a rapid turnover of cells, repopulation contributes significantly to the recovery of the tissue. Several authors have found no difference in repopulation in skin after neutrons and X-rays (reviewed by Field, 1976). With a strongly decreased repair capacity after neutrons, repopulation becomes the most important factor contributing to the total recovery, as reflected by a modified "Ellis formula" proposed for neutron irradiation of the skin: $D_N \sim N^{0.04} \times T^{0.11}$ (Field, 1972). For late effects developing in tissues with a slow turnover of cells, repopulation is usually of minor importance during the first weeks of irradiation. The slope of 0.06 for the neutron curve in Figure 7.2 represents the sum of the exponents for N and T in an isoeffect formula. For X-ray induced progressive radiculopathy (region L2-L5), the mean exponent for T for treatment times of 1-4 weeks is about 0.02 (see 6.3.5). If the rate of repopulation is not different for neutrons as compared to X-rays, an isoeffect formula for the present spinal cord results could be derived as: $D_N \sim N^{0.04} \times T^{0.02}$. This formula only differs in the exponent for T from the one proposed by Field for skin.

Another factor which might increase the effectiveness of neutrons versus X-rays for the induction of late effects is slow repair, which is suggested to take place with X-rays but not with neutrons (Field, 1977). However, the phenomenon of slow repair has been demonstrated only for damage to the lung up to now.

7.3.2 The RBE in relation to survival curve characteristics

In Chapter VI, isosurvival curve characteristics have been derived for the various types of X-ray induced lesions and the different target cells. The relative contribution of a linear (a_1) and quadratic

(a_2) term in the equation:

$$S = e^{-(a_1 D + a_2 D^2)} \quad (1)$$

were determined by plotting the inverse of the total dose versus the dose per fraction required for a given endpoint (Figure 6.4). In the present experiments with neutron induced damage in the lumbar spinal cord, the lesions are similar to the progressive radiculopathy as observed with X-rays. In Figure 7.3, the data presented in Figure 6.4

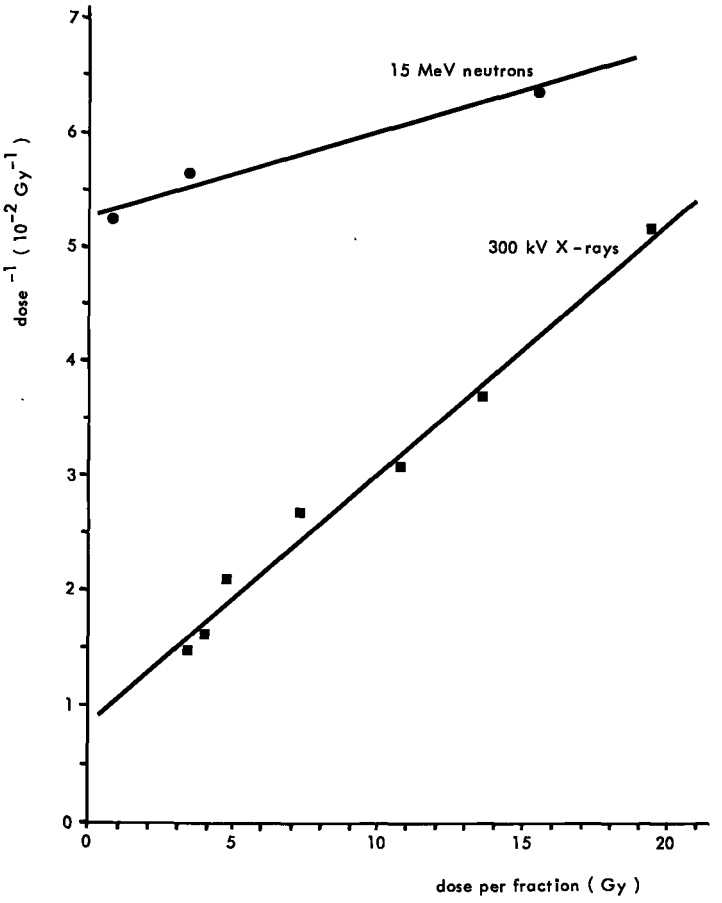

Figure 7.3

Relationship between reciprocal of the isoeffect dose for induction of lumbar progressive radiculopathy and the dose per fraction. Values of the intercept and slope of the curves are shown in Table 7.2.

for X-rays are compared with those obtained for neutrons. The curves are described by the formula $\frac{1}{D_N} = a + bD$, in which a and b are proportional to a_1 and a_2 in formula (1), respectively. From the values presented in Table 7.2, it can be seen that for neutrons a is larger by a factor of 6 and b smaller by a factor of 3 as compared to X-rays. As a consequence, the ratio a/b is increased from 3.85 Gy for X-rays to about 75 Gy for neutrons. Thus, for doses in the clinical range of 1-2 Gy per fraction, the contribution of the quadratic term is almost negligible and virtually no accumulation of repairable subeffective damage will occur at the doses employed.

These observations are comparable with the results of Kellerer et al. (1976) who estimated the values of a_1 and a_2 from survival curves of V-79 cells *in vitro* after irradiation with neutrons of various energies. For 15 MeV neutrons, the effectiveness for the production of one-hit lethal events (a_1) is increased by a factor of 3.5 as compared to X-rays, while the value of (a_2) is decreased by a factor of 2.5.

It might be assumed that the similarity between the present data obtained for the spinal cord with an indirect method and the data obtained from experiments on *in vitro* cell survival indicate the existence of similar mechanisms. If this is correct, it can be concluded that the observation of a greatly reduced influence of the capacity for repair of subeffective damage for equivalent effects with doses per fraction of less than 5 Gy is probably due to the combination of an increased effectiveness for the production of single hit type lethal events and a decreased effectiveness for the production of repairable sublethal events.

TABLE 7.2.

ISOSURVIVAL CURVE CHARACTERISTICS FOR PROGRESSIVE RADICULOPATHY

	$a(10^{-2}\ Gy^{-1})$	$b(10^{-3}\ Gy^{-2})$	$\frac{1}{a}$ (Gy)	$\frac{a}{b}$ (Gy)
300 kV X-rays	0.85 ± 0.11	2.2 ± 0.16	118 ± 15	3.85 ± 0.75
15 MeV neutrons	5.28 ± 0.11	0.7 ± 0.14	29 ± 1	75 ± 20

Whether the repair capacity of the target cells is actually reduced cannot be concluded from the present experiments. The occurrence of repair after neutron irradiation has been demonstrated in various experimental systems: T1 cells of human kidney origin (Broerse and Barendsen, 1969), Chinese hamster ovary cells (Gragg et al., 1977), mouse intestinal crypt cells (Hornsey et al., 1977). The failure to observe repair in other experimental systems might be attributed to the use of relatively small total doses (Nias et al., 1971) or to the use of neutrons with a low mean energy (Erichsen et al., 1976), for which the value of a_1 is greatly increased relative to that of high energy neutrons.

The data presented in Figure 7.2 show an increasing RBE with decreasing dose per fraction, due to the repair capacity of cells for subeffective damage induced with X-rays. A question of clinical importance is whether a limit exists for the increasing RBE values. From the curves in Figure 7.3, it can be seen that, with decreasing doses per fraction, a maximum RBE of 15 MeV neutrons is calculated from the ratio of the maximal tolerated doses, i.e., the values $\frac{1}{a}$ for neutrons and X-rays in formula $\frac{1}{D_N} = a + bD$. This extrapolated maximum RBE value is about 6 for data obtained in the present experiments on spinal cord damage.

7.3.3 Variation in RBE for different tissues and target cells A possible explanation of the differential response of CNS to neutrons and X-rays

Experiments with cells *in vitro* as well as with cellular assay systems *in vivo* have shown considerable differences in RBE values (Broerse and Barendsen, 1973). For one cell type, the RBE varies with the extent of cell survival, while, at a given survival level, the RBE may vary among different cell types. Thus, variation in RBE values for effects in the target cells involved in the development of normal tissue damage must generally be expected and this might result in different RBE values for the organized tissue responses dependent on different cell types. In Figure 7.4, RBE values as obtained by several investigators in the Radiobiological Institute for various tissue endpoints after irradiation with 15 MeV D-T neutrons are presented. The lowest values are observed for the hemopoietic tissues. This can be explained by the small shoulder of the X-ray cell survival curve of hemopoietic stem cells. For most other tissues, the RBE increases with decreasing dose per fraction, although this increase appears to be

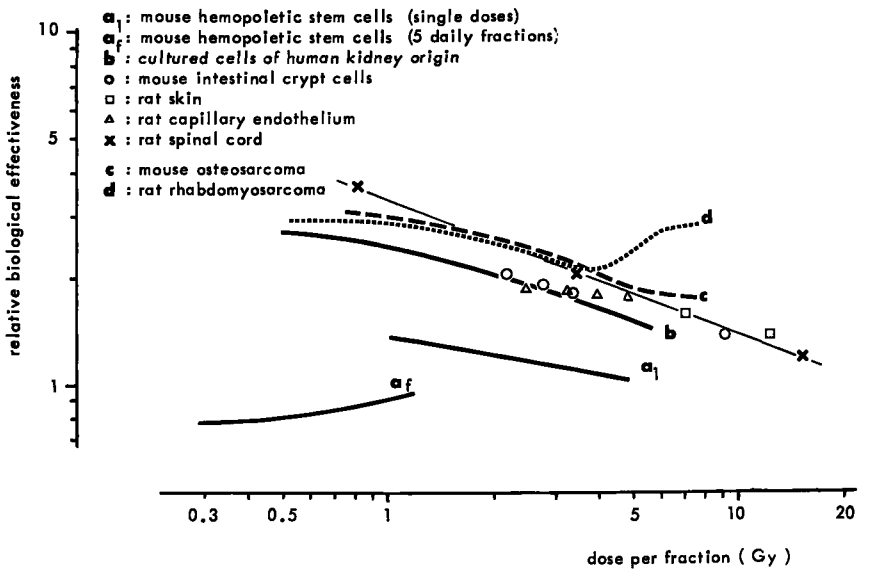

Figure 7.4

Relationships between the relative biological effectiveness of 15 MeV neutrons and the dose per fraction for a variety of endpoints in tumors and normal tissues.

smaller for intestine and vascular endothelium than for the spinal cord. It should be mentioned that other investigators have not observed the low values for intestine with either 15 MeV D-T neutrons or other energies (reviewed by Field and Hornsey, 1979). For some tissues such as murine tail, cartilage and esophagus, high RBE values were found with large doses per fraction. This is probably mainly due to the presence of a significant fraction of hypoxic cells in these tissues under experimental conditions employed, because, at doses of 1-2 Gy of fast neutrons, the difference with most other tissues disappears. In addition to the hemopoietic tissues, the lung appears to be the only tissue with relatively low RBE values over the entire dose range of about 1-2 Gy. These values were all obtained from observing the death of animals after irradiation of the whole thorax. With more specific endpoints which are used to assess damage after lower doses, higher RBE values were observed for the lung (Travis et al., 1979) and this might be clinically more relevant.

Apart from the question of whether experimental data are relevant for man, an important problem is that most normal tissue RBE values were derived with doses larger than 1-2 Gy per fraction, while lower doses per fraction are used in clinical applications. Extrapolation of the experimental curves of the type shown in Figure 7.4 might lead to an underestimation of RBE values to be applied for treatment of cancer in man. This is illustrated by the development of brain damage in human patients irradiated with neutrons, for which treatments in general an RBE value of 3 has been used. That for the CNS for doses per fraction of about 1 Gy the RBE is close to 4, is shown in the present experiments and in experiments on the mouse spinal cord (Geraci, 1978).

For most tissues studied, qualitative differences in reactions have not been reported for neutrons as compared to gamma or X-rays. The brain damage reported for man after neutron irradiations, however, appears to show marked differences from X-ray induced lesions, namely:

1. the latent period is about six months for neutrons, while, for X-rays, this period is in most cases from 1-2 years;
2. after neutron irradiation, the main histopathological aspect is demyelination of the white matter, while vascular damage is predominant after X-rays.

The present results obtained for the rat spinal cord may provide an explanation for the observed differences. The most common type of X-ray induced CNS damage in man is chronic progressive myelopathy or encephalopathy, which is comparable with the type 2 vascular lesions induced with X-rays in the rat cervical cord, developing after a latent period of 1-1.5 year. After a dose which is 10-15% larger than the threshold dose for type 2 vascular lesions, rats will develop paralysis within six months due to demyelination and white matter necrosis. It has been observed that, starting a few weeks after irradiation with doses as low as 15 Gy X-rays, a chronic process of diffuse demyelination and remyelination takes place. It can be assumed that, depending on the dose, this damage may progress to white matter necrosis or is repaired and vascular damage may develop later in these animals. With neutrons, repair during the early phase of demyelination may be inhibited, resulting in the development of large demyelinated areas and necrosis after a relatively short latent period. That this early repair is diminished is suggested by the observed short latent periods as compared to X-rays in the present experiments on the lumbosacral cord.

The difference in effectiveness of neutrons as compared to X-rays in the brain might also be due to a different RBE for the target cells involved namely, the glial cell for the demyelinating lesions and the

endothelium for the vascular lesions. As can be seen in Figure 7.4, RBE values determined for damage to the capillary endothelium are smaller than for the spinal cord. Furthermore, relatively high RBE values were observed for the late response (30 and 180 days postirradiation) of glial cells in the subependymal plate of the rat brain, which is regarded as a stem cell region (Chauser et al., 1977). A high RBE for damage to glial cells is also suggested by the observation of demyelination in the brains of seven monkeys irradiated with 850 rep (approximately 7 Gy) of 14 MeV neutrons (Vogel and Pickering, 1956). Even in monkeys surviving 22 months after irradiation, vascular damage was minimal.

It can be concluded that the RBE of fast neutrons for the target cells involved in the development of demyelinating lesions (glial cells) is probably higher than for the development of vascular damage in the brain and spinal cord. This difference can explain the predominance of early death in patients treated with neutrons for brain tumors. This insight in fundamental aspects of late CNS damage derived from an experimental model supports the conclusion drawn from clinical results that neutron therapy does not provide an advantage for treatment of brain tumors.

ABSTRACT

Late effects of ionizing radiation are generally observed in organs or tissues which are characterized by a slow turnover of cells, e.g., the lung, liver, kidney and central nervous system. In contrast, acute effects are mainly observed in tissues with a rapid turnover of cells such as the skin, intestinal tract and the hemopoietic system. This correlation between the development of radiation damage in tissues and the rate of cellular turnover suggests that the loss of reproductive capacity of cells is one of the most important effects of radiation. While much is known about the kinetics of acute effects and the cell types involved, this information is mostly lacking for late effects. Experiments described in this thesis are concerned with the mechanisms of the development of late radiation damage in the spinal cord. Histopathological observations of the irradiated cord showed specific types of lesions in relation to dose and time after irradiation. This suggests the involvement of different target cells.

In clinical radiotherapy, one of the important factors determining the dose of radiation that can be administered to the tumor is the normal tissue tolerance. Brain and spinal cord are for the treatment of tumors in various locations among the most critical dose limiting tissues. A part of this thesis deals with the tolerance of the spinal cord and the dependence on various factors such as dose fractionation, overall time of treatment, dose rate and type of radiation.

In Chapter I, the effects of radiation on tissues and cells are discussed. Irreversible loss of integrity and function of an organ after irradiation is thought to be the result of a decrease in the number of surviving cells below a critical level. The dose at which severe damage is observed is not similar for all tissues, but depends on, e.g., the kinetics of cells and their progression through various maturation compartments, the intrinsic radiosensitivity of cells and the capacity to repair sublethal damage during fractionated irradiation. Some of these characteristics of individual cells can be derived from cell survival curves, which can be obtained from cells in culture, or, with limitations, from cells in rapidly proliferating tissues. However, for tissues in which turnover of cells occurs at a low rate, information on cell survival can be obtained only in an indirect way (see Chapter VI) or by stimulating the cells to divide.

The concept of tolerance doses and the value of isoeffect formulas in clinical radiotherapy are introduced. It is pointed out that recent clinical and experimental studies caution against the use of one formula to predict tolerance doses in various fractionation schemes for all tissues at risk. Finally, the possibilities of improving tumor treatment by the use of high LET radiation are discussed in Chapter I.

In Chapter II, the structure of the spinal cord is described, as an introduction to the histopathological studies and the analysis of target cells involved in the various types of lesions. The structure of the spinal cord in man and the rat is largely similar, although the anatomical locations of various long fiber systems show great variation among different species. This explains the differences in neurological signs observed in radiation myelopathy in man and the rat, while the lesions are similarly distributed in the cord.

The function and the reactions to injury of the three types of glial cells (astrocytes, oligodendrocytes, microglial cells) in the spinal cord and of the Schwann cells in the nerve roots are briefly reviewed.

The experimental techniques used for studies of late radiation damage in the spinal cord are presented in Chapter III. Male rats of the inbred WAG/Rij strain were used in most experiments. Two strains, the BN/Bi and the (WAG/Rij x BN/Bi)F1 hybrid were used in comparative studies. The effects of 300 kV X-rays or 15 MeV neutrons were evaluated for different regions of the spinal cord, corresponding to vertebral levels C5-T2, T12-L2 and L2-L5. During irradiation, the animals were routinely anesthetized with Nembutal, but, especially in multifraction experiments, inhalation anesthesia with halothane or ethrane was used. For the assessment of damage, different grades of neurological signs were distinguished and separate scoring systems were used for the cervical and lumbar regions. A stage of definite paresis was used as the endpoint in estimations of the latent period.

The factors which influence the latent period such as the dose, rat strain, age at the time of irradiation or type of anesthesia are analyzed in Chapter IV. A general phenomenon seems to be that, with increasing dose, the length of the latent period decreases. After doses of less than 30 Gy, the length of the latent period is strain dependent, but the differences disappear with higher dose. All variables studied (strain, age, anesthesia) appeared to influence the threshold dose for the cervical cord, but not for the lumbosacral cord.

The development of definite paralytic signs, used as an endpoint for the determination of latent periods, reflects only the presence of

damage without revealing its pathological characteristics. These are described in Chapter V. Various types of lesions were observed, suggesting that different pathological mechanisms are involved in the induction of paralysis, depending on dose and time after irradiation. In the cervical cord, after irradiation with doses in the range of 20-40 Gy of X-rays, the latent period decreases with increasing dose from 7 to 4 months. The primary lesion observed in demyelination and necrosis of the white matter, which is mainly attributed to damage to the oligodendrocytes. After irradiation with single doses in the range of 17-20 Gy, i.e., below the level for induction of the demyelinating lesions, paralysis may develop after very long latent periods, up to the end of the lifespan of the rats. The lesions observed in these rats all seem to have a vascular origin, varying from telangiectasis and small hemorrhages and developing into either a chronic inflammatory process or an acute hemorrhagic infarction. Because the lesions apparently start in the capillaries or small venules, the endothelial cell is the most probable target.

In the lumbosacral region, the type of damage is completely different from that in the cervical cord and it is concluded that mainly the nerve roots are involved. With doses above a threshold of about 20 Gy, the nerve roots show demyelination and necrosis, which is attributed to damage to Schwann cells.

In the final part of Chapter V, the different syndromes of human radiation myelopathy are described and compared with the lesions observed in the rats. It is concluded that the general characteristics of the various lesions are similar in man and the rat, which emphasizes the suitability of the rat as an animal model in studies on radiation myelopathy.

The effect of dose fractionation on the tolerance of the spinal cord is presented in Chapter VI. For the induction of the various syndromes as described in Chapter V, isoeffect curves showing the relationship between the total dose and the number of fractions are presented. The slope of the curves presented on log-log scale is between 0.4 and 0.46, indicating that the spinal cord has a great capacity for repair of subeffective damage. The kinetics of this type of repair is similar to that of Elkind repair of sublethal damage, which is completed within about 6 hours. As could be expected for a tissue with a slow turnover of cells (the glial and endothelial cells), recovery by repopulation is minimal for short overall times. The relative contribution of time-dependent recovery has been estimated in split-dose experiments with varying time intervals. In the lumbosacral nerve roots, some additional recovery is observed to start between 1 and 4 weeks,

which suggests a proliferative reaction of Schwann cells. In the cervical cord, additional recovery appeared to start only after 2 months. Thus, the repair characteristics of the various target cells assumed to be involved in the development of damage appear to be different. This conclusion is also drawn from an analysis of isosurvival curve parameters. These showed that with an increasing number of fractions the maximally tolerated dose of the spinal cord is between 120 and 210 Gy for the various syndromes. These values are higher than those obtained for other normal tissues.

The strong dependence on the number of fractions as observed for the rat spinal cord tolerance appears to be similar for the human spinal cord. This is reflected in the proposed isoeffect formula $D = NSD \times N^{0.4}$, which can be used to predict the spinal cord tolerance in different fractionation schemes. For treatment periods of 1-2 months, the time factor is negligible.

The results of irradiation of the spinal cord with 15 MeV neutrons are presented in the final chapter. Data were obtained mainly for the lumbosacral cord. Histopathological observations showed lesions similar to those induced with X-rays, although the latent periods were shorter after neutrons. With fractionated irradiation, the influence of repair was greatly reduced relative to X-rays, which resulted in an RBE of 3.7 at a neutron dose of 0.9 Gy per fraction. The finding of a high RBE for nervous tissue supports the conclusions drawn from clinical results that neutrons offer no advantage for the treatment of brain tumors. However, the results presented in Chapter VI suggest a better alternative for the treatment of brain tumors to be irradiation with gamma rays in a large number of small fractions within a short overall time, e.g., 2-3 fractions per day. This type of treatment would take advantage of the large repair capacity for subeffective damage during fractionated irradiation of the central nervous system.

SAMENVATTING

Onder late effecten van straling worden meestal die effecten verstaan die later dan enkele maanden na bestraling optreden. Bij de stralingsbescherming, waarbij het gaat om kleine doses straling, is het belangrijkste late effect het ontstaan van kanker. In de radiotherapie van kanker, waarbij hogere doses straling worden gebruikt, wordt met late effecten bedoeld het optreden van ernstige schade in organen of weefsels in de omgeving van de behandelde tumor. De meeste van deze late effecten ontstaan in organen die een langzame vervanging van cellen vertonen, zoals longen, lever, nieren, hersenen en ruggemerg. Daarentegen worden acute of vroege effecten van straling voornamelijk gevonden in weefsels met een hoge celdelingsactiviteit, zoals huid, maag-darmkanaal en het beenmerg. Bij deze weefsels vindt echter dikwijls een snel herstel van de toegebrachte schade plaats. De gevonden relatie tussen het optreden van stralingsschade en de celdelingsactiviteit in een bepaald orgaan wijst erop, dat het verlies van het vermogen van celdeling een van de meest belangrijke effecten van ioniserende straling is.

Over het ontstaan van de acute effecten en de daarbij betrokken celtypen, is veel bekend. Inzicht in het ontstaan van late effecten ontbreekt echter voor veel weefsels. Het in dit proefschrift beschreven onderzoek over het ontstaan van late stralingsschade in het ruggemerg van de rat is uitgevoerd om dit inzicht uit te breiden.

Bij de radiotherapie wordt de dosis straling die aan een tumor kan worden toegediend voornamelijk beperkt door de tolerantie van de omliggende gezonde weefsels. Hersenen en ruggemerg behoren tot de meest kritieke dosis-limiterende weefsels, gezien de ernst van eventueel optredende complicaties. Een deel van dit proefschrift beschrijft het onderzoek over de factoren die de tolerantie van het ruggemerg beïnvloeden. Hierbij is gelet op o.a. de totale dosis die nodig is om een bepaald effect te veroorzaken, het effect van het verdelen van een dosis in een aantal kleine fracties en de invloed van het dosistempo. Ook is de werking van röntgenstralen vergeleken met neutronenstraling.

Hoofdstuk I geeft een introductie over de effecten van straling op weefsels en cellen. Het ontstaan van ernstige stralingsschade in een orgaan wordt toegeschreven aan een zodanig celverlies dat het aantal

overlevende cellen te gering is voor een blijvend herstel. De dosis, waarbij onherstelbare schade optreedt is niet gelijk voor alle weefsels, maar is afhankelijk van o.a. de celkinetiek, de stralingsgevoeligheid van cellen en hun vermogen tot herstel van z.g. sublethale schade tijdens gefractioneerde bestraling. Voor cellen in weefselkweek kunnen sommige van deze eigenschappen worden bestudeerd aan de hand van overlevingscurven, die de relatie geven tussen de dosis en het aantal overlevende cellen. In beperkte mate is dit ook mogelijk voor snel prolifererende cellen in b.v. de darmcrypten en het huidepitheel. Echter van weefsels die een lage delingsactiviteit vertonen kunnen gegevens over celoverleving slechts verkregen worden via een indirecte methode, zoals beschreven in Hoofdstuk VI.

Vervolgens worden in Hoofdstuk I beschreven het concept van de tolerantiedosis en de waarde van z.g. isoeffectformules in de radiotherapie. Benadrukt wordt, dat recente klinische en experimentele gegevens een waarschuwing inhouden met betrekking tot het berekenen van tolerantiedoses voor alle normale weefsels met behulp van één formule met vaste exponenten. Tevens worden in Hoofdstuk I de mogelijkheden tot verbetering van kankertherapie met behulp van snelle neutronen besproken.

De structuur van het ruggemerg is beschreven in Hoofdstuk II, als inleiding tot de latere histopathologische studies. De histologische structuur van het ruggemerg van de rat vertoont grote gelijkenis met dat van de mens, hoewel de ligging van de verschillende zenuwbanen belangrijke verschillen laat zien. Dit verklaart waarom het optreden van stralingsmyelopathie bij de mens en de rat gepaard gaat met verschillende neurologische symptomen, ondanks de aanwezigheid van identieke lesies. Van de drie typen gliacellen (steuncellen) in het ruggemerg, de astrocyten, oligodendrocyten en microglia cellen, en van de Schwann cellen in de zenuwwortels, is een kort overzicht gegeven van hun functie en hun reacties bij verschillende soorten schade.

De opzet van de verschillende experimenten en van de gebruikte technieken is beschreven in Hoofdstuk III. Voor de meeste experimenten zijn mannelijke albino ratten van de WAG/Rij stam gebruikt. Ter vergelijking met de bij deze ingeteelde stam verkregen resultaten, zijn enkele experimenten uitgevoerd met ratten van de BN/Bi stam en met (WAG/Rij x BN/Bi)F1 hybriden. Drie gebieden van het ruggemerg, nl. een cervicaal deel en twee aansluitende lumbale gedeelten zijn bestraald met 300 kV röntgenstraling of 15 MeV neutronenstraling. Bestraling vond plaats onder verdoving met Nembutal, alleen bij bestralingen met een groot aantal fracties (30 of 60 fracties in 6 weken) werd gebruik gemaakt van het gasvormige anestheticum halothaan of ethraan. Bij de

ontwikkeling van schade konden verschillende neurologische symptomen worden onderscheiden, op basis waarvan een scoringssysteem werd ontwikkeld. Het moment van optreden van duidelijke verlammingsverschijnselen werd beschouwd als het eind van de z.g. latente periode.

Een analyse van de factoren, die de lengte van de latente periode beïnvloeden, is gegeven in Hoofdstuk IV. De latente periode is o.a. afhankelijk van de dosis, gebruikte rattestam, leeftijd en de soort anesthesie. In het algemeen wordt de latente periode korter bij toenemende dosis. Ook is bij deze experimenten gelet op de drempeldosis, die gedefinieerd is als de hoogste dosis waarbij geen verlammingen optreden. Gebleken is dat de drempeldosis voor het cervicale gebied sterker afhankelijk is van de onderzochte variabelen dan voor het lumbale gebied.

Hoewel de ontwikkeling van duidelijke verlammingsverschijnselen op de aanwezigheid van schade duidt, geeft dit geen informatie over het ontstaansmechanisme van de schade. De histopathologische kenmerken zijn beschreven in Hoofdstuk V. Verschillende soorten schade zijn gevonden, zowel in de verschillende gebieden van het ruggemerg als binnen één gebied, afhankelijk van de dosis en tijd na bestraling. Dit wijst erop dat verschillende mechanismen betrokken zijn bij het ontstaan van verlammingen. Na bestraling van het cervicale ruggemerg met doses tussen 20 en 40 Gy neemt de latente periode af met toenemende dosis, van 7 tot 4 maanden. De hierbij geinduceerde schade wordt gekenmerkt door demyelinisatie en necrose van de witte stof. Dit wordt primair toegeschreven aan beschadiging van de oligodendrocyten. Na bestraling met doses tussen ongeveer 17 en 20 Gy, waarbij bovenstaande lesies niet optreden, kunnen nog tot zeer lang na bestraling (1 à $1\frac{1}{2}$ jaar) verlammingen ontstaan tengevolge van bloedvatschade. Deze schade kan beginnen met kleine bloedingen en vaatverwijding en zich vervolgens ontwikkelen tot een chronisch ontstekingsproces of een acute uitgebreide bloeding. Het bij dit proces primair betrokken celtype is waarschijnlijk de endotheel cel. In het lumbosacrale gebied beperkt de schade zich voornamelijk tot demyelinisatie en necrose van de zenuwwortels, na doses van 20 Gy en hoger. Schade aan het ruggemerg zelf wordt hierbij niet gevonden. Het voornamelijk bij deze lesie betrokken celtype is de Schwann cel.

Hoofdstuk V wordt besloten met een beschrijving van de verschillende bij de mens waargenomen syndromen van stralingsmyelopathie. Deze vertonen een grote gelijkenis met de verschillende bij de rat voorkomende lesies, hetgeen de geschiktheid van de rat als diermodel voor studies over stralingsmyelopathie benadrukt.

Hoofdstuk VI geeft een analyse van de verschillende factoren die de stralingstolerantie van het ruggemerg beïnvloeden, zoals fractionering van de dosis en de totale tijdsduur van een bestralingsserie. Voor het ontstaan van de verschillende in Hoofdstuk V beschreven syndromen geven z.g. isoeffectcurven de relatie weer tussen de totale dosis en het aantal fracties. De helling van deze curven op dubbel logarithmische schaal heeft een waarde tussen de 0.4 en 0.46, hetgeen betekent dat het ruggemerg een grote capaciteit tot herstel van subeffectieve schade heeft. De snelheid van dit type herstel is gelijk aan die van Elkind herstel van sublethale schade, waargenomen in gekweekte zoogdiercellen, en vindt plaats in ongeveer 6 uur. Zoals verwacht kon worden bij een weefsel met lage celdelingsactiviteit (de glia- en endotheelcellen) is de bijdrage van celproliferatie tot het herstel gering tijdens korte bestralingsperioden. Of deze bijdrage groter wordt voor langere perioden is nagegaan in experimenten, waarbij 2 doses straling met verschillende tijdsintervallen worden toegediend. Voor de zenuwwortels in het lumbosacrale gebied lijkt een tweede fase van herstel te beginnen tussen 1 en 4 weken, hetgeen wijst op een proliferatieve reactie van Schwann cellen. In het cervicale ruggemerg bleek dit type van herstel pas bij tijdsintervallen vanaf 2 maanden te beginnen.

Bij een toename van het aantal fracties en een vermindering van de dosis per fractie, stijgt de tolerantiedosis. Hierbij wordt een maximum bereikt, dat niet voor alle weefsels gelijk is. Voor het ruggemerg lijkt deze maximaal tolerabele dosis hoger te zijn dan voor andere weefsels. Deze sterke afhankelijkheid van het aantal fracties zoals waargenomen bij het ruggemerg van de rat, lijkt ook te bestaan voor het menselijk ruggemerg. Dit is weergegeven in de isoeffect formule $D = NSD \times N^{0.4}$, welke gebruikt kan worden om de ruggemergtolerantie te berekenen voor verschillende fractioneringsschema's. Voor bestralingstijden van 1 tot 2 maanden is de tijdsfactor zoals gebruikt in de Ellis formule te verwaarlozen.

In het laatste hoofdstuk zijn de resultaten beschreven van bestraling van voornamelijk het lumbale gebied met 15 MeV neutronen. Het histopathologisch beeld van de geïnduceerde schade was vergelijkbaar met dat, veroorzaakt door röntgenstraling. De latente periode was echter korter na bestraling met neutronen. Bij gefractioneerde bestraling bleek het herstel van subeffectieve schade in vergelijking met röntgenstraling sterk verminderd, en de relatieve biologische effectiviteit (RBE) was 3.7 bij een neutronendosis van 0.9 Gy per fractie. Een hoge RBE van neutronen voor zenuwweefsel komt overeen met de conclusie uit klinische waarnemingen, dat neutronen waarschijnlijk

geen voordeel bieden bij de behandeling van hersentumoren. Daarentegen suggereren de in Hoofdstuk VI beschreven resultaten mogelijk een beter alternatief, n.l. bestraling met een groot aantal fracties röntgen- of gammastraling in korte tijd, b.v. met 2 à 3 fracties per dag. Dit type behandeling zou gebruik maken van de sterke herstelcapaciteit voor subeffectieve schade tijdens gefractioneerde bestraling van het centraal zenuwstelsel.

ABBREVIATIONS

BBB	blood-brain barrier
C5	fifth cervical vertebra
CNS	central nervous system
D_N	total dose applied in N fractions
D_o	dose required to reduce the surviving fraction of cells by a factor of e^{-1}
D_Q	dose at which the extrapolated exponential part of a survival curve intersects the abscissa at 100% survival
ED_{50}	dose at which 50 percent of the animals develop a defined endpoint
F_1	(WAG/Rij x BN/Bi)F_1 hybrid
Gy	gray. 1 Gy = 1 $J.kg^{-1}$ = 100 rad
HPS	hematoxylin phloxine saffron (histological stain)
L2	second lumbar vertebra
LD_{50}	dose which is lethal to 50 percent of the animals
LET	linear energy transfer
LFB-PAS	luxol fast blue - periodic acid Schiff (histological stain)
N	number of fractions
NSD	nominal single dose
OER	oxygen enhancement ratio
PNS	peripheral nervous system
RBE	relative biological effectiveness
T2	second thoracic vertebra
T	overall time of fractionated irradiation
TD	tolerance dose

ACKNOWLEDGEMENTS

Thanks are due to all those members of the REP-Institutes who contributed to the work described in this thesis. In particular, I would like to express my gratitude to:

- Prof. Dr. G.W. Barendsen, who introduced me in the field of radiation biology and gave the impulse to perform these studies. His support and criticisms during the preparation of this thesis are gratefully acknowledged;
- Mrs. H.A. Sissingh for her skilled technical assistance during all these years;
- Prof. Dr. D.W. van Bekkum for providing the facilities to perform the experiments;
- Prof. Dr. C.F. Hollander, Prof. Dr. K. Breur, Dr. C. Zurcher and Dr. M.J. van Zwieten for their critical reading and suggestions to improve the manuscript;
- Dr. J.J. Broerse, Dr. J. Zoetelief, Mr. A.C. Engels and Mr. C.J. Bouts for their cooperation in the time-consuming neutron experiments;
- Mrs. A.L. Nooteboom, Mr. E.H. Offerman and their collaborators of the histological laboratory for preparing the many thousands of histological slides;
- Mrs. C.D.F. van den Berg for technical assistance;
- Mrs. L. van der Burg-Verweij and Mrs. E.N. Janse-Over for their help with the X-irradiations;
- Dr. A.C. Ford for editing the English text;
- Mr. A.A. Glaudemans for preparation of the photomicrographs;
- Mrs. M.C. von Stein for typing the various versions of the manuscript;
- Mrs. D. van der Velden for preparation of the final manuscript and last but not least,
- Mr. J.Ph. de Kler, who expertly prepared the figures and designed the front cover.

REFERENCES

Adams, H.R. (1970) Prolongation of barbiturate anesthesia by chloramphenicol in laboratory animals. J. Am. Vet. Med. Assoc. 157, 1908-1913.

Adrian, E.K. and Williams, M.G. (1973) Cell proliferation in injured spinal cord. An electron microscopic study. J. Comp. Neurol. 151, 1-24.

Asbell, S.O. and Kramer, S. (1971) Oxygen effect on the production of radiation-induced myelitis in rats. Radiology 98, 678-681.

Asscher, A.W. and Anson, S.G. (1962) Arterial hypertension and irradiation damage to the nervous system. Lancet, 1343-1346 (December).

Atkins, H.L. and Tretter, P. (1966) Time-dose considerations in radiation myelopathy. Acta Radiol. 5, 79-93.

Barendsen, G.W. (1966) Possibilities for the application of fast neutrons in radiotherapy: recovery and oxygen enhancement of radiation induced damage in relation to linear energy transfer. Eur. J. Cancer 2, 333-345.

Barendsen, G.W. (1968) Responses of cultured cells, tumours and normal tissues to radiations of different linear energy transfer. Curr. Top. Radiat. Res. 4, 295-356.

Barendsen, G.W., Beusker, T.L.J., Vergroesen, A.J. and Budke, L. (1960) Effects of different ionizing radiations on human cells in tissue culture. II. Biological experiments. Radiat. Res. 13, 841-849.

Barendsen, G.W., Broerse, J.J. and Putten, L.M. van (1971) Guest editors. Fundamental and practical aspects of the application of fast neutrons in clinical radiotherapy. Eur. J. Cancer 7, 97-267.

Barendsen, G.W., Broerse, J.J. and Putten, L.M. van (1974) Guest editors. Proc. of the second meeting on fundamental and practical aspects of the application of fast neutrons in clinical radiotherapy. Eur. J. Cancer 10, 199-398.

Barendsen, G.W., Broerse, J.J. and Breur, K. (1979) Guest editors. High LET radiations in clinical radiotherapy. Proc. 3rd Meeting on Fundamental and Practical Aspects of Fast Neutrons and Other High LET Particles in Clinical Radiotherapy. Eur. J. Cancer, Suppl. 6, in press.

Beal, J.A. and Hall, J.L. (1974) A light microscopic study of the effects of X-irradiation on the spinal cord of neonatal rats. J. Neuropath. Exp. Neurol. 33, 128-143.

Berg, B.N., Wolf, A and Simms, H.S. (1962) Degenerative lesions of spinal roots and peripheral nerves in aging rats. Gerontologia 6, 72-80.

Berg, N.O. and Lindgren, M. (1958) Time-dose relationship and morphology of delayed radiation lesions of the brain in rabbits. Acta Radiol. [Suppl.] 167, 1-118.

Bergonié, J. and Tribondeau, L. (1906) Interprétation de quelques résultats de la radiotherapie et essoi de fixation d'une technique rationelle. Compt. Rend. Acad. Sci. 143, 983-985.

Berry, R.J., Wiernik, G., Patterson, T.J.S. and Hopewell, J.W. (1974) Excess late subcutaneous fibrosis after irradiation of pig skin, consequent upon the application of the NSD formula. Br. J. Radiol. 47, 277-281.

Berthold, C.-H (1974) A comparative morphological study of the developing node-paranode region in lumbar spinal roots. II. Light microscopy after Osmium-tetroxyde alpha-naphtylamine (OTAN) staining. Neurobiology 4, 117-131.

Blakemore, W.F. (1972) Observations on oligodendrocyte degeneration, the resolution of status spongiosus and remyelination in cuprizone intoxication in mice. J. Neurocytol. 1, 413-426.

Boden, G. (1950) Radiation myelitis of the brain-stem. J. Faculty Radiol. 2, 79-94.
Bradley, W.G., Fewings, J.D., Cumming, W.J.K., Harrison, R.M. and Faulds, A.J. (1977) Delayed myeloradiculopathy produced by spinal X-irradiation in the rat. J. Neurol. Sci. 31, 63-82.
Broerse, J.J. (1976) Editor. Basic physical data for neutron dosimetry. Publication EUR 5629e of the Commission of the European Communities, Luxembourg.
Broerse, J.J. and Barendsen, G.W. (1967) Measurements of biological effects and physical parameters of neutrons from the $^{9}Be(^{3}He,n)^{11}C$ reaction; possibilities for fast neutron radiotherapy. Int. J. Radiat. Biol. 13, 189-194.
Broerse, J.J. and Barendsen, G.W. (1969) Recovery of cultured cells after fast neutron irradiation. Int. J. Radiat. Biol. 15, 335-339
Broerse, J.J. and Barendsen, G.W. (1973) Relative biological effectiveness of fast neutrons for effects on normal tissues. Curr. Top. Radiat. Res. Quart. 8, 305-350.
Bunge, R.P. (1968) Glial cells and the central myelin sheath. Physiol. Rev. 48, 197-251.
Burek, J.D., Kogel, A.J. van der and Hollander, C.F. (1976) Degenerative myelopathy in three strains of aging rats. Vet. Pathol. 13, 321-331.
Burns, R.J., Jones, A.N. and Robertson, J.S. (1972) Pathology of radiation myelopathy. J. Neurol. Neurosurg. Psychiatry 35, 888-898.
Cairnie, A.B. and Millen, B.H. (1975) Fission of crypts in the small intestine of the irradiated mouse. Cell Tissue Kinet. 8, 189-196.
Caldwell, W.L. (1975) Time-dose factors in fatal post-irradiation nephritis. In: Cell survival after low doses of radiation: theoretical and clinical implications (ed. T. Alper), pp. 328-334, The Institute of Physics. John Wiley and Sons.
Cammermeyer, J. (1970) The life history of the microglial cell: a light microscopic study. In: Neurosciences research, vol. 3 (eds. S. Ehrenpreis and O.C. Solnitzky), pp. 43-129, Academic Press, New York.
Cavanagh, J.B. (1968) Effects of X-irradiation on the proliferation of cells in peripheral nerve during Wallerian degeneration in the rat. Br. J. Radiol. 41, 275-281.
Caveness, W.F., Tanaka, A. and Hess, K.H. (1974) Delayed brain swelling and functional derangement after X-irradiation of the right visual cortex in the Macaca mulatta. Radiat. Res. 57, 104-120.
Chadwick, K.H. and Leenhouts, H.P. (1973) A molecular theory of cell survival. Phys. Med. Biol. 18, 78-87.
Chauser, B.M., Hudson, F.R. and Law, M.P. (1976) Renal function in the rat following irradiation. Radiat. Res. 67, 86-97.
Chauser, B., Morris, C., Field, S.B. and Lewis, P.D. (1977) The effects of fast neutrons and X-rays on the subependymal layer of the rat brain. Radiology 122, 821-823.
Cheng, H. and Leblond, C.P. (1974) Origin, differentiation and renewal of the four main epithelial cell types in the mouse small intestine. Am. J. Anat. 141, 537-562.
Combes, P.F., Daly, N., Schlienger, M., Humeau (1975) Les myélopathies radiques tardives progressives. J. Radiologie 56, 815-825.
Cook, R.D. and Wisniewski, H.M. (1973) The role of oligodendroglia and astroglia in Wallerian degeneration of the optic nerve. Brain Res. 61, 191-206.
Corbin, K.B. and Gardner, E.D. (1937) Decrease in number of myelinated fibres in human spinal roots with age. Anat. Rec. 68, 63-74.
Coy, P. and Dolman, C.L. (1971) Radiation myelopathy in relation to oxygen level. Br. J. Radiol. 44, 705-707.
Denekamp, J. (1973) Changes in the rate of repopulation during multifraction irradiation of mouse skin. Br. J. Radiol. 46, 381-387.

Donaldson, H.H. (1924) The Rat. Reference tables and data for the albino rat (Mus Norvegicus Albinus) and the Norway rat (Mus Norvegicus), 2nd ed., Memoirs of the Wistar Institute of Anatomy and Biology, No. 6, Philadelphia.

Douglas, B.G. and Fowler, J.F. (1976) The effect of multiple small doses of X-rays on skin reactions in the mouse and a basic interpretation. Radiat. Res. 66, 401-426.

Durand, R.E. and Sutherland, R.M. (1975) Intercellular contact: its influence on the Dq of mammalian survival curves. In: Cell survival after low doses of radiation: theoretical and clinical implications (ed. T. Alper), pp. 237-247, The Institute of Physics, John Wiley and Sons.

Dutreix, J., Wambersie, A. and Bounik, C. (1973) Cellular recovery in human skin reactions: application to dose fraction number overall time relationship in radiotherapy. Eur. J. Cancer 9, 159-167.

Dynes, J.B. and Smedal, M.I. (1960) Radiation myelitis. Am. J. Roentgenol. 83, 78-87.

Elkind, M.M. (1976) Fractionated dose radiotherapy and its relationship to survival curve shape. Cancer Treat. Rev. 3, 1-15.

Elkind, M.M. and Sutton, H. (1959) X-ray damage and recovery in mammalian cells in culture. Nature (London) 184, 1293-1295.

Ellis, F. (1968) The relationship of biological effect to dose-time-fractionation factors in radiotherapy. Curr. Top. Radiat. Res. Quart. 4, 357-397.

Erichsen, E.A., Baker, M.L., Moss, A.J., Prior, R.M. and Dalrymple, G.V. (1976) Survival of mouse L-929 cells following neutron irradiation. Radiology 119, 467-469.

Field, S.B. (1972) The Ellis formulae for X-rays and fast neutrons. Br. J. Radiol. 45, 315-317.

Field, S.B. (1976) An historical survey of radiobiology and radiotherapy with fast neutrons. Curr. Top. Radiat. Res. Quart. 11, 1-86.

Field, S.B. (1977) Early and late normal tissue damage after fast neutrons. Int. J. Radiat. Oncol. Biol. Phys. 3, 203-210.

Field, S.B. and Bewley, D.K. (1974) Effects of dose-rate on the radiation response of rat skin. Int. J. Radiat. Biol. 26, 259-267.

Field, S.B. and Hornsey, S. (1977) Repair in normal tissues and the possible relevance to radiotherapy. Strahlentherapie 153, 371-379.

Field, S.B. and Hornsey, S. (1979) Neutron RBE for normal tissues. Eur. J. Cancer, in press.

Field, S.B., Hornsey, S. and Kutsutani, Y. (1976) Effects of fractionated irradiation on mouse lung and a phenomenon of slow repair. Br. J. Radiol. 49, 700-707.

Gänshirt, H. (1975) Strahlenmyelopathie. Nervenarzt 46, 562-568.

Geraci, J.P., Jackson, K.L., Christensen, G.M., Thrower, P.D. and Mariano, M. (1978) RBE for late spinal cord injury following multiple fractions of neutrons. Radiat. Res. 74, 382-386.

Geraci, J.P., Jackson, K.L., Christensen, G.M., Thrower, P.D. and Weyer, B.J. (1977) Acute and late damage in the mouse small intestine following multiple fractionations of neutrons or X-rays. Int. J. Radiat. Oncol. Biol. Phys. 2, 693-696.

Geraci, J.P., Thrower, P.D., Jackson, K.L., Christensen, G.M., Parker, R.G. and Fox, M.S. (1974) The relative biological effectiveness of fast neutrons for spinal cord injury. Radiat. Res. 59, 496-503.

Gilmore, S.A. (1972) Spinal nerve root degeneration in aging laboratory rats: a light microscopic study. Anat. Rec. 174, 251-258.

Gragg, R.L., Humphrey, R.M. and Meyn, R.E. (1977) The response of chinese hamster ovary cells to fast neutron radiotherapy beams. II. Sublethal and potentially lethal damage recovery capabilities. Radiat. Res. 71, 461-470.

Greenfield, M.M. and Stark, F.M. (1948) Post-irradiation neuropathy. Am. J. Roentgenol. 60, 617-622.

Griffiths, I.R. and Duncan, I.D. (1975) Age changes in the dorsal and ventral lumbar nerve roots of dogs. Acta Neuropathol. (Berl.) 32, 75-85.

Hassler, O. and Movin, A. (1966) Microangiographic studies on changes in the cerebral vessels after irradiation. Acta Radiol. 4, 279-288.

Hegazy, M.A.H. and Fowler, J.F. (1973) Cell population kinetics and desquamation skin reactions in plucked and unplucked mouse skin. II. Irradiated skin. Cell Tissue Kinet. 6, 587-602.

Hendry, J.H., Rosenberg, I., Greene, D. and Stewart, J.G. (1976) Tolerance of rodent tails to necrosis after "daily" fractionated X-rays or D-T neutrons. Br. J. Radiol. 49, 690-699.

Herndon, R.M., Price, D.L. and Weiner, L.P. (1977) Regeneration of oligodendroglia during recovery from demyelinating disease. Science 195, 693-694.

Hildebrand, C. (1977) Presence of marchi-positive myelinoid bodies in the spinal cord white matter of some vertebrate species. J. Morphol. 153, 1-22.

Hollander, C.F. (1976) Current experience using the laboratory rat in aging studies. Lab. Anim. Sci. 26, 320-328.

Hopewell, J.W. (1977). Annual Report of the Research Institute, Churchill Hospital, Oxford.

Hopewell, J.W. and Berry, R.J. (1975) Radiation tolerance of the pig kidney: A model for determining overall time and fraction factors for preserving renal function. Int. J. Radiat. Oncol. Biol. Phys. 1, 61-68.

Hopewell, J.W. and Wright, E.A. (1970) The nature of latent cerebral irradiation damage and its modification by hypertension. Br. J. Radiol. 43, 161-167.

Hopewell, J.W. and Wright, E.A. (1975) The effects of dose and field size on late radiation damage to the rat spinal cord. Int. J. Radiat. Biol. 28, 325-333.

Hornsey, S., Andreozzi, U. and Warren, P.R. (1977) Sublethal damage in cells of the mouse gut after mixed treatment with X-rays and fast neutrons. Br. J. Radiol. 50, 513-517.

Hornsey, S., Kutsutani, Y. and Field, S.B. (1975) Damage to mouse lung with fractionated neutrons and X-rays. Radiology 116, 171-174.

Hornsey, S. and White, A. (1979). Isoeffect curve for radiation myelopathy. In the press.

Hubbard, B.M. (1977) Late effects of ionising radiation on the central nervous system of the rat. D. Phil. Thesis, University of Oxford.

Hubbard, B.M. and Hopewell, J.W. (1978) The dose-latent period relationship in the irradiated cervical spinal cord of the rat. Radiology 128, 779-781.

ICRP (1975). Report of the Task Group on Reference Man. ICRP Report 23. Pergamon Press, Oxford.

ICRU (1977). Neutron Dosimetry for Biology and Medicine. ICRU Report 26.

Innes, J.R.M. and Carsten, A. (1962) A demyelinating or malacic myelopathy and myodegeneration - delayed effect of localized X-irradiation in experimental rats and monkeys. In: Response of the nervous system to ionizing radiation (eds. T.J. Haley and R.S. Snider), pp. 233-247, Academic Press, New York.

Jellinger, K. and Sturm, K.W. (1971) Delayed radiation myelopathy in man. J. Neurol. Sci. 14, 389-408.

Johnson, R., Fowler, J.F., Zanelli, G.D. (1976) Changes in mouse blood pressure, tumor blood flow and core and tumor temperatures following nembutal or urethane anesthesia. Radiology 118, 697-703.

Jones, A. (1964) Transient radiation myelopathy. Br. J. Radiol. 37, 727-744.

Kaczmarczyk, G. and Reinhardt, H.W. (1975) Arterial blood gas tensions and acid-base status of Wistar rats during thiopental and halothane anesthesia. Lab. Anim. Sci. 25, 184-190.

Kellerer, A.M., Hall, E.J., Rossi, H.H. and Teedla, P. (1976) RBE as a function of neutron energy. II. Statistical analysis. Radiat. Res. 65, 172-186.
Kellerer, A.M. and Rossi, H.H. (1972) The theory of dual radiation action. Curr. Top. Radiat. Res. Quart. 8, 85-158.
Kerns, J.M. and Hinsman, E.J. (1973) Neuroglial response to sciatic neurectomy. I. Light microscopy and autoradiography. II. Electron microscopy. J. Comp. Neurol. 151, 237-280.
Kerr, F.W.L. (1975) Neuroanatomical substrates of nociception in the spinal cord. Pain 1, 325-356.
Kim, Y.S. (1974a) Human tissues: Chemical composition and photon dosimetry data. Radiat. Res. 57, 38-45.
Kim, Y.S. (1974b) Human tissues: Chemical composition and photon dosimetry data. A correction. Radiat. Res. 60, 361-362.
Kogel, A.J. van der (1977) Radiation tolerance of the rat spinal cord: time-dose relationships. Radiology 122, 505-509.
Kogel, A.J. van der and Barendsen, G.W. (1974) Late effects of spinal cord irradiation with 300 kV X-rays and 15 MeV neutrons. Br. J. Radiol. 47, 393-398.
Korr, H., Schultze, B. and Maurer, W. (1975) Autoradiographic investigations of glial proliferation in brain of adult mice. II. Cycle time and mode of proliferation of neuroglia and endothelial cells. J. Comp. Neurol. 160, 477-490.
Kristensen, O., Melgard, B. and Schiodt, A.V. (1977) Radiation myelopathy of the lumbo-sacral spinal cord. Acta Neurol. Scand. 56, 217-222.
Kristensson, K., Molin, B. and Sourander, P. (1967) Delayed radiation lesions of the human spinal cord. Acta Neuropathol. 9, 34-44.
Lambert, P.M. (1978) Radiation myelopathy of the thoracic spinal cord in long-term survivors treated with radical radiotherapy using conventional fractionation. Cancer 41, 1751-1760.
Lampert, P.W. and Davis, R.L. (1964) Delayed effects of radiation on the human central nervous system. "Early" and "late" delayed reactions. Neurology 14, 912-917.
Lewis, P.D. (1968) A quantitative study of cell proliferation in the subependymal layer of the adult rat brain. Exp. Neurol. 20, 203-207.
Liu, H.M. (1973) Schwann cell properties: 1. Origin of Schwann cell during peripheral nerve regeneration. J. Neuropathol. Exp. Neurol. 32, 458-473.
Liversage, W.E. (1969) A general formula for equating protracted and acute regimes of radiation. Br. J. Radiol. 42, 432-440.
Madrazo, A.A. and Churg, J. (1976) Radiation nephritis. Chronic changes following moderate doses of radiation. Lab. Invest. 34, 283-290.
Mastaglia, F.L., McDonald, W.I., Watson, J.V. and Yogendran, K. (1976) Effects of X-radiation on the spinal cord: an experimental study of the morphological changes in central nerve fibres. Brain 99, 101-122.
Masuda, K., Reid, B.O. and Withers, H.R. (1977) Dose effect relationship for epilation and late effects on spinal cord in rats exposed to gamma rays. Radiology 122, 239-242.
Mazze, R.I., Calverley, R.K. and Smith, N.T. (1977) Inorganic fluoride nephrotoxicity: prolonged enflurane and halothane anesthesia in volunteers. Anesthesiology 46, 265-271.
McDonald, L.W. and Hayes, T.L. (1967) The role of capillaries in the pathogenesis of delayed radionecrosis of brain. Am. J. Pathol. 50, 745-758.
Michenfelder, J.D., Milde, J.H. and Sundt, T.M.Jr. (1976) Cerebral protection by barbiturate anesthesia. Arch. Neurol. 33, 345-350.
Moosavi, H., McDonald, S., Rubin, P., Cooper, R., Stuard, I.D. and Penney, D. (1977) Early radiation dose-response in lung: an ultrastructural study. Int. J. Radiat. Oncol. Biol. Phys. 2, 921-931.

Nias, A.H.W., Greene, D. and Major, D. (1971) Constancy of biological parameters in a 14 MeV neutron field. Int. J. Radiat. Biol. 20, 145-151.
Ornitz, R.D., Bradley, E.W., Mossman, K.L., Fender, F.M. and Rogers, C.C. (1977) Clinical observations of early and late normal tissue injury in patients receiving fast neutron irradiation. Int. J. Radiat. Oncol. Biol. Phys. 2, suppl. 2, 166-167.
Pallis, C.A., Louis, S. and Morgan, R.L. (1961) Radiation myelopathy. Brain 84, 460-479.
Palmer, J.J. (1972) Radiation myelopathy. Brain 95, 109-122.
Pardridge, W.M. and Oldendorf, W.H. (1977) Transport of metabolic substrates through the blood-brain barrier. J. Neurochem. 28, 5-12.
Parker, R.G., Berry, H.C., Gerdes, A.J., Soronen, M.D. and Shaw, C.M. (1976) Fast neutron beam radiotherapy of glioblastoma multiforme. Am. J. Roentgenol. 127, 331-335.
Peters, A. and Vaughn, J.E. (1970) Morphology and development of the myelin sheath. In: Myelination (eds. A.N. Davison and A. Peters), p. 3-79, Charles C. Thomas, Springfield, Illinois.
Phillips, T.L. (1966) An ultrastructural study of the development of radiation injury in the lung. Radiology 87, 49-54.
Phillips, T.L., Barschall, H.H., Goldberg, E., Fu, K. and Rowe, J. (1974) Comparison of RBE values of 15 MeV neutrons for damage to an experimental tumour and some normal tissues. Eur. J. Cancer 10, 287-292.
Phillips, T.L. and Buschke, F. (1969) Radiation tolerance of the thoracic spinal cord. Am. J. Roentgenol. 105, 659-664.
Price, H.L. (1975) General anesthetics. In: Pharmacological basis of therapeutics (eds. L.S. Goodman and A. Gilman), Chapter 7, pp. 89-96, MacMillan Publishing Comp. Inc., New York.
Raju, M.R. and Richman, C. (1972) Negative pion radiotherapy: physical and radiobiological aspects. Curr. Top. Radiat. Res. Quart. 8, 159-233.
Rapoport, S.I. (1976) Opening of the blood-brain barrier by acute hypertension. Exp. Neurol. 52, 467-479.
Reese, T.S. and Karnovsky, M.J. (1967) Fine structural localization of a blood-brain barrier to exogenous peroxidase. J. Cell Biol. 34, 207-217.
Reinhold, H.S. and Buisman, G.H. (1973) Radiosensitivity of capillary endothelium. Br. J. Radiol. 46, 54-57.
Reinhold, H.S. and Buisman, G.H. (1975) Repair of radiation damage to capillary endothelium. Br. J. Radiol. 48, 727-731.
Reinhold, H.S. and Hopewell, J.W. (1979) Late changes in the architecture of blood vessels of the rat brain after irradiation. Br. J. Radiol., in press.
Reinhold, H.S., Kaalen, J.G.A.H. and Unger-Gils, K. (1976) Radiation myelopathy of the thoracic spinal cord. Int. J. Radiat. Oncol. Biol. Phys. 1, 651-657.
Research Plan for Radiation Oncology (1976) Committee for radiation oncology studies, S. Kramer, chairman. Cancer 37, 2031-2148.
Rider, W.D. (1963) Radiation damage to the brain - a new syndrome. J. Can. Assoc. Radiol. 14, 67-69.
Rizzuto, N. and Gambetti, P.L. (1976) Status spongiosus of rat central nervous system induced by actinomycin D. Acta Neuropathol. 36, 21-30.
Rubin, P. and Casarett, G.W. (1968) Clinical radiation pathology, W.B. Saunders Comp., Philadelphia.
Rubin, P. and Casarett, G. (1972) A direction for clinical radiation pathology. The tolerance dose. In: Front. Radiation Ther. Onc., vol. 6 (ed. J.M. Vaeth), Karger, Basel and University Park Press, Baltimore.
Sadowsky, C.H., Sachs, E. and Ochoa, J. (1976) Postradiation motor neuron syndrome. Arch. Neurol. 33, 786-787.

Scholz, W., Schlote, W. and Hirschberger, W. (1962) Morphological effect of X-irradiation to the central nervous system. In: Response of the nervous system to ionizing radiation (eds. T.J. Haley and R.S. Snider), pp. 211-232, Academic Press, New York.

Skoff, R.P. (1975) The fine structure of pulse labeled (^{3}H-thymidine cells) in degenerating rat optic nerve. J. Comp. Neurol. 161, 595-612.

Smith, M.E. (1968) The turnover of myelin in the adult rat. Biochim. Biophys. Acta 164, 285-293.

Spencer, P.S. and Thomas, P.K. (1974) Ultrastructural studies of the dying-back process. II. The sequestration and removal by Schwann cells and oligodendrocytes of organelles from normal and diseased axons. J. Neurocytol. 3, 763-783.

Stenwig, A.E. (1972) The origin of brain macrophages in traumatic lesions, Wallerian degeneration and retrograde degeneration. J. Neuropathol. Exp. Neurol. 31, 696-704.

Stone, R.S. (1948) Neutron therapy and specific ionization. Amer. J. Roentgenol. 59, 771-785.

Stone, R.S., Lawrence, J.H. and Aebersold, P.C. (1940) Preliminary report on the use of fast neutrons in the treatment of malignant disease. Radiology 35, 322-327.

Strandqvist, M. (1944) Studien über die kumulative Wirkung der Röntgenstrahlen bei Fraktionierung. Erfahrungen aus dem Radiumhemmet an 280 Haut und Lippenkarzinomen. Acta Radiologica, Suppl. 55, 1-300.

Thomas, P.K., Lascelles, R.G. and Stewart, G. (1975) Hypertrophic neuropathy. Handbook Clin. Neurol., vol. 21, part 1, pp. 145-170, North Holland Publ. Comp., Amsterdam.

Travis, E.L., Harley, R.A., Fenn, J.O., Klobukowski, C.J. and Hargrove, H.B. (1977) Pathologic changes in the lung following single and multi-fraction irradiation. Int. J. Radiat. Oncol. Biol. Phys. 2, 475-490.

Travis, E.L., Hobson, B., Holmes, S.J. and Field, S.B. (1979) Quantitative histological changes in mouse lungs after single doses of X-rays and neutrons. In: Proc. 3rd Meeting on Fundamental and Practical Aspects of Fast Neutrons and Other High LET Particles in Clinical Radiotherapy. Eur. J. Cancer, Suppl. 6, in the press.

Tsubouchi, S. and Matsuzawa, T. (1974) Rapid radiation cell death and cell proliferation in intestinal epithelium after 1000 rad irradiation. Radiat. Res. 57, 451-458.

Tveten, L. (1976) A microangiographic and stereomicroscopic study of the spinal cord vascularity in man and rat. Monograph, University Institute of Pathological Anatomy, Rikshospitalet, Oslo.

Tveten, L. and Loken, A.C. (1975) Spinal cord vascularity. A histopathological and angiographic study of the effects of thoracic-lumbar aortic mobilization in the rat. Neuropathol. Appl. Neurobiol. 1, 379-395.

Van den Brenk, H.A.S., Richter, W. and Hurley, R.H. (1968) Radiosensitivity of the human oxygenated cervical spinal cord based on analysis of 357 cases receiving 4 MeV X-rays in hyperbaric oxygen. Br. J. Radiol. 41, 205-214.

Vaughn, J.E. and Skoff, R.P. (1972) Neuroglia in experimentally altered central nervous tissue. In: Structure and function of nervous tissue, vol. VI (ed. G.H. Bourne), pp. 39-72, Academic Press, New York.

Verhaart, W.J.C. (1970) Comparative anatomical aspects of the mammalian brain stem and the cord. Van Gorcum & Comp. N.V., Assen.

Vogel, F.S. and Pickering, J.E. (1956) Demyelinization induced in the brains of monkeys by means of fast neutrons. J. exp. Med. 104, 435-441.

Waibl, H. (1973) Zur Topographie der Medulla spinalis der Albinoratte (Rattus norvegicus). Adv. Anat. Embryol. Cell Biol. 47, 1-42.

Wara, W.M., Phillips, T.L., Margolis, L.W. and Smith, V. (1973) Radiation pneumonitis: a new approach to the derivation of time-dose factors. Cancer 32, 547-552.
Wara, W.M., Phillips, T.L., Sheline, G.E. and Schwade, J.G. (1975) Radiation tolerance of the spinal cord. Cancer 35, 1558-1562.
White, A. and Hornsey, S. (1978) Radiation damage to the rat spinal cord: the effect of single and fractionated doses of X-rays. Br. J. Radiol. 51, 515-523.
Withers, H.R. (1967) The dose-survival relationship for irradiation of epithelial cells of mouse skin. Brit. J. Radiol. 40, 187-194.
Withers, H.R. (1975) The four R's of radiotherapy. In: Advances in Radiation Biology, vol. 5 (eds. J.T. Lett and H. Adler), pp. 241-271, Academic Press, New York.
Withers, H.R., Chu, A.M., Reid, B.O. and Hussey, D.H. (1975) Response of mouse jejunum to multifraction radiation. Int. J. Radiat. Oncol. Biol. Phys. 1, 41-52.
Withers, H.R., Flow, B.L., Huchton, J.I., Hussey, D.H., Jardine, J.H., Mason, K.A., Raulston, G.L. and Smathers, J.B. (1977) Effect of dose fractionation on early and late skin responses to γ-rays and neutrons. Int. J. Radiat. Oncol. Biol. Phys. 3, 227-233.
Wolff, J.R. and Bär, Th. (1976) Development and adult variations of the pericapillary glial sheath in the cortex of rat. In: The cerebral vessel wall (eds. J. Cervos-Navarro et al.), pp. 7-13, Raven Press, New York.
Zeman, W. (1966) Oxygen effect and selectivity of radiolesions in the mammalian neuraxis. Acta Radiol. Ther. Phys. Biol. 5, 204-216.